GEOLOGY AND MINERAL POTENTIAL OF THE WESTERN SKEENA ARCH:
Evolution of an Arc-Transverse Structural Corridor, West-Central British Columbia

Joel J. Angen, Craig J. R. Hart, Joanne L. Nelson, and Mana Rahimi

Geoscience BC Report 2022-09
British Columbia Geological Survey Open File 2019-09
MDRU Publication 458

Geoscience BC

BRITISH COLUMBIA GEOLOGICAL SURVEY est. 1895

MDRU
MINERAL DEPOSIT RESEARCH UNIT

UBC THE UNIVERSITY OF BRITISH COLUMBIA

GEOLOGY AND MINERAL POTENTIAL OF THE WESTERN SKEENA ARCH:
Evolution of an Arc-transverse Structural Corridor, West-Central British Columbia

Joel J. Angen[1,2], Craig J.R. Hart[1], JoAnne L. Nelson[3], Mana Rahimi[1]

Geoscience BC* Report 2022-09

British Columbia Geological Survey Open File 2019-09

MDRU† Publication 458

[1] MDRU – Mineral Deposit Research Unit, The University of British Columbia, Vancouver, British Columbia, Canada

[2] corresponding author, angenjoel@gmail.com

[3] British Columbia Geological Survey, British Columbia Ministry of Energy, Mines and Low Carbon Innovation, Victoria, British Columbia

Keywords: Skeena arch, Hazelton Group, Skeena Group, Bulkley suite, Babine suite, Nanika suite, Stikine Terrane, folding, arc transverse, porphyry

Suggested Citation:
Angen, J.J., Hart, C.J.R., Nelson, J., and Rahimi, M. (2022): Geology and Mineral Potential of the Western Skeena Arch: Evolution of an Arc-transverse Structural Corridor, West-Central British Columbia. Geoscience BC Report 2022-09, BCGS Open File 2019-09, MDRU Publication 458, 47 p.

Report prepared by MDRU

Dept. Earth, Ocean and Atmospheric Sciences, The University of British Columbia
Vancouver, BC V6T 1Z4, Canada
Tel: +1-604-822-6136
Email: mdru@eoas.ubc.ca

Includes bibliographic references.
Electronic monograph issued in PDF format.
ISBN 978-0-88865-480-9

*Geoscience BC is an independent, non-profit organization that generates earth science in collaboration with First Nations, local communities, government, academia and the resource sector. Our independent earth science enables informed resource management decisions and attracts investment and jobs. Geoscience BC gratefully acknowledges the financial support of the Province of British Columbia.

†MDRU—Mineral Deposit Research Unit is an internationally-recognized collaborative venture between the mining industry and Earth, Ocean and Atmospheric Sciences Department at The University of British Columbia (UBC), established with assistance from the Natural Sciences and Engineering Research Council of Canada (NSERC), and devoted to solving mineral exploration-related problems.

Cover image: *Looking northwest at the CuLater rhyolite dome, northern flank of Ventura Peak.*

CONTENTS

1. INTRODUCTION

The Skeena arch is an ENE-trending paleotopographic high in central British Columbia that transects the Stikine terrane. Lower Jurassic and older rocks exposed along its crest are flanked by Middle Jurassic to Lower Cretaceous units that were deposited in the Bowser basin to the north and Nechako basin to the south (Figure 1.1; Tipper and Richards, 1976). The Skeena arch is a highly prospective region for mineral deposits, with over 220 metallic mineral occurrences documented in the western Skeena arch alone (MINFILE, 2020). Economically significant porphyry and related mineralization within the Skeena arch is genetically associated with the Bulkley (Late Cretaceous) and Babine/Nanika plutonic suites (Eocene) that post-date terrane accretion (MacIntyre, 2006). These occurrences have the potential to generate new wealth and provide employment for the residents of central British Columbia. However, none of these deposits are currently being exploited, and exploration to find new deposits benefits from new ideas and geoscience.

Reactivation of pre-existing structures is regarded as a favourable mechanism to localize the emplacement and focussing of porphyry intrusions and can provide conduits for the flow of mineralizing hydrothermal fluids (Heidrick and Titley, 1982; Richards, 2000; Tosdal and Richards, 2001). In arc terranes, transverse structures are recognized as features that can control the emplacement of porphyry intrusions and mineralization, particularly where they intersect arc-parallel structures (Schmitt, 1966; Glen and Walshe, 1999; Richards et al., 2001; Garwin et al., 2005; Gow and Walshe, 2005).

The distribution of the prospective Bulkley and Babine/Nanika plutonic suites, as well as the Topley and Kleanza plutonic suites (Late Triassic to Early Jurassic), mostly align along the northeasterly trend of the Skeena arch (Figure 1.1). Despite regional (Tipper and Richards, 1976b) and more detailed (MacIntyre et al., 1989a; MacIntyre et al., 1989b; Desjardins et al., 1990a; Desjardins et al., 1990b; Nelson et al., 2006; Nelson and Kennedy, 2007; Nelson et al., 2008a; Nelson, 2009) geological mapping, the structural history of the Skeena arch and, in particular, the significance of its arc-transverse orientation, has not been well established. An improved understanding of the tectonic and structural history of the western Skeena arch and its influence on mineralization will improve the efficacy and provide targeting criteria for future mineral exploration efforts.

Interpretations of recently-acquired, Search project phase 1 aeromagnetic survey data in 2015 (Precision GeoSurveys, 2016) is the foundation for this project. The survey included a total of 29,820 line km at 250 m line spacing to cover a total area of 6756 km^2. The data are herein integrated with historical geological data and new structurally-focused mapping to provide an improved understanding of the geological and structural framework of the western Skeena arch.

Targeted field mapping was conducted during the summer of 2016, with preliminary geological interpretations released as a BC Geological Survey Fieldwork article (Angen et al., 2017). In addition, extensive processing and review of Advanced Spaceborne Thermal Emission Radiometer (ASTER) data within the Search Phase 1 area was carried out in 2017 to test its effectiveness as a tool to potentially identify alteration related to mineralizing processes. Results were reported in a Geoscience BC Summary of Activities paper (Rahimi et al., 2018). Portions of these previous reports are incorporated herein with additional information acquired through subsequent laboratory and office-based investigations. This report accompanies MDRU Map 17-2018/Geoscience BC Map 2019-03-01/BCGS Map 2019-07 and Geoscience BC Map 2019-03-02/MDRU Map 18-2018/BCGS Open File 2019-08, which are bedrock geology and aeromagnetic correlation maps, respectively.

Geological Setting

The Search study area is in the west-central Stikine terrane and overlaps along its western margin, with the intrusions of the eastern Coast Plutonic Complex (Figure 1.1). The Stikine terrane records episodic Devonian to Jurassic island arc volcanism and sedimentation. It was accreted to the western margin of North America during the Middle Jurassic along with the other Intermontane terranes, Quesnel and Cache Creek terranes (Monger et al., 1982). The Insular terranes were proximal to the new continental margin that formed outboard from the amalgamated Intermontane terranes at least by the Middle Jurassic, as evidenced by detrital zircon signatures, overlapping strata, and coincident deformation (McClelland and Gehrels, 1990; van der Heyden, 1992; Kapp and Gehrels, 1998; Gehrels, 2001; Israel et al., 2006; Israel at al., 2014). Subsequent magmatism generated largely through subduction-related convergence of the Insular terranes formed the Coast Plutonic Complex (CPC), a Middle Jurassic to Eocene continental margin batholith that stitches the Insular and Intermontane Terranes (van der Heyden, 1992).

The core of the western Skeena arch represents a broadly eastward-younging section through typical Stikine terrane stratigraphy. Mississippian to Permian volcanic and lesser sedimentary rocks of the Mt. Attree Formation are overlain by Ambition Formation limestone (Permian); these two units constitute the Zymoetz Group which is equivalent to the Stikine assemblage defined farther north (Monger, 1977; Nelson et al., 2008a). A relatively thin (<50 m) unit of Upper Triassic chert and argillite overlies the Zymoetz Group (Nelson et al., 2006). This unit is assigned to the Stuhini Group. Upper Triassic to Lower Jurassic subaerial to submarine volcanic rocks of the Telkwa Formation are widespread in the western Skeena arch where they preserve a transition from primarily proximal subaerial deposition in the west to progressively more distal and

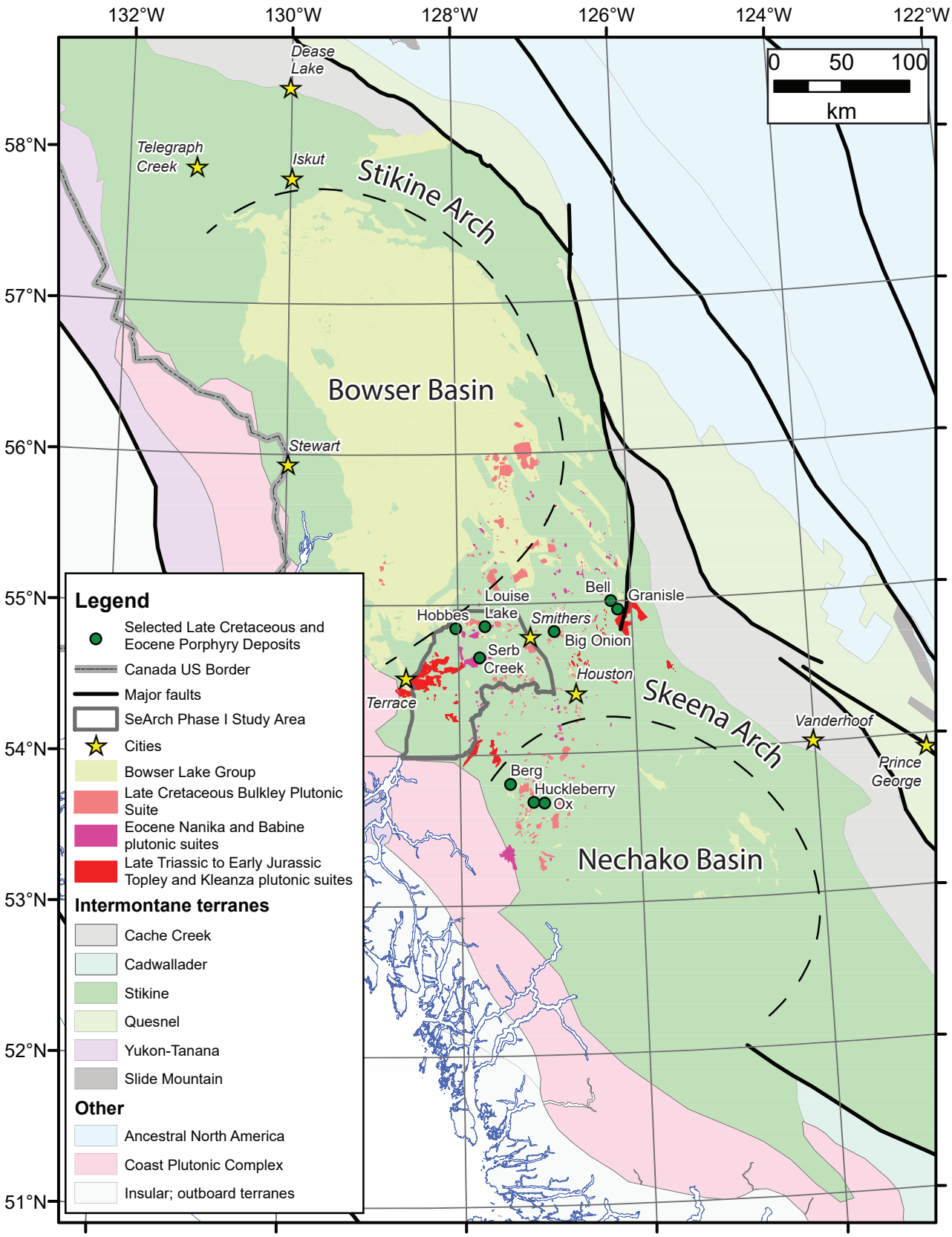

Figure 1.1: Location of the study area in the terrane context of west-central British Columbia. Terranes modified after Colpron and Nelson (2011) and Nelson et al. (2013). Outlines of the Bowser and Nechako basins modified after Tipper and Richards (1976).

submarine deposition to the east (Tipper and Richards, 1976). The Telkwa Formation represents the lower Hazelton Group at this latitude (Gagnon et al., 2012; Barresi et al., 2015a; Barresi et al., 2015b). It records the onset and voluminous main-stage magmatic activity of the Hazelton arc.

The lower Hazelton Group and related intrusions elsewhere in the Stikine terrane host large porphyry and epithermal deposits (e.g., 'Golden Triangle' and Toodoggone districts). Equivalent mineralization has not yet been recognized in the Skeena arch. The Telkwa Formation is conformably overlain by Lower to Middle Jurassic mixed sedimentary and volcanic rocks of the Nilkitkwa, Saddle Hill, Smithers, and Quock formations; these are collectively referred to as the upper Hazelton Group and record the waning stages of Hazelton arc activity (Gagnon et al., 2012). Termination of the Hazelton arc corresponds to accretion of the Intermontane terranes to the western margin of North America during the Middle Jurassic and a transition to non-arc-magma-generating processes (Barresi et al., 2015a; van Straaten and Nelson, 2016; van Straaten and Gibson, 2017).

Marine sedimentation continued across much of Stikine terrane following accretion. The upper Hazelton Group is overlain by Middle Jurassic to Early Cretaceous marine sedimentary rocks of the Bowser Lake Group in the Bowser Basin, and equivalent strata in the Nechako Basin. Chert-rich detritus in the Bowser Lake Group was shed from the uplifted Cache Creek terrane (Gabrielse and Yorath, 1991). A gradational contact has been well-documented between the Quock Formation and the lower Bowser Lake Group along the northern margin of the Skeena arch (Evenchick et al., 2010; Gagnon et al., 2012). Middle Jurassic marine sedimentary rocks of the Bowser Lake Group are limited to only a few localities across the Skeena arch: Callovian fossils (and zircons) have been recovered from an isolated exposure of Bowser Lake Group near Telkwa Pass (Pálfy et al., 2000) and fine-grained Bajocian to Callovian marine sedimentary rocks occur in the headwaters of Tenas Creek (MacIntyre et al., 1989a; MacIntyre et al., 1989b). Thick accumulations of Bowser Lake Group strata are limited to the Bowser Basin and Nechako Basin where their thicknesses have been estimated at up to 4000 m and 1500 m, respectively (Evenchick, 1991; Diakow et al., 1997). The Trout Creek assemblage, a distinctive Late Jurassic delta facies of the Bowser Lake Group that occurs along the northern margin of the Skeena arch, has been interpreted to reflect uplift and erosion of the arch (Tipper and Richards, 1976; MacIntyre et al., 1989a; this study). A Late Jurassic origin for the Skeena arch as a paleotopographic high is supported by the basal contact of the Skeena Group. The Skeena Group records a transition from Early Cretaceous predominantly marine deposition to Late Cretaceous predominantly fluvial deposition (Basset and Kleinspehn, 1997). Within the southern Bowser Basin, the Bowser Lake Group is gradationally overlain by the Lower Cretaceous Skeena Group (Smith and Mustard, 2005; 2006). In contrast, in the central Skeena arch, the Skeena Group rests unconformably on the Telkwa Formation (Palsgrove and Bustin, 1991).

The Coast Plutonic Complex spans the length of western margin of North America from northern Washington, USA up to southwestern Yukon. Geochemically, it resembles the roots to other subduction-related magmatic arcs (Roddick, 1983; Samson et al., 1991; Cui and Russel, 1995; Friedman and Armstrong, 1995; Patchett and Gehrels, 1998; Boghossian and Gehrels, 2000; Mahoney et al., 2009). Between the Late Cretaceous and Eocene, it formed through east-dipping subduction beneath the accreted Intermontane and Insular terranes. Associated magmatic activity inboard, or behind, the continental arc axis is relatively sparse and documented by the Bulkley (Late Cretaceous) and Nanika/Babine (Eocene) plutonic suites. The vast majority of mineralization throughout the Skeena arch is interpreted to be genetically related to these intrusions (MacIntyre, 2006).

Previous Work

This study benefited from excellent previous geological investigations, with most areas being covered by two or more generations of regional mapping since 1950 (Fig. 1.2). The Terrace map area, covering the eastern boundary of the Coast Plutonic Complex and westernmost limit of the Skeena arch, was mapped at 1:250,000 scale by Duffell and Souther (1964). Details of the geological relationships and mineralization within this region were outlined in an associated memoir (Duffell and Souther, 1964). The geology of the eastern half of the Terrace map area was revised during 1:125,000 mapping by Woodsworth et al. (1985), and subsequently refined through 1:50,000 mapping during the Terrace mapping project (Nelson et al., 2006; Nelson et al., 2007; Nelson et al., 2008a; Nelson et al., 2008b; Nelson, 2009). The first geological compilation of the western Skeena arch was produced by Carter and Kirkham (1969) at 1:250,000 scale. The stratigraphic framework and tectonic setting of the Stikine terrane and overlap assemblages was established in a detailed review of Jurassic stratigraphy of north-central British Columbia by Tipper and Richards (1976). This bulletin was released along with an updated 1:250,000 compilation of the Smithers map area (Richards and Tipper, 1976). Geological contacts in the central Smithers map area were refined through subsequent 1:50,000 mapping during the late 1980s as part of the Telkwa project (MacIntyre et al., 1989a; MacIntyre et al., 1989b; Desjardins et al., 1990a; Desjardins et al., 1990b). The Telkwa Coalfields area was remapped at 1:20,000 to facilitate coal exploration efforts (Ryan, 1993). Evenchick et al. (2008) recompiled mapping along the northern margin of the Skeena arch (i.e., southern margin of the Bowser Basin) at 1:125,000. Detailed study areas for the current project were preferentially selected to fill in the gap between the Terrace mapping project

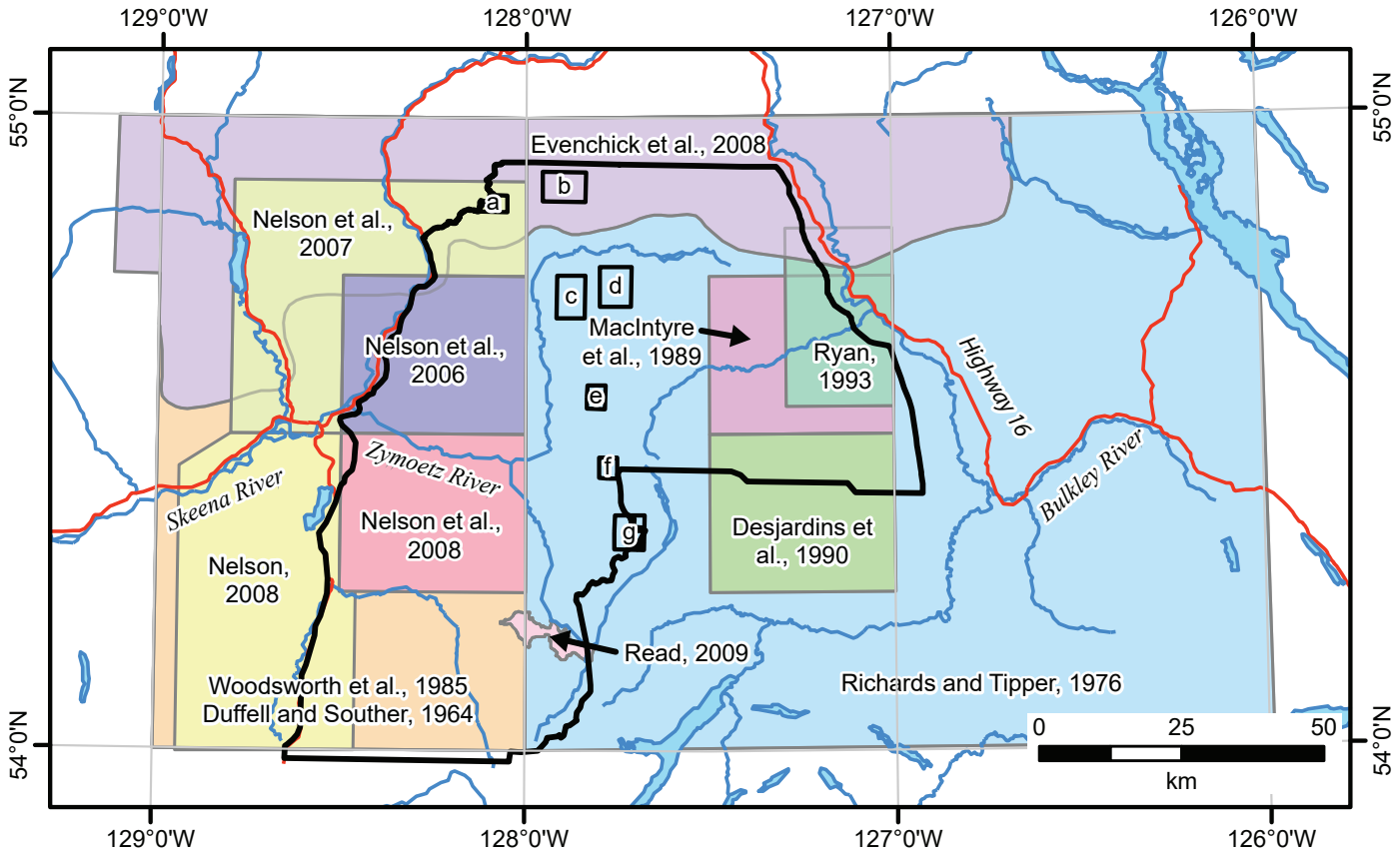

Figure 1.2: Sources of information for the Search compilation map. The Search phase 1 aeromagnetic survey and detailed study areas are outlined in black: a – Zymo ridge; b – Paleo peak; c – Ventura Peak; d – Cariboo Mountain; e – Limonite Creek; f – south of Outcast Peak; g – Tatsi Creek.

to the west and the Telkwa mapping project to the east (Figure 1.2). A 1:20,000 map of the region surrounding Mount Nimbus was produced by Peter Read for planning of the Northern Gateway pipeline right of way. This map, which also fills in part of the intervening gap (Figure 1.2), was incorporated into the current project and can be found in an AMEC geotechnical report on the Northern Gateway pipeline project (AMEC, 2009).

A number of theses previously carried out in the current study area have contributed significantly to the understanding of geological relationships in the western Skeena arch and eastern Coast Plutonic Complex. Most of these theses were focused on specific stratigraphic intervals: Mihalynuk (1987) mapped an east-west transect through the Telkwa Formation south of the Zymoetz River, focusing on stratigraphy, structure and metamorphism; Barresi (2015) investigated the geochemistry, geochronology, and volcanic facies of the Telkwa Formation near Terrace as part of a project detailing the tectono-magmatic and metallogenic evolution of the Hazelton Group; Gagnon (2010) investigated stratigraphy and sedimentary facies of the upper Hazelton Group and lower Bowser Lake Group along the northern margin of the Skeena arch as part of a project detailing the transition from deposition in the Hazelton trough to the Bowser Basin; and Bassett (1995) refined the stratigraphy and distribution of the Skeena Group.

The intrusions of the Coast Plutonic Complex with a focus on eastern apophyses into the Stikine terrane was evalauted with results being incorporated into GSC Memoir 329 (Duffell and Souther, 1964). Carter (1974) undertook a metallogenic investigation focused on the age and distribution of porphyry deposits across west-central British Columbia; this was subsequently published as British Columbia Geological Survey Bulletin 64 (Carter, 1981).

Other metallogenic investigations have been deposit specific: Deyell et al. (2000) investigated high-sulfidation epithermal mineralization at the Limonite Creek prospect; and McKeown et al. (2008) investigated potential VMS-style mineralization on the Gazelle property (now the Midas property, MINFILE 103I 185). Structurally-focused studies have been rare in this area: Heah (1991) detailed high strain zone deformation in the vicinity of Shames River, west of the current study area; Evenchick (1979) investigated a northeasterly-trending high-strain zone immediately south of the current study area at Atna Peak; and Angen (2009) carried out a geospatial structural analysis of data collected during the Terrace mapping project.

Other targeted studies in this region mainly focused on relationships between mineral deposits, geochronology and stratigraphy. Hanson and Klassen (1995) provided an overview

of the Louise Lake porphyry deposit which at the time was interpreted to be Eocene. Friedman and Panteleyev (1997) reassigned Louise Lake to the Bulkley suite based on new U-Pb zircon geochronology. Gareau et al. (1997) refined assignments of volcanic and plutonic rocks along the western limit of the Skeena arch using U-Pb zircon geochronology. Pálfy et al. (2000) tightened chronological constraints on stratigraphy near the Hazelton Group to Bowser Lake Group contact at several localities in the study area through a combination of U-Pb zircon geochronology and ammonite biostratigraphy. Palsgrove and Bustin (1991) assessed stratigraphy and coal quality of the Skeena Group in the Telkwa coalfield area. All of these studies significantly improved our understanding of the geological framework of the western Skeena arch.

2. LITHOLOGIC UNITS

The following is a summary of lithologic units that are present in the Search I project area. They are included in the legend of the geological map (Geoscience BC Map 2019-03-01) that accompanies this report (Angen et al., 2019a, Figure 2.1). Seven selected areas that were mapped at 1:20,000 are presented as insets within Figure 2.1. Lithological units in these areas are discussed in detail, whereas units that occur within the Search area but not encountered during the more detailed investigations are only given cursory review. The regional geological information for the Search area outside of the detailed study areas has been modified from the digital BC geological map compilation (Cui et al., 2017) to accommodate newly-compiled mapping as well as new observations and geochronology from both inside and outside of the in the detailed study areas. Contacts were modified or refined from interpretations of Search Phase 1 aeromagnetic data, where applicable (Figure 2.2)(Precision GeoSurveys Inc., 2016). The shapefiles used to generate Figure 2.1 are available for download from http://www.geosciencebc.com/projects/2016-038/. Further information regarding specific sources of data have been preserved in feature attributes.

To improve confidence of the timing of formation of lithological units and related geological events, U-Pb geochronological results were obtained for 14 samples (Appendix A). To improve the geological map, surface geological mapping was integrated and interpreted with the aeromagnetic data. To better understand the magnetic character of the rock units, magnetic susceptibility measurements were carried out at each outcrop using a handheld KT-9 magnetic susceptibility meter. Magnetic susceptibility data for major lithological units are shown in Figure 2.3 and details of data collection and raw data are in Appendix B.

Plutonic suites have, on average, higher magnetic susceptibilities than stratified rocks. Regions of higher magnetic responses in the aeromagnetic data locally correspond to plutonic rocks. All of the volcanic and sedimentary units have overlapping ranges of magnetic susceptibility, making their distinctions on the basis of magnetic characteristics difficult. The sedimentary units generally exhibit lower magnetic susceptibilities and have less variability than other units. The three volcanic units have large variability but generally low magnetic susceptibilities. The Mount Attree volcanics, which may have initially contained considerable magnetite, have undergone extensive magnetite-destructive alteration and deformation. The magnetic susceptibility range of the Telkwa Formation is large and reflects the rare occurrence of strongly-magnetic basalt flows within mostly maroon, hematite-bearing volcanic rocks with low magnetic susceptibility. The Netalzul volcanics include abundant intercalated sedimentary rocks and have been affected by extensive magnetite-destructive alteration surrounding Late Cretaceous Bulkley suite intrusions—both contribute to its low magnetic susceptibility.

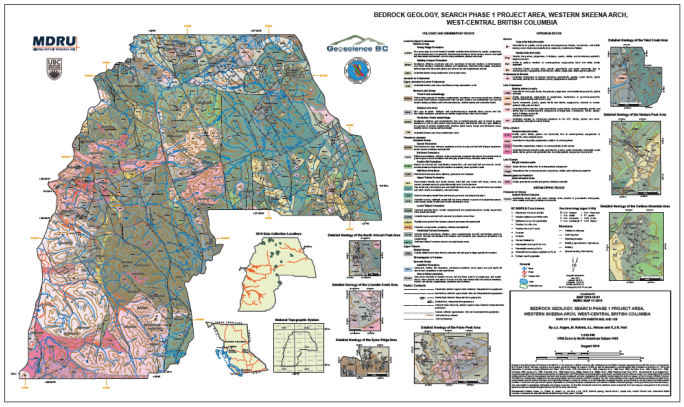

Figure 2.1: Bedrock geology of the Search Phase 1 project area, west central British Columbia. Inset maps: a – Zymo ridge; b – Paleo peak; c – Ventura peak; d – Cariboo Mountain; e – Limonite Creek; f – South of Outcast Peak; and g – Tatsi Creek. Available as Angen et al. (2019a); http://www.geosciencebc.com/i/project_data/2016-038/GBCMap2019-03-01MDRUMap17-2018BCGS2019-07_Geo.pdf

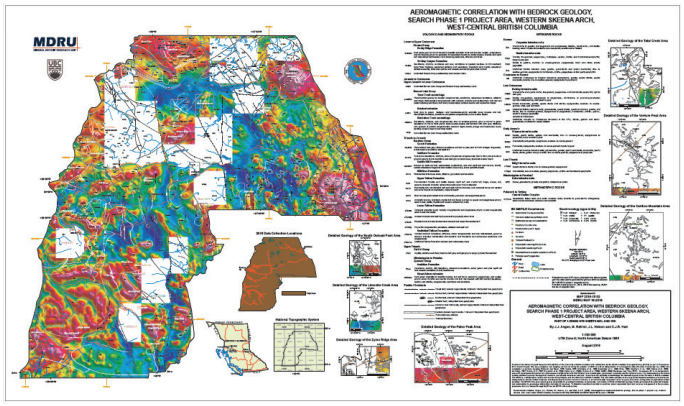

Figure 2.2: Aeromagnetic correlation with bedrock geology of the Search Phase 1 project area, west central British Columbia. Available as Angen et al. (2019b); http://www.geosciencebc.com/i/project_data/2016-038/GBCMap2019-03-02MDRUMap18-2018BCGS2019-08_GPH.pdf

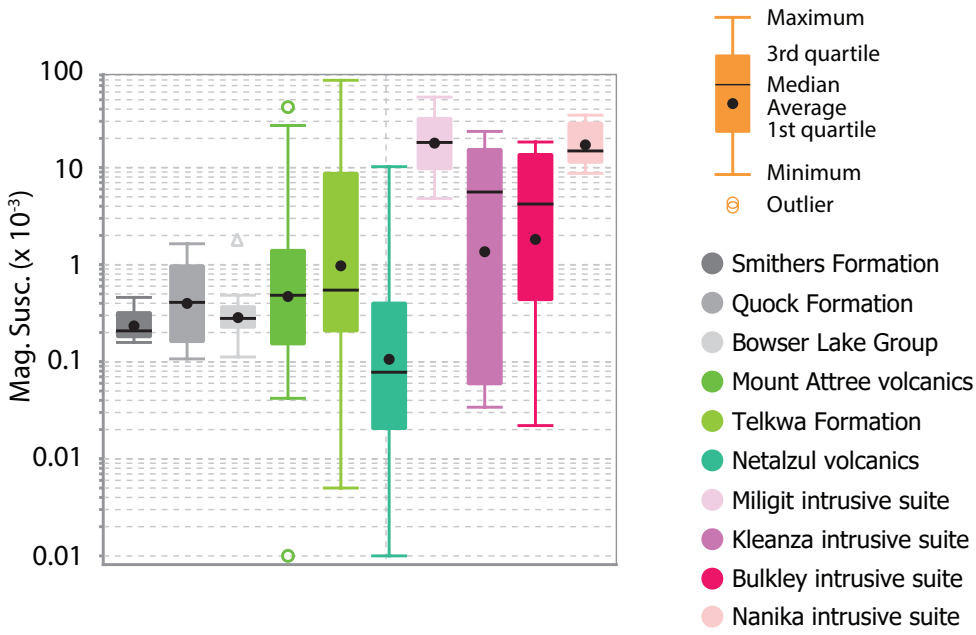

Figure 2.3: Box and whisker plot of magnetic susceptibility values for major lithologic units documented in the Search area. Data were collected during mapping in 2016, and presented in Appendix B.

Stratigraphy

Stratigraphic units in the western Skeena arch range in age from Mississippian to Upper Cretaceous (Figure 2.4). The oldest rocks are Mississippian to Permian volcanic and sedimentary rocks of the Mount Attree volcanics that are overlain by Permian limestone of the Ambition Formation, which combined, make up the Zymoetz Group (Nelson et al., 2006; Nelson et al., 2008a). Sparse Middle Triassic marine sedimentary rocks are assigned to the Stuhini Group (Nelson et al., 2006; Nelson et al., 2008a). The Zymoetz Group is unconformably overlain by Upper Triassic to Lower Jurassic volcanic and minor sedimentary rocks of the Telkwa Formation, which are assigned to the lower Hazelton Group (Tipper and Richards, 1976; Nelson et al., 2008a). In the Skeena arch region, the upper Hazelton Group includes the Nilkitkwa, Saddle Hill, Smithers and Quock formations. Lower Jurassic sedimentary rocks of the Nilkitkwa Formation overlie the Telkwa Formation in the southeastern Search area (MacIntyre et al., 1989a). Elsewhere a paraconformity separates the Telkwa Formation from nearly indistinguishable Lower Jurassic volcanic rocks of the Saddle Hill Formation (MacIntyre et al., 2001). The Saddle Hill Formation is conformably overlain by Middle Jurassic tuffaceous sedimentary rocks of the Smithers Formation and Middle to Upper Jurassic tuffaceous sedimentary rocks of the Quock Formation, which is equivalent to Ashman Formation. The Quock Formation is gradationally overlain by the Upper Jurassic to Lower Cretaceous Bowser Lake Group, which includes the slope facies Richie-Alger assemblage, shelf facies Muskaboo Creek assemblage, Netalzul volcanics and the deltaic-facies Trout Creek assemblage (Evenchick et al., 2010; note that the Trout Creek assemblage is not recognized in this reference). The Skeena Group conformably to unconformably overlies older units and includes the shelf to delta facies Bulkley Canyon Formation, the slope facies Laventie Formation and volcanic rocks of the Rocky Ridge Formation (Bassett and Kleinspehn, 1997).

Zymoetz Group

The oldest stratified rocks in the Skeena arch region are Mississippian to Permian volcanic and sedimentary rocks of the Zymoetz Group in and west of the Howson Range (Figure 2.1). The Zymoetz Group is equivalent to the Stikine assemblage of northwestern British Columbia (Brown et al., 1991). The Zymoetz Group includes Mississippian to Permian volcanic and minor sedimentary rocks of the Mount Attree volcanics that are unconformably overlain by Permian limestone assigned to the Ambition Formation (Nelson et al., 2006; Nelson et al., 2008a). The Zymoetz Group correlates with metavolcanic rocks and Permian limestone mapped in the eastern Skeena arch as the Asitka Group (MacIntyre et al., 2001)

Mount Attree Volcanics

Mississippian to Permian, variably metamorphosed volcanic and minor sedimentary rocks occur in isolated exposures through the western half of the Search area. They have been informally named the Mount Attree volcanics (Nelson et al., 2008a). The Mount Attree volcanics consist mainly of interbedded plagioclase- and pyroxene-phyric andesite and basalt flows and associated volcanic breccia and lapilli tuff, but also include minor rhyolite to dacite, marble, conglomerate

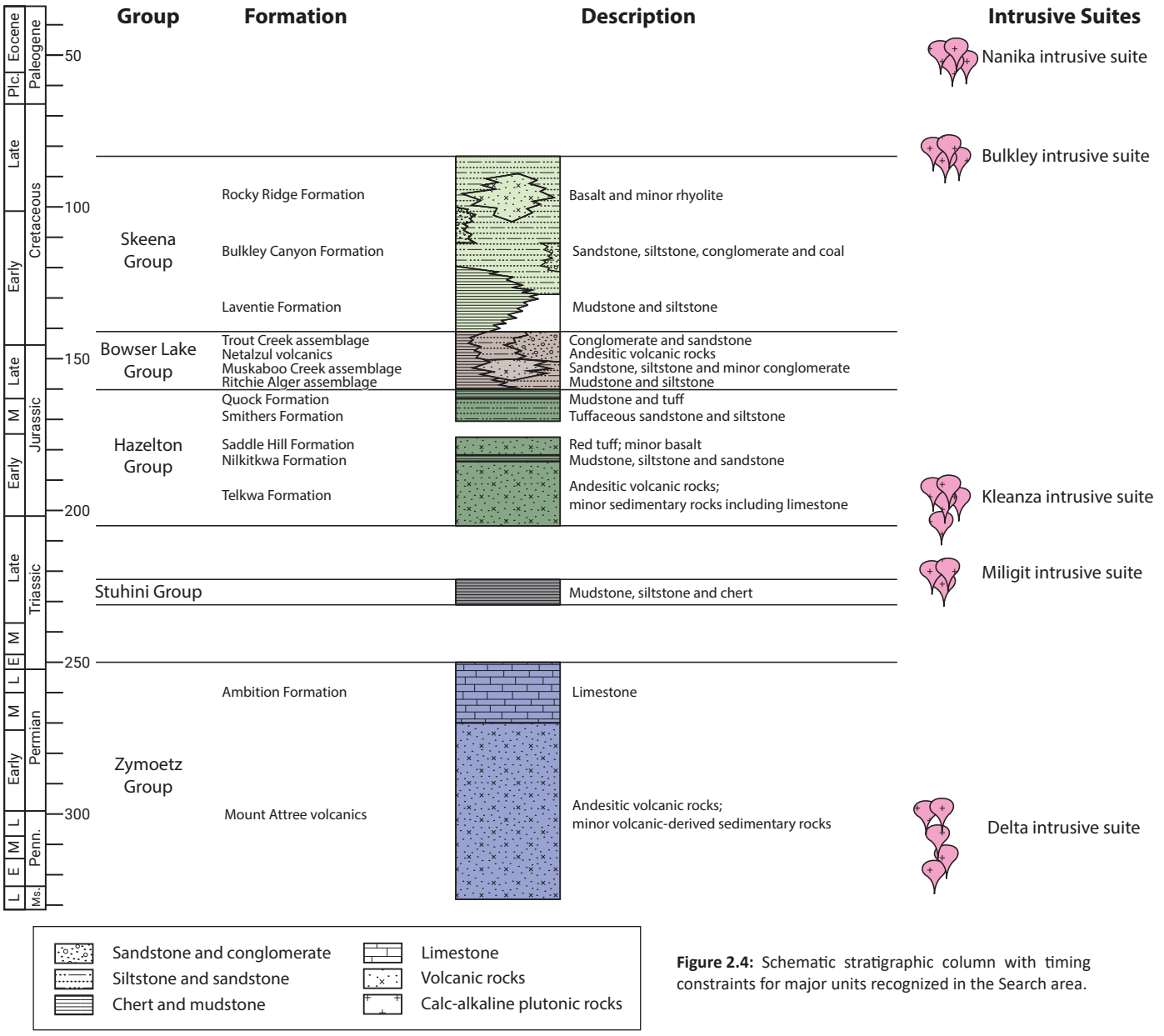

Figure 2.4: Schematic stratigraphic column with timing constraints for major units recognized in the Search area.

and phyllite. They are metamorphosed to greenschist to amphibolite facies and are well foliated (Nelson et al., 2008a). Their lower contact has not been identified. The Mount Attree volcanics are unconformably(?) overlain by Permian Ambition Formation limestone. Available isotopic dates include 285 ± 9 Ma U-Pb zircon from a feldspar crystal-bearing tuff collected ~5 km upstream from the mouth of the Zymoetz River (Gareau et al., 1997) and 322.2 ± 1.0 Ma U-Pb zircon from quartz-phyric dacite ~10 km NNW of Kitimat (Nelson, 2017; Nelson and Friedman, 2017). The Mount Attree volcanics are also crosscut by Mississippian intrusions (Nelson, 2017). They therefore represent Mississippian to Permian arc-related magmatism (Nelson, 2017). In this study, the Mount Attree volcanics have been recognized farther east than previously recognized in two localities in the Howson Range: at Limonite Creek (Figure 2.1 inset e) where they host Late Triassic intrusions of the Miligit plutonic suite; and south of Outcast Peak (Figure 2.1 inset f) where they are unconformably overlain by the Telkwa Formation.

A succession of mafic volcanic rocks in the headwaters of Limonite Creek (Figure 2.1 inset e) were previously assigned to the Telkwa Formation (Lower Jurassic) (Richards and Tipper, 1976), but they are cut by two Late Triassic plutons (see Late Triassic Miligit plutonic suite section) indicating that the volcanic rocks must be Late Triassic or older. The volcanic rocks are poorly exposed and variably deformed with locally intense propylitic and phyllic alteration. Where phyllic alteration is intense, the volcanic rocks have a steep, ENE-striking foliation parallel to Telkwa Pass (Figure 2.1 inset e). A few pyroxene- and plagioclase-

phyric basalt to andesite flows have primary volcanic textures. They contain 6% plagioclase and 8% pyroxene phenocrysts in a dark green fine-grained groundmass with chlorite and epidote alteration throughout. Andesitic lapilli tuff contains andesite fragments up to 5 cm in a light grey ash groundmass with 10% anhedral chlorite-altered mafic minerals. Glassy, pale purple, aphanitic dacite is exposed towards the western limit of volcanic rocks within the saddle. The upper and lower contacts of this unit have not been identified. A phyllic-altered lapilli tuff was collected for U-Pb zircon geochronology but yielded no zircons, so the volcanic package lacks an absolute age constraint.

Mafic volcanic rocks are also exposed along the western slope of the Howson Range south of Outcast Peak (Figure 2.1 inset f). At this locality they are intensely chlorite- and epidote-altered and locally exhibit a strong, shallowly southeast-dipping foliation. The volcanic rocks include very fine-grained, aphyric to sparsely plagioclase- and hornblende-phyric, dark green basalt and andesitic lapilli tuff. Lapilli tuff contains up to 15% subangular lapilli of white, plagioclase- and hornblende-phyric rhyolite as well as dark green, fine-grained andesite in an ash groundmass with 1% hornblende crystal fragments and 5% plagioclase crystal fragments. A fine-grained, dark green-grey basalt flow contains 5% each of plagioclase and hornblende as phenocrysts up to 1 mm in an intensely chlorite- and sericite-altered groundmass overprinted by epidote. This basalt flow is unconformably overlain by conglomerate at the base of the Telkwa Formation.

The mafic volcanic rocks at Limonite Creek and south of Outcast Peak are interpreted to belong to the Mount Attree volcanics based on their pre-Late Triassic age and lithological similarity to the Mount Attree volcanics further west, towards Terrace.

Ambition Formation

The Ambition Formation was defined by Gunning et al. (1994) to refer to Permian limestone in northwestern Stikine terrane. It has been identified in the western Search area, extending from the lower Zymoetz River valley to the lower Chist Creek valley (Nelson et al., 2006; Nelson et al., 2008a; Nelson et al., 2008b). Limestone has not been recognized between the Mount Attree volcanics and the Hazelton Group in the Howson Range (Figure 2.1).

Stuhini Group

The Stuhini Group is represented in the western Skeena arch by thin bedded argillite, siltstone and chert that is exposed in the lower Zymoetz River valley (Nelson et al., 2006; Nelson et al., 2008a). This is in contrast to the Stikine terrane north of the Bowser Basin where the Stuhini Group includes thick pyroxene-phyric basalt flows and associated volcaniclastic rocks (Monger et al., 1991). The conspicuous lack of a volcanic component in the Stuhini Group has been recognized from the Skeena arch south to the Whitesail Lake and Nechako Plateau regions (Diakow et al., 1997; Nelson et al., 2006). Like the Ambition Formation, the fine-grained sedimentary rocks comprising the Stuhini Group in the western Skeena arch were not recognized between the Mount Attree volcanics and the Telkwa Formation during this study.

Hazelton Group

Telkwa Formation

The Telkwa Formation is extensively exposed across the western Skeena arch (Figure 2.1). It was first named by Tipper and Richards (1976) who subdivided it into the western Howson subaerial facies, the central subaerial to shallow marine Babine shelf facies, and the eastern Kotsine submarine facies at the latitude of the Skeena arch. Subsequent, more detailed work has identified considerable lateral and vertical variation leading to a somewhat more complex subdivision of the Telkwa Formation (MacIntyre et al., 1989a; Desjardins et al., 1990a; Nelson et al., 2008a; Barresi et al., 2015b). It is now recognized to include an uppermost Triassic to lowermost Jurassic lower component and a Lower Jurassic upper component in the western Skeena arch. The lower Telkwa Formation is exposed in the southwestern part of the Search area south of Kleanza Creek and in the Howson Range. It consists mainly of massive andesite to basalt flows and breccia deposits. Extensive exposures south of Kleanza Creek that are interpreted to represent a volcanic centre referred to as the Mount Henderson complex (Barresi et al., 2015b).

North of Kleanza Creek, the upper Telkwa Formation is a thick, highly variable volcanic sequence of andesite with lesser dacite, rhyolite and basalt, the Mount O'Brien volcanic complex (Barresi et al., 2015b). Farther east, in the current study area, the upper Telkwa Formation comprises well-bedded andesite to dacite tuffs with minor basalt flows. Rhyolite occurs throughout the package as isolated lenses and flow domes, as well as rare, laterally extensive tuff beds. Sedimentary rocks including rare limestone are also interspersed throughout the volcanic package, becoming more common to the east. Telkwa Formation units are herein presented in approximate stratigraphic order from oldest to youngest, although lateral variations and inter-fingering of units occur throughout.

Basal Conglomerate

The base of the Telkwa Formation is a major unconformity with a locally developed basal conglomerate. In the western part of the Search area, between Chist Creek and the Zymoetz River, the basal conglomerate contains plutonic, volcanic and limestone fragments (Nelson et al., 2006). The basal conglomerate is exposed at one locality on the western slope of the Howson Range, south of Outcast Peak (Figure 2.1 inset f). It overlies dark green chlorite- and epidote- altered mafic volcanic rocks that are herein interpreted as Mount Attree volcanics (see above). The conglomerate contains subangular to well-

rounded cobbles of dark green chlorite- and epidote-altered mafic volcanic rocks, similar to the underlying Mount Attree volcanics, within a maroon to dark purple ash matrix (Figure 2.5a). The conglomerate is overlain by well-bedded maroon to dark purple volcaniclastic rocks and mafic flows of the lower Telkwa Formation.

Lower Telkwa Rhyolite

A lower Telkwa rhyolite unit is recognized west of the Howson Range. It includes local rhyolite centres at the base of the Telkwa Formation; one such centre returned a U-Pb zircon age of 204.29 ± 0.45 Ma (Barresi et al., 2015b). Rhyolite also occurs at the boundary between the lower and upper Telkwa Formation at Tatsi Creek. A characteristic pale purple plagioclase- and quartz-bearing crystal lithic tuff in the Tatsi Creek area has also been assigned to this lower Telkwa rhyolite unit (Figure 2.1 inset g). It occurs at the boundary between the lower and the upper Telkwa Formation in the Tatsi Creek area (Figure 2.1 inset g). The marker bed contains up to 35% plagioclase crystals and trace quartz crystals (both up to 3 mm), and maroon lapilli similar to the underlying andesitic tuffs, set in a pale grey to purple groundmass.

Lower Telkwa Andesite Flows

The Telkwa Formation south of the Zymoetz River and west of the Kitnayakwa River comprises mostly andesitic flows with rare thin intervals of rhyolite and tuffaceous sedimentary strata. The andesites are dark grey to purple to maroon and typically amygdaloidal. Most are plagioclase-phyric with typically 2–3 mm crystals and rare flows containing >1 cm crystals (Nelson and Kennedy, 2007). This thick accumulation of andesite flows may represent a major volcanic centre with volcaniclastic equivalents deposited distally (Barresi et al., 2015b).

Lower Telkwa Andesite Breccia

East of the Kitnayakwa River and north of the Zymoetz River the lower Telkwa Formation consists mostly of dark grey to purple to maroon andesitic volcaniclastic rocks (Figure 2.1). It includes massive monomict to polymict breccia dominated intervals north of the Zymoetz River and well-bedded predominantly

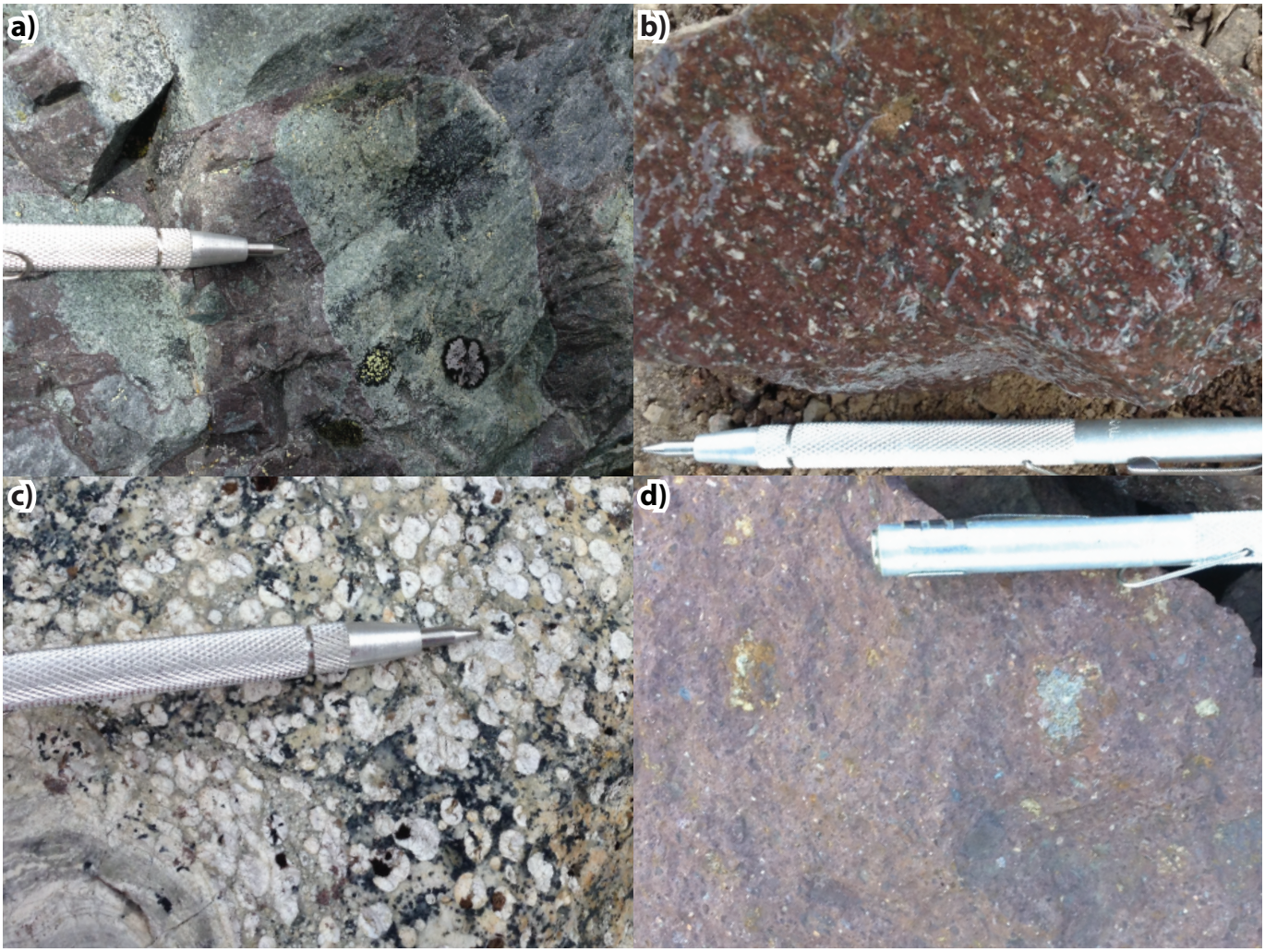

Figure 2.5: Characteristic rock types of the Telkwa Formation: (a) basal conglomerate; (b) plagioclase-phyric andesite; (c) spherulitic rhyolite; (d) upper Telkwa Formation dacitic tuff from the eastern end of Microwave ridge.

subaerial volcaniclastic rocks in the southern Howson Range, referred to as the Howson facies by Tipper and Richards (1976). The lower Telkwa andesite breccia is well exposed in the Tatsi and Outcast Peak areas (Figure 2.1 insets f and g). At Outcast Peak, it conformably overlies the basal conglomerate in a well-bedded, shallowly east-dipping panel with intervals of plagioclase crystal tuff, lapilli tuff, and minor dark green amygdaloidal basalt flows. Individual beds vary from 0.5 to 20 m thick. Basalt flows decrease in abundance up section. Minor dark grey siltstone and very fine-grained sandstone are interbedded with tuff, indicating partial subaqueous deposition. In the Tatsi Creek area, the base of the Telkwa Formation is not exposed. The stratigraphically lowest rocks are thick-bedded (up to 30 m) maroon andesitic lapilli tuffs. An ~300 m thick section of andesitic lapilli tuffs is conformably overlain by a light grey to purple crystal-lithic lapilli tuff marker bed assigned to the lower Telkwa rhyolite (see above).

A sample of plagioclase crystal tuff ~50 m stratigraphically above the basal contact of the Telkwa Formation on the southwestern slope of Outcast Peak was collected for U-Pb zircon geochronology (Figure 2.1 inset f). Sample 16JA110 has equant to slightly elongate subhedral zircons up to 100 µm with variably developed oscillatory zoning. Of 20 analyzed zircons, five are Mississippian and interpreted to be inherited from the underlying Mount Attree volcanics; nine are scattered between ca. 220 and 210 Ma and are interpreted to be inherited from the nearby Miligit suite. The remaining six analyses are overlapping and concordant, returning a weighted mean $^{206}Pb/^{238}U$ age of 204.0 ± 2.8 Ma (Figure 2.6; Table 2.1). This is the interpreted eruptive age of the tuff.

The lower Telkwa andesite breccia also occurs on Microwave Ridge west of the Stock MINFILE occurrence (093L 085) where it is conformably overlain by calcareous sedimentary rocks (Figure 2.1). Sample 16JA198 is from crystal lithic tuff immediately beneath the sedimentary rocks. It yielded slightly elongate, prismatic zircons up to 100 µm, with both sector and oscillatory zoning. Of 20 analyzed zircons, five slightly older zircons are interpreted to be inherited from the underlying Telkwa volcanic stratigraphy. The youngest 15 analyses are overlapping and concordant, returning a weighted mean $^{206}Pb/^{238}U$ age of 200.1 ± 1.2 Ma (Figure 2.6; Table 2.1).

Upper Telkwa Andesite Flows and Breccia

Volcanic rocks of the upper Telkwa Formation are also primarily andesitic composition. Upper Telkwa maroon to purple, plagioclase-phyric andesite flows and breccias occur in the detailed study areas north of Ventura Peak and near Cariboo Mountain (Figure 2.1 insets c and d). Plagioclase phenocrysts are ubiquitous, comprising 15 to 30% of the rock. Flow banding is locally represented by maroon and purple layering (Figure 2.5b).

Upper Telkwa Basalt

Basalt forms a relatively minor but distinctive component of the upper Telkwa Formation in the study area. It can be fine-grained and aphyric or pyroxene- and plagioclase-phyric (MacIntyre et al., 1989a; Desjardins et al., 1990a). Pyroxene and plagioclase-phyric basalt flows and volcaniclastic equivalents with an overall 100 m thickness underlie the western part of the Ventura Peak map area (Figure 2.1 inset c). The flows contain up to 15% euhedral pyroxene phenocrysts, typically 3–5 mm, but locally up to 20 mm, and 20% plagioclase phenocrysts to 1–3 mm, in a fine-grained, dark green groundmass. Relationships between this basalt unit and other Telkwa Formation units were not observed, but it is apparently stratigraphically below the east-dipping rhyolite tuff that transects the ridge to the east (Figure 2.1 inset c). Abundant float of euhedral pyroxene- and plagioclase-phyric basalt was recognized in the Tatsi Creek area amongst well-bedded dacitic tuff, but the source was not identified.

Upper Telkwa Rhyolite

On the north slope of Ventura Peak (Figure 2.1 inset c) rhyolite forms a coherent flow-dome complex near the CuLater prospect, as a series of flow-banded dikes on the western ridge and as breccia to lapilli tuff as much as 300 m thick along the NE-trending ridge of Ventura Peak (Figure 2.1 inset c). Where it is coherent, the rhyolite is fine-grained to aphanitic and beige to pale pink with 1 mm to 5 cm thick flow bands that are planar to contorted. Trace albite and quartz phenocrysts occur in a fine groundmass of quartz, feldspar and hematite. The breccia to lapilli tuff is massive to well bedded, with angular fragments mainly of rhyolite but including rare plagioclase-phyric andesite. Tuffs locally grade upwards to fine ash. Spherulites occur in coherent flows and rhyolite breccia where they reach 3 cm in diameter. A roughly 200 x 300 m area in the saddle is gossanous due to intense phyllic alteration, with between 2 and 10% finely disseminated pyrite and patches of pale green phengite. The rhyolite that makes up the southernmost northeast-trending ridge contains a different alteration assemblage of quartz and tourmaline prisms up to 5 mm long with minor epidote. Tourmaline crystals occur within spherulites, suggesting that they grew after devitrification of the rhyolite (Figure 2.5c). Rhyolite crosscuts and overlies maroon Telkwa Formation andesite and underlies red tuff of the Saddle Hill Formation. Samples of flow-banded rhyolite and rhyolitic lapilli tuff with conspicuous quartz crystal fragments were collected from two localities in the Ventura Peak area for U-Pb zircon geochronology, but neither yielded zircons.

On Cariboo Mountain, rhyolite also occurs as an intrusive dome and associated lapilli tuff. Rhyolitic lapilli tuff forms lenses within the Telkwa Formation andesite. The dome follows a north-striking fault with minimal displacement that crosscuts

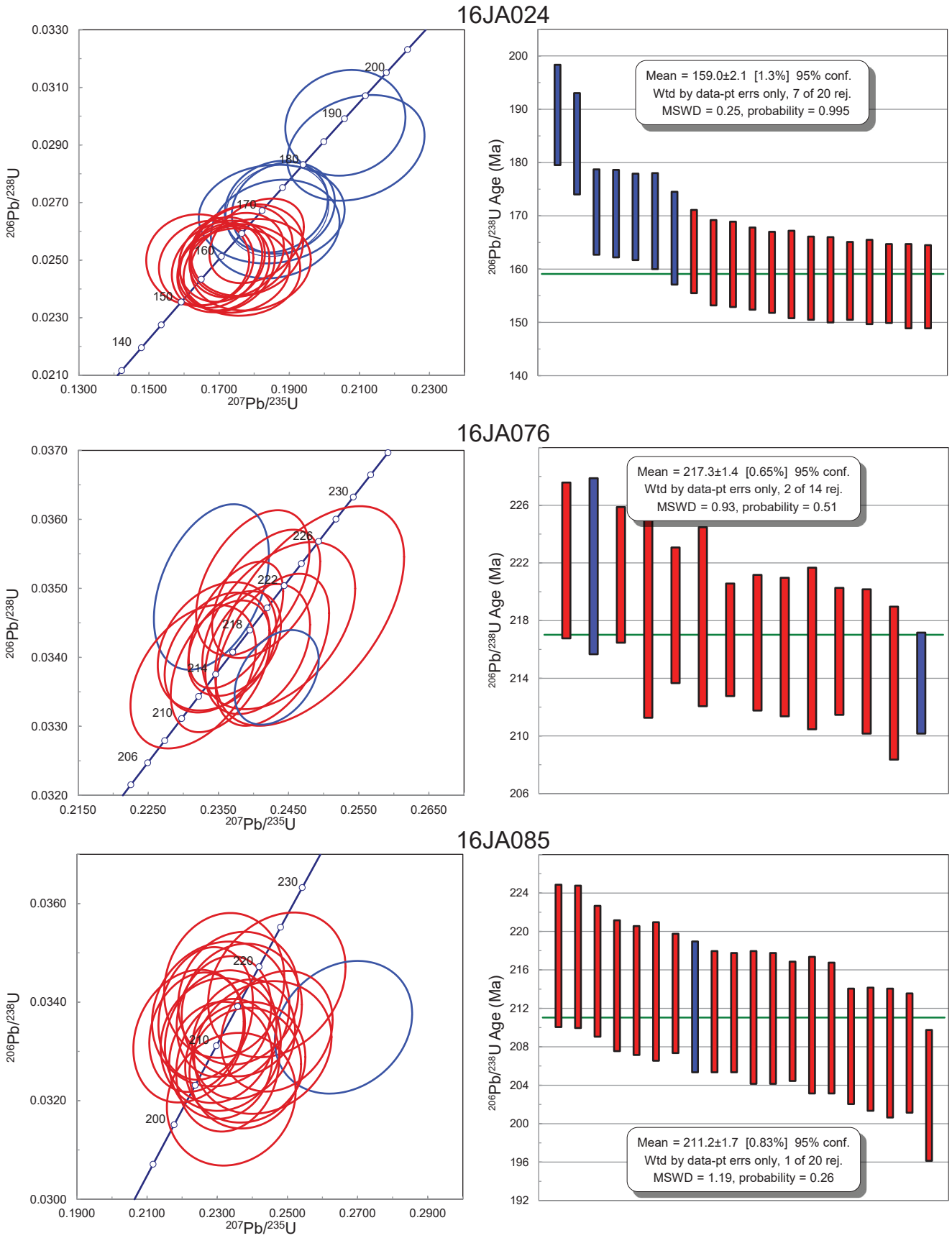

Figure 2.6: U-Pb standard Concordia and $^{206}Pb/^{238}U$ isochron plots for igneous zircon samples collected in 2016. Error ellipses and error bars are plotted at 2σ. Analyses plotted in red are included in the final age determination, analyses plotted in blue are not. MSWD = mean square weighted deviation. Methods and corresponding data provided in Appendix A.

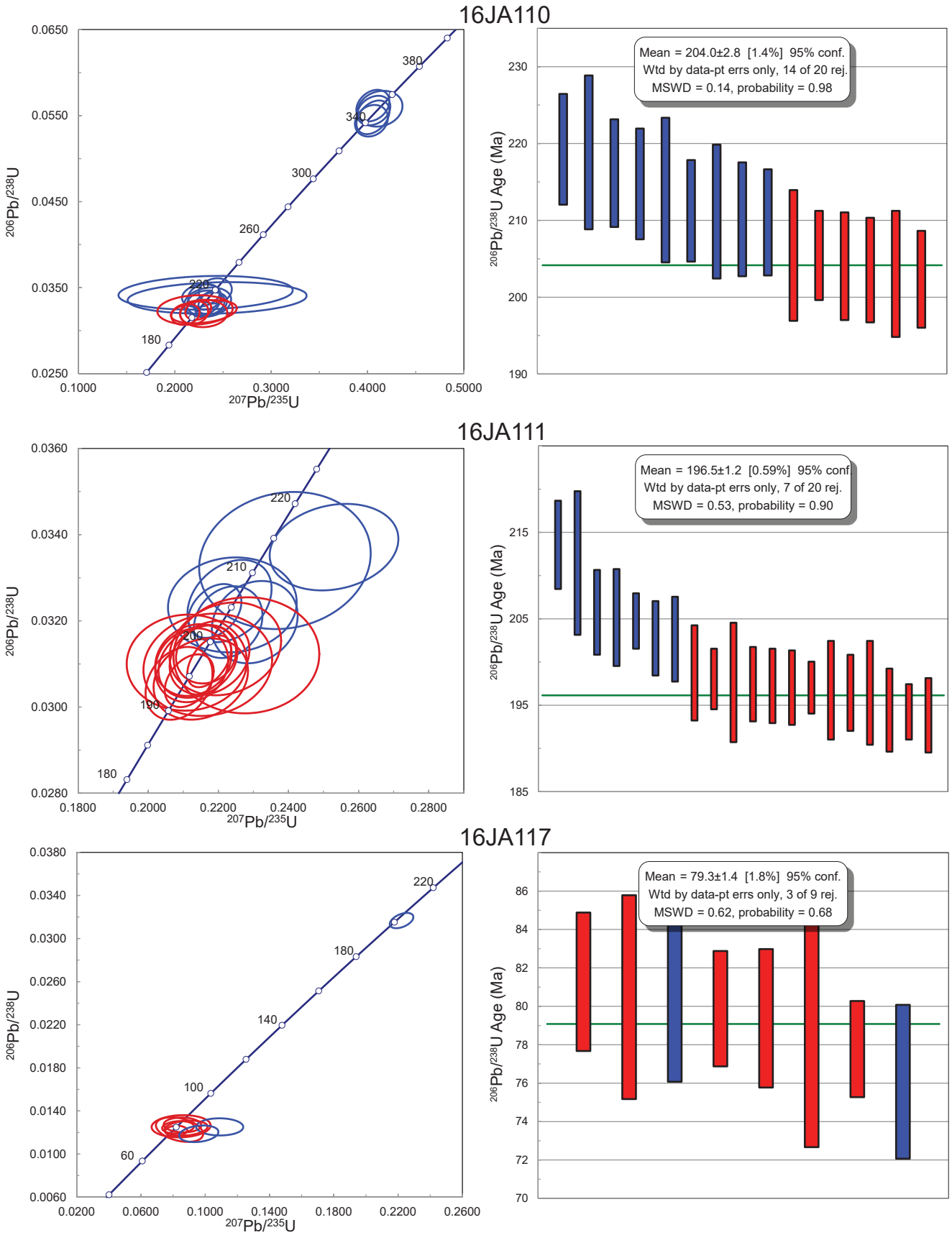

Figure 2.6 (continued)

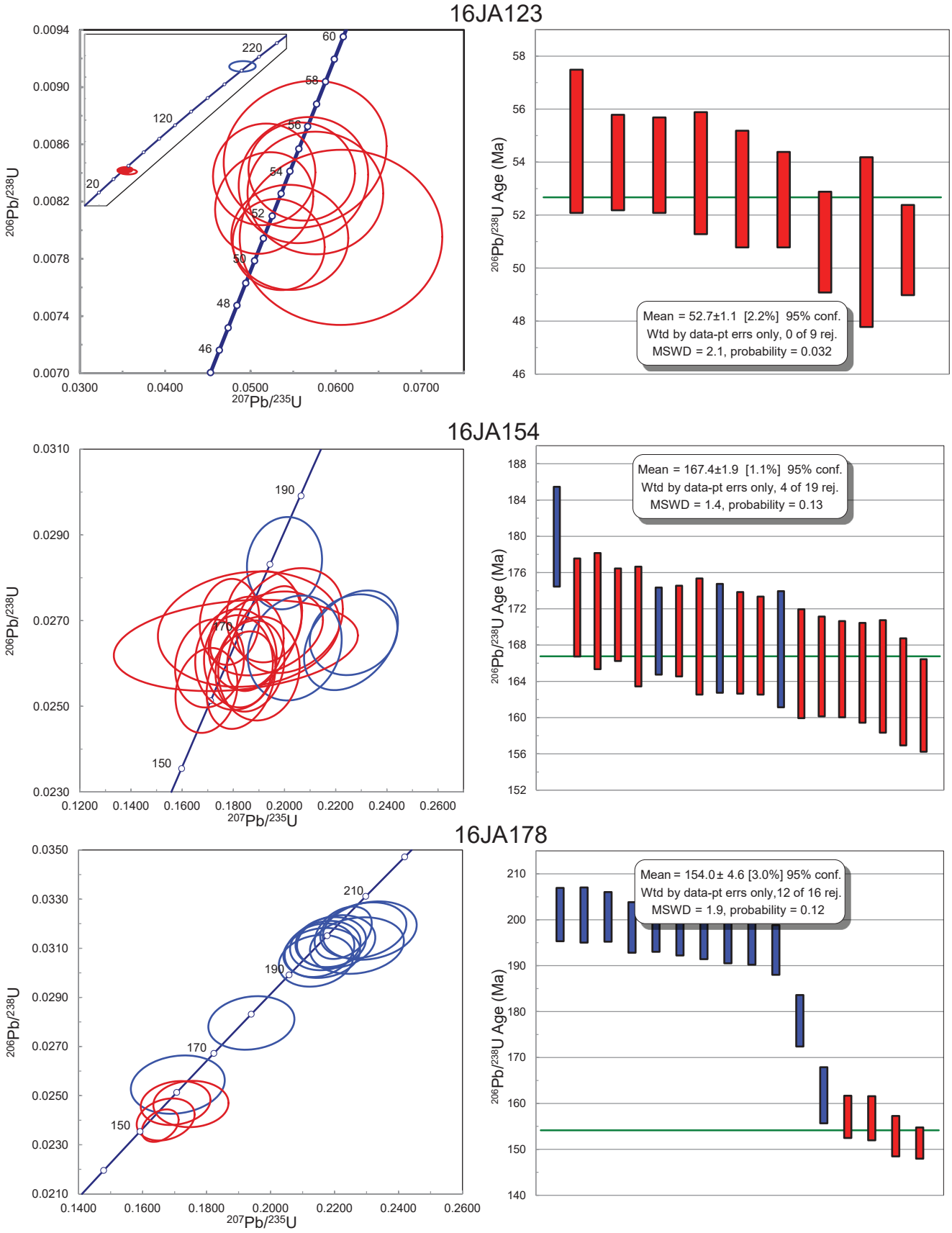

Figure 2.6 (continued)

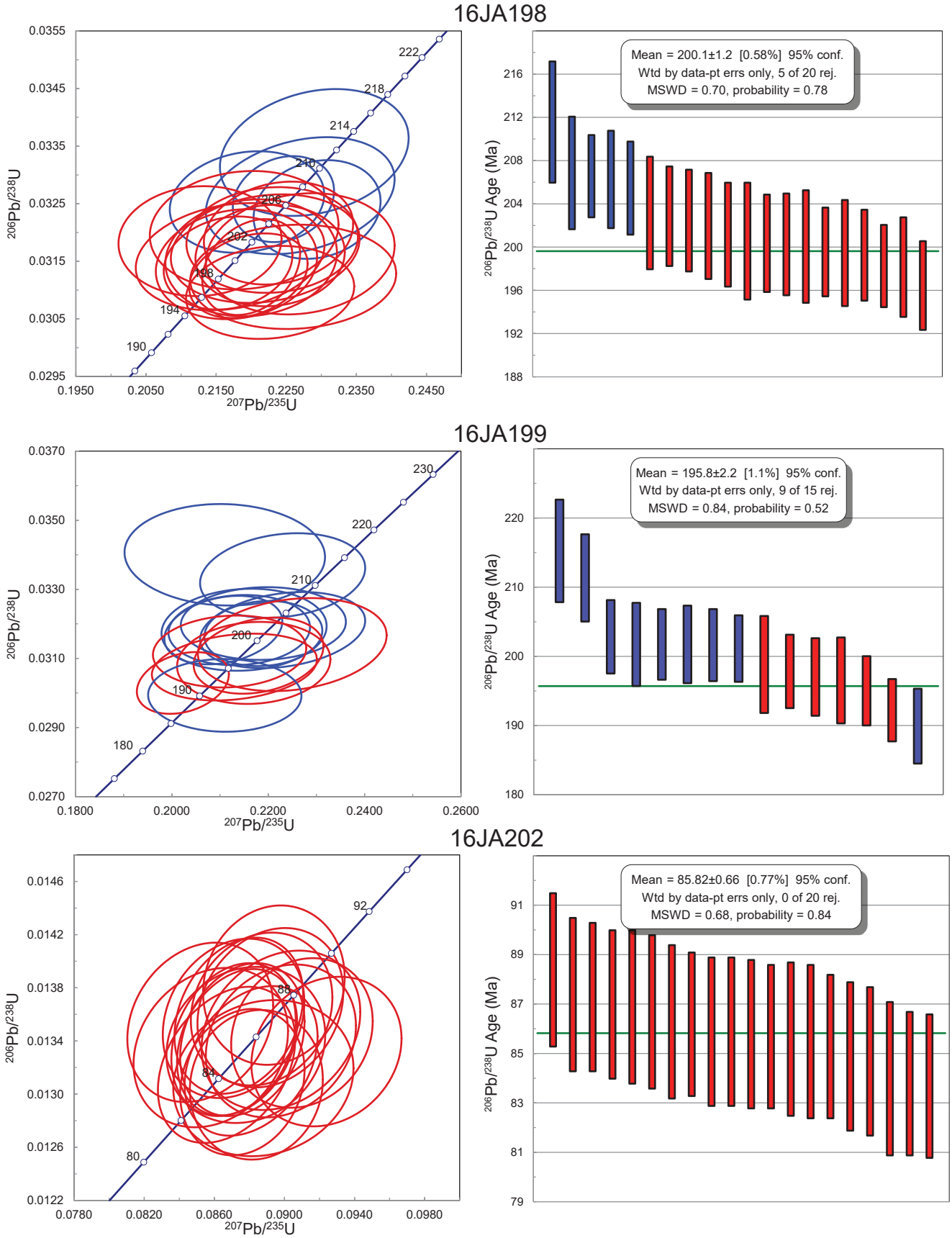

Figure 2.6 (continued)

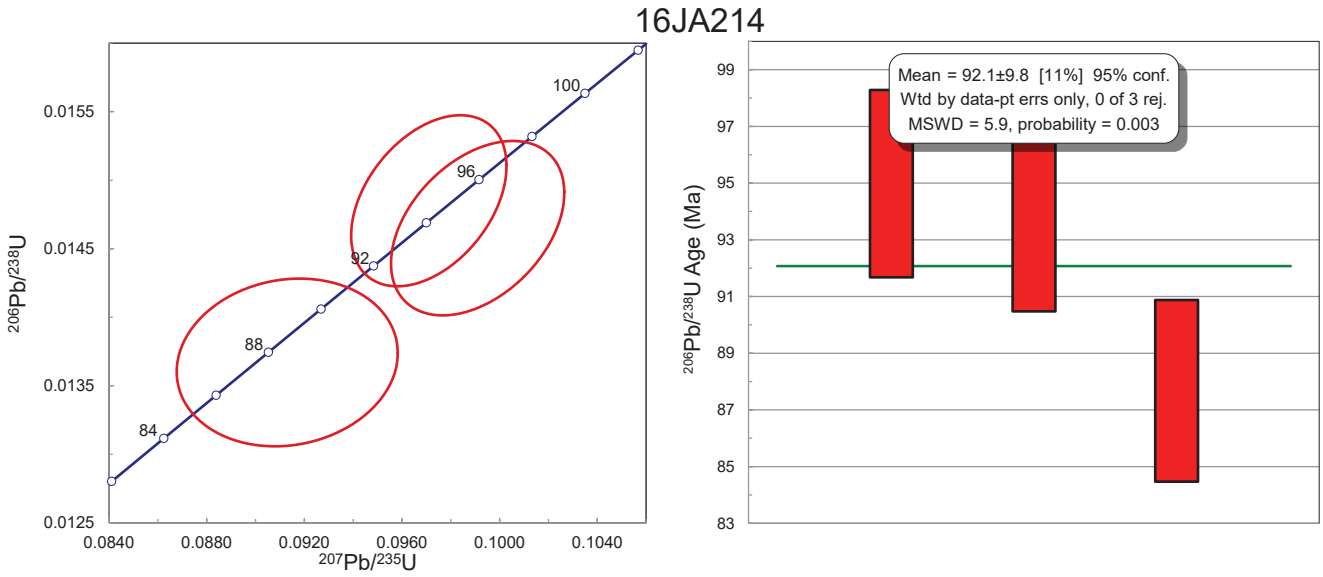

Figure 2.6 (continued)

Telkwa Formation andesite (Figure 2.1 inset d). The lapilli tuff is locally normally graded, indicating younging to the east.

Upper Telkwa Dacitic Tuff

Well-bedded maroon tuff makes up significant portions of the Telkwa Formation both north of Kleanza Creek and east of the Howson Range (Figure 2.1). This unit is interpreted to cap the Telkwa Formation throughout the Telkwa Range, where it locally includes fine-grained to plagioclase- and pyroxene-phyric basalt (MacIntyre et al., 1989a; Desjardins et al., 1990a). Dacitic tuff conformably overlies lower Telkwa andesite flows, breccia, and tuff in the southern Howson Range (Figure 2.1 insets f and g). At this locality it occurs as at least 200 m of well-bedded brick red dacitic lapilli, crystal and ash tuff crosscut by dikes and sills of Nanika plutonic suite granite. Individual tuff beds vary between 5 cm and 5 m thick.

Well-bedded, brick red tuff with minor rhyolite is exposed on the eastern half of Microwave Ridge, where it gradationally overlies calcareous sedimentary rocks. This sequence had been interpreted to belong to the Nilkitkwa Formation by (MacIntyre et al., 1989a) and reassigned to the Saddle Hill Formation by MacIntyre et al. (1994). A quartz-bearing tuff near the eastern limit of exposure along Microwave Ridge, ~1 km stratigraphically above the sedimentary horizon was collected for U-Pb zircon geochronology (Figure 2.5d. It yielded nearly equant prismatic zircons 50 to 100 µm with oscillatory and sector zoning. A cluster of analyses between 201 and 215 Ma are interpreted as inherited from the underlying older Telkwa Formation and possibly the Miligit plutonic suite. Six concordant, overlapping analyses returned a weighted mean $^{206}Pb/^{238}U$ age of 195.8 ± 2.2 Ma (Figure 2.6, Table 2.1). A single younger analysis was discarded as the analysed zircon appears metamict, suggesting possible Pb loss. This age confirms that the well-bedded brick red tuffs on Microwave Ridge are equivalent and belong to the upper Telkwa Formation dacitic tuff unit and not the Saddle Hill Formation.

Telkwa Formation Sedimentary Rocks

In addition to the basal conglomerate, the Telkwa Formation contains sporadic intercalated sedimentary rocks. A lens of volcanic-derived conglomerate, siltstone, calcareous tuff, and limestone that is too narrow to be represented at the current map scale bisects the Telkwa Formation on Microwave Ridge at the boundary between the lower Telkwa andesite breccia and the upper Telkwa dacitic tuff (Figure 2.1). Conglomerate beds contain well-rounded cobbles to boulders of volcanic rock units similar to the underlying lower Telkwa Formation in a coarse sand matrix (Figure 3b). Carbonate-rich sandstone and tuff beds weather recessively. Fine- to coarse-grained epiclastic sandstone defines planar beds, 5–10 cm thick, some of which fine upwards. This lens was previously assigned to the Nilkitkwa Formation (Pliensbachian to Toarcian)(MacIntyre et al., 1989a). It is bracketed between U-Pb zircon sample 16JA198 in the lower Telkwa andesite breccia unit and 16JA199 in the upper Telkwa dacitic tuff unit, confirming that it forms part of a continuous, conformable, east-dipping homocline of predominantly Hettangian red tuffs. It is therefore reassigned as a sedimentary inlier of the Telkwa Formation and not part of the Nilkitkwa Formation.

Nilkitkwa Formation

The Nilkitkwa Formation is a Lower Jurassic, predominantly fine-grained, marine sedimentary sequence that conformably to unconformably overlies the Telkwa Formation near Morice

Table 2.1: Results of new U-Pb zircon geochronology.

Sample	UTM East	UTM North	UTM Zone	Unit	Rock Description	Age (Ma)	Error (Ma)	Age Note
16JA024	567914	6083101	9	Quock Formation	Dark grey shale with rhyolitic and massive sulfide fragments	159.0	2.1	Age is weighted mean $^{206}Pb/^{238}U$ isochron of 14 youngest, overlapping concordant analyses. Older zircons interpreted as inherited from underlying tuffaceous Smithers Formation as detrital grains. There are no distinguishing characteristics of either zircon population in CL images or chemistry.
16JA076	578054	6047125	9	Miligit suite	Quartz diorite	217.3	1.4	Age is weighted mean $^{206}Pb/^{238}U$ isochron of 12 concordant overlapping analyses. Two zircons rejected for discordance. All zircons are small with low luminescence in CL images. Some have high luminescence rims but not large enough to analyze. There are no identified distinctions that could indicate multiple populations in CL images or geochemistry.
16JA085	575919	6045815	9	Miligit suite	Biotite hornblende granodiorite	211.2	1.7	Age is weighted mean $^{206}Pb/^{238}U$ isochron of 19 concordant and nearly overlapping analyses. One zircon rejected for discordance. All zircons are prismatic with well-developed oscillatory zoning. There is no apparent indication of damage that might suggest Pb loss in CL image of the youngest analysis. There are no distinct populations identified based on geochemistry.
16JA110	578828	6034104	9	Telkwa Formation	Plagioclase crystal tuff	204.0	2.8	Age is weighted mean $^{206}Pb/^{238}U$ isochron of six youngest, overlapping concordant analyses. There are five Mississippian zircons as well as nine older Triassic zircons which have been rejected as probable inherited/detrital. Detrital zircons are expected in a crystal tuff. The three populations do not represent clearly distinct, internally consistent characteristics in CL images. Some of the Mississippian grains have more pronounced oscillatory zoning (black and white vs grey) while some older Triassic grains appear abraded. There are no geochemically distinct populations.
16JA111A	578697	6033703	9	Kleanza suite	Hornblende granodiorite	196.5	1.2	Age is weighted mean $^{206}Pb/^{238}U$ isochron of the 13 youngest, overlapping concordant analyses. Seven slightly older zircons interpreted to represent antecrysts or xenocrysts were rejected. There are no distinct populations detected via CL or geochemistry.
16JA117B	582700	6022019	9	Bulkley suite	Biotite hornblende granodiorite	79.3	1.4	Age is weighted mean $^{206}Pb/^{238}U$ isochron of the 6 youngest, overlapping concordant analyses. Two discordant analyses are rejected as is one ~200 Ma xenocryst. The xenocryst is much larger with better developed oscillatory zoning than all other grains. There are no distinct geochemical signatures detected for different populations.
16JA123	582357	6023353	9	Nanika suite	Plagioclase biotite hornblende porphyritic granodiorite	52.7	1.1	Age is weighted mean $^{206}Pb/^{238}U$ isochron of 9 concordant overlapping analyses. One ~200 Ma zircon is rejected (probable xenocryst). All zircons have well developed oscillatory zoning and prismatic habit. The ~200 Ma zircon has no distinct geochemical characteristics when compared to the Eocene population.
16JA154	558773	6079991	9	???	Biotite hornblende microdiorite	167.4	1.9	Age is weighted mean $^{206}Pb/^{238}U$ isochron of 15 concordant and nearly overlapping analyses. One ~180 Ma possible xenocryst is rejected as well as three discordant analyses. There are no distinct populations detected in geochemistry. The reported age for this sample is older than the Bowser Lake Group rocks that it crosscuts. It is possible that all of the zircons in this sample are inherited and do not reflect the crystallization age. Many zircons appear abraded or resorbed in CL images.
16JA176	556093	6079497	9	Trout Creek assemblage	Silty sandstone interbedded with polymict conglomerate	149.7	4.1	Reported age is the $^{206}Pb/^{238}U$ age of the youngest detrital zircon. This is a maximum depositional age for this sedimentary unit. Unimodal distribution with peak at ~155 Ma and range of 150 Ma to 164 Ma.
16JA178	571625	6084300	9	Netalzul volcanics	Andesitic lapilli to block tuff	154.0	4.6	Age is weighted mean $^{206}Pb/^{238}U$ isochron of four youngest, concordant overlapping analyses. The four included zircons form a distinct population with well-developed oscillatory zoning, good prismatic shape, and low U/Th ratios. One slightly older zircon (~162Ma) has very poorly developed oscillatory zoning, blocky shape, and very high U/Th in common with a single older zircon. The remaining zircons have typically poorly developed oscillatory zoning, sometimes with an apparent rim too small to analyze, and low U/Th ratios.
16JA198	599034	6063558	9	Telkwa Formation	Andesitic lapilli tuff	200.1	1.2	Age is weighted mean $^{206}Pb/^{238}U$ isochron of 15 concordant and overlapping analyses. Five slightly older zircons are interpreted as detrital/reworked grains incorporated from the underlying Telkwa. Zircons are typically prismatic with sector zoning well-developed in most regardless of age. There are no distinct populations based on CL images or chemistry.
16JA199	601292	6061399	9	Telkwa Formation	Andesitic ash tuff	195.8	2.2	Age is weighted mean $^{206}Pb/^{238}U$ isochron of six concordant overlapping analyses. The youngest grain is discarded as it appears metamict in CL suggesting possible Pb loss. The 201–215 Ma zircons are interpreted as inherited from the underlying Telkwa Formation and possibly Triassic Miligit suite intrusions. There are no distinct characteristics of these populations based on geochemistry or CL images.
16JA202	583103	6079701	9	Bulkley suite	Plagioclase hornblende porphyritic quartz monzonite	85.8	0.7	Age is weighted mean $^{206}Pb/^{238}U$ isochron of all 20 analyses which are concordant and overlapping. All zircons exhibit well-developed oscillatory zoning and are typically doubly terminated euhedral prisms up to 200 µm long.
16JA214	577223	6078047	9	Bulkley suite	Plagioclase hornblende quartz porphyritic diorite	92.1	9.8	Age is weighted mean $^{206}Pb/^{238}U$ isochron of only three recovered zircons from this sample. The older two are both slender prisms with sector zoning. The one younger zircon is a stubbier prismatic grain with oscillatory zoning (suspiciously similar to zircons from 16JA202). It is considered only an approximate age. The sampled dyke could not have inherited zircons of that age from the immediate country rock.

Lake and east-northeast of Smithers (Tipper and Richards, 1976). As originally defined, it included locally abundant volcanic rocks that have subsequently been separated out as the Saddle Hill Formation (MacIntyre et al., 2001). A few exposures of sedimentary rocks overlying the Telkwa Formation in and northeast of the Telkwa Range have been assigned to the Nilkitkwa Formation (MacIntyre et al., 1989a; MacIntyre et al., 1989b; see Figure 2.1). From Hudson Bay Mountain to Quinlan Mountain, the Nilkitkwa Formation appears to be missing, with the Saddle Hill Formation resting directly on the upper Telkwa Formation (Figure 2.1). Investigation of a locality previously mapped as Nilkitkwa Formation sedimentary rocks in the Microwave Ridge area confirmed that it is a sedimentary lens within the Telkwa Formation. Further investigation may indicate that other Nilkitkwa Formation occurrences should be reassigned to the Telkwa Formation as well.

Saddle Hill Formation

The Saddle Hill Formation was introduced by Richards (1990) and formally defined by MacIntyre et al. (2001) to refer to a section, up to 1 km thick, of andesitic to rhyolitic volcanic rocks that are stratigraphically between the Nilkitkwa Formation and the Smithers Formation in the Babine Lake area. These rocks had previously been referred to as the Red Tuff Member of the Nilkitkwa Formation (Tipper and Richards, 1976). Equivalent strata in the western Skeena Arch was referred to as the Eagle Peaks Formation (MacIntyre et al., 1994); however, that name was never formalized. Evenchick et al. (2008) adopted the term Saddle Hill Formation for the former Red Tuff Member at Ashman Ridge and Hudson's Bay Mountain. The Saddle Hill Formation is difficult to distinguish from the tuff and basalt unit of the upper Telkwa Formation. This is made even more difficult with the lack of Nilkitkwa Formation sedimentary rocks as a marker horizon between the two. Two regions were identified during the current study that can be confidently correlated with the Saddle Hill Formation: the northern limit of the Howson Range and the east slope of Cariboo Mountain.

The Saddle Hill Formation (formerly Red Tuff Member) was recognized by Richards and Tipper (1976) along a northeast trending ridge at the very northern limit of the Howson Range (Figure 2.1 inset c) . It occurs as a series of well-bedded, shallowly northwest-dipping, brick red ash, lapilli and block tuffs typically between 0.5 and 5 m thick with minor interbedded aphanitic black basalt. The Saddle Hill Formation paraconformably overlies maroon andesite to dacite of the Telkwa Formation. Lapilli are heterolithic, including pale grey to green aphanitic rhyolite, maroon and dark grey plagioclase- phyric and aphanitic andesite, vesicular black basalt, microdiorite and limestone. All are in a fine-grained, red to pink, ash groundmass with up to 10% of 1–2mm plagioclase fragments. Recessive weathering of limestone lapilli and surrounding tuff yields 5 to 30 cm pits in outcrop surfaces (Figure 2.7a). Some fragments record prior alteration: rhyolitic lapilli are pale green due to phengite (Figure 2.7b), many andesite fragments are epidote-altered, and one fragment contains a quartz-calcite vein that terminates at its margins. A sample from a similar limestone clast-bearing 'holey tuff' ~5 km southeast of Quinlan Mountain yielded a U-Pb zircon age of 178.90 ± 0.28 Ma (Barresi et al., 2015b). A northeast-trending dike swarm crosscuts the Telkwa Formation approximately 1.5 km southeast of the exposed Saddle Hill Formation (Figure 2.1 inset c). These dikes are interpreted as local feeders to the Saddle Hill Formation. They are dark grey and maroon, aphanitic, and amygdaloidal with irregular chilled margins. Vesicles are filled with quartz and calcite.

The Saddle Hill Formation is also exposed on the eastern slope of Cariboo Mountain, where it dips shallowly to the east (Figure 2.1 inset d). The characteristic 'holey tuff' observed to the west was not identified here but it is otherwise the same as documented in the northern Howson Range, with rare aphanitic vesicular basalt and well-bedded brick red ash to lapilli tuffs. As at other localities, it paraconformably overlies maroon andesite and cream coloured rhyolite of the Telkwa Formation.

Smithers Formation

The Smithers Formation comprises Lower to Middle Jurassic fossiliferous and tuffaceous sandstone and siltstone (Tipper and Richards, 1976; Gagnon et al., 2012). Gagnon et al. (2012) assigned the Quinlan Mountain section as the formal type section of the Smithers Formation, where it unconformably overlies red tuff of the Saddle Hill Formation. The Smithers Formation occurs on the western slope of Paleo Peak (Figure 2.1 inset b). At this locality, the Smithers Formation consists of brown weathering, light grey tuffaceous sandstone and dark grey tuffaceous siltstone with calcareous cement. Beds are 1cm to 3m thick with common trough cross stratification. Rare lenses of volcanic granule conglomerate occur throughout. Beds rich in fossil casts are common and primary sedimentary structures are heavily modified by bioturbation (Figure 2.7c). Recovered fossils include: *Astarte (Coelastarte) livingstonensis; Myophorella sp.; Trigonia sp.; Mytilus sp.* (middle to upper Bajocian, 19JA013); *Cobbanites talkeetnanus,* var. *dansicostata; Trigonia sp.; Pholadomya sp.* (upper Bajocian to lower Callovian, 16JA017), and *Myophorella (Scaphogonia) sp.; Trigoniida; Iotrigonia sp.* (upper Bajocian to Oxfordian, 16JA021) (Fossil identifications by B. Najafian). The sequence is at least 300 m thick but may be thicker, as its lower contact was not identified. At Ashman Ridge to the southeast, it is reported to disconformably overlie the Saddle Hill Formation (Gagnon et al., 2012). It is conformably overlain by black shale, siltstone and tuff of the Quock Formation on the western slope of Paleo Peak.

Quock Formation

The Quock Formation is a Middle Jurassic to lowest Upper Jurassic sequence of typically thin-bedded siliceous mudstone

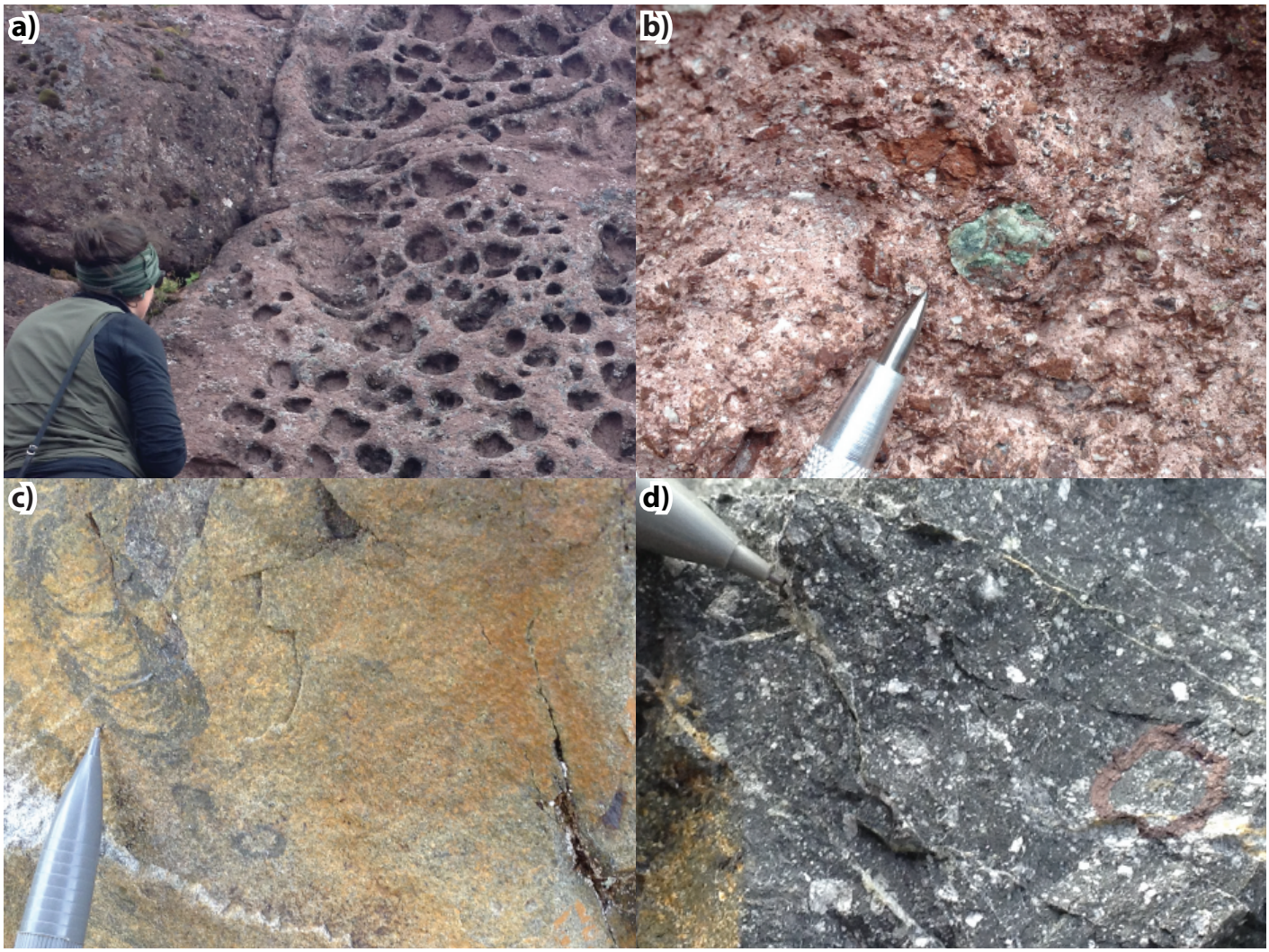

Figure 2.7: Characteristics of upper Hazelton Group rock types: (a) characteristic weathering pattern of limestone-fragment-bearing Saddle Hill Formation; (b) green phengite-altered rhyolite fragment in the Saddle Hill Formation; (c) Zoophycos(?) ichnofossil in sandstone of the Smithers Formation; (d) volcanic and massive sulfide fragments in Quock Formation mudstone.

and tuff (Thomson et al., 1986; Gagnon et al., 2012). It is exposed on the periphery of the Bowser basin and reflects a relatively low-energy marine environment that spanned much of the central Stikine terrane. Three distinct lithofacies of the Quock Formation occur on Paleo Peak (Figure 2.1 inset b). Rhyolitic lapilli breccia on the northwest ridge is made up of angular lapilli of aphanitic to plagioclase-phyric, white and pale pink rhyolite and minor, dark grey, plagioclase-phyric andesite. Lapilli are set in a fine siliceous groundmass with 5% plagioclase and 2% quartz crystal fragments. Both the fragments and the groundmass contain up to 10% finely disseminated pyrite. The exposure is crosscut by rhyolitic and basaltic dikes. The lapilli breccia grades laterally into more typical black shale interbedded with tuffaceous siltstone exposed in the western cirque of Paleo Peak. A 10-cm thick tuff bed is normally graded, indicating right way up. The shale contains up to 10% feldspar crystal fragments, aphanitic cream coloured rhyolite fragments, and fragments of massive pyrite up to 5 mm across (Figure 2.7d). Plant fossils recovered from this unit were identified as *Neocalamites* of possible Upper Jurassic age (Fossil identifications at MDRU by B. Najafian). The Quock Formation continues onto the southwest slope of Paleo Peak, where consists of ~100 m of well-bedded black shale with rare tuffaceous beds and common bivalve and belemnite casts. A fault separates this northeast-dipping panel from Ashman Ridge, where the Quock Formation is exposed within a northwest dipping panel as "…220 m of thinly bedded blocky-weathering dark grey siliceous mudstone with recessive laminations and very thin (<3 cm) beds of pale orange-weathered ash tuff" (Gagnon et al., 2012).

A U-Pb zircon sample of *Neocalamite*-bearing, pyritic, black shale and tuff (16JA024) returned prismatic, slightly elongate zircons up to 300 µm with well-developed oscillatory zoning. Of 17 analyses, three are slightly older and interpreted to reflect inheritance from the underlying tuffaceous Smithers

Formation. The remaining 14 analyses yield a weighted mean $^{206}Pb/^{238}U$ age of 159.0 ± 2.1 Ma, confirming the Upper Jurassic age of the Quock Formation locally as well as the contained *Neocalamite* fossils. This is slightly younger than the Bathonian to Callovian (Middle Jurassic) age interpreted from macrofossil collections at Quinlan Mountain to the west and Ashman Ridge to the southeast. but supports the earliest Oxfordian upper age limit suggested (Gagnon et al., 2012).

Bowser Lake Group

The Bowser Lake Group refers to Jurassic to Cretaceous marine and non-marine sedimentary strata deposited into the Bowser basin. The Bowser Lake Group has been subdivided into eight lithofacies assemblages that interfinger with one another at a variety of scales (Evenchick and Thorkelson, 2005). They represent coeval depositional environments within the basin that migrated laterally with time.

Three lithofacies were recognized in the current study area by Evenchick et al. (2008). They are the Ritchie-Alger fan assemblage, the Muskaboo Creek shelf assemblage, and the Netalzul volcanics. We propose that the Trout Creek assemblage of Tipper and Richards (1976) be retained in this area to acknowledge the occurrence of Upper Jurassic and or Lower Cretaceous conglomerate-rich deltaic sedimentary rocks that are sufficiently different from the Muskaboo Creek shelf assemblage.

Muskaboo Creek assemblage

The Muskaboo Creek assemblage is consists mainly of planar-bedded, medium-grained sandstone with interbedded fine-grained sandstone, siltstone, and conglomerate (Evenchick and Thorkelson, 2005). It is well bedded in thin to thick beds, with abundant bioturbation and macrofossils.

The Muskaboo Creek assemblage has been documented at Ashman Ridge, where it gradationally overlies the Quock Formation, with the boundary placed at the uppermost discrete tuff horizon (Evenchick et al., 2010; Gagnon et al., 2012). The same relationship is exposed on the southwest and west slopes of Paleo Peak (Figure 2.1 inset b). Tuffaceous shale is overlain by well-bedded, fine- to coarse-sandstone, siltstone, and rare granule conglomerate. Clasts are typically 40% chert with 20% each of quartz, feldspar, and red to green volcanic rocks. Sandstone beds are 30 cm to 5 m thick, laterally continuous and grey to brown weathering (Figure 2.8a); the latter reflecting a calcareous cement. Bivalve coquinas occur throughout the section.

Undifferentiated Bowser Lake and Skeena Groups

Localities lacking a dominant Bowser Lake Group facies or where outcrop or observations are limited, are mapped as undifferentiated Bowser Lake Group. Where sedimentary rocks are exposed but cannot be confidently assigned to the Bowser Lake Group or Skeena Group, they are assigned to a mixed unit. For instance, on the north slope of Zymo Ridge, fine-grained, orange-red-weathering sandstone, siltstone and shale gradationally overlie conglomerate of the Trout Creek assemblage. Sandstone and siltstone beds are 10 to 100 cm thick, laterally continuous, and lack sedimentary structures. Shale beds are rare, but can be over 4 m thick. Local bivalve and gastropod coquinas occur close to the base of the unit. This unit was assigned to the Laventie Formation of Bassett and Kleinspehn (1997) by Angen et al. (2017). As noted by Ferri et al. (2005) the distinction between the Laventie Formation and the Richie-Alger assemblage of the Bowser Lake Group is ambiguous in this region.

Netalzul Volcanics

Oxfordian (Upper Jurassic) volcanic rocks recognized along the southern and eastern margins of the Bowser Basin are referred to as the Netalzul volcanics (Tipper and Richards, 1976). They are of andesitic to basaltic composition and include flows, breccia and tuff with minor intercalated sandstone, conglomerate and coal (Tipper and Richards, 1976). The Netalzul volcanics are well exposed on Paleo Peak, on the north slope of Ashman Ridge, and the northeast ridge of Quinlan Mountain (Figure 2.1). On Ashman Ridge they conformably overlie the Muskaboo Creek assemblage and, in turn, are overlain by undifferentiated sedimentary rocks of the Bowser Lake Group (Evenchick et al., 2008).

On the northern slope of Paleo Peak, the most common lithology in the Netalzul volcanics is andesitic to basaltic block breccia to lapilli tuff. Fragments are dark green and maroon, angular to subrounded, plagioclase- ± hornblende-phyric andesite. Plagioclase is typically euhedral, 1 to 3 mm, and comprises up to 15% of the fragments and groundmass. Where present, hornblende is euhedral, up to 5 mm long and makes up to 3% of fragments. Trace anhedral quartz phenocrysts up to 2 mm occur in some fragments as well. The lower contact is gradational, with the abundance of plagioclase-phyric andesite fragments increasing up-section from the siliciclastic Muskaboo Creek assemblage into lapilli tuff of the Netalzul volcanics. The Netalzul volcanics form a resistant cap on the northwestern ridge of Paleo Peak. The basal contact is sharp and apparently erosional, cutting bedding planes within the underlying Muskaboo Creek assemblage (Figure 2.8a). This variability is attributed to local erosional channels scouring into the underlying unconsolidated sedimentary rocks and depositing coarse volcaniclastic material. The upper contact of the unit was not observed in this area.

On Zymo Ridge, the Netalzul volcanics overlie and are intercalated with Bowser Lake Group sedimentary rocks. Dark grey plagioclase-phyric flows, breccias and lapilli tuffs occur with pebbly sandstone, siltstone and shale. One shale bed

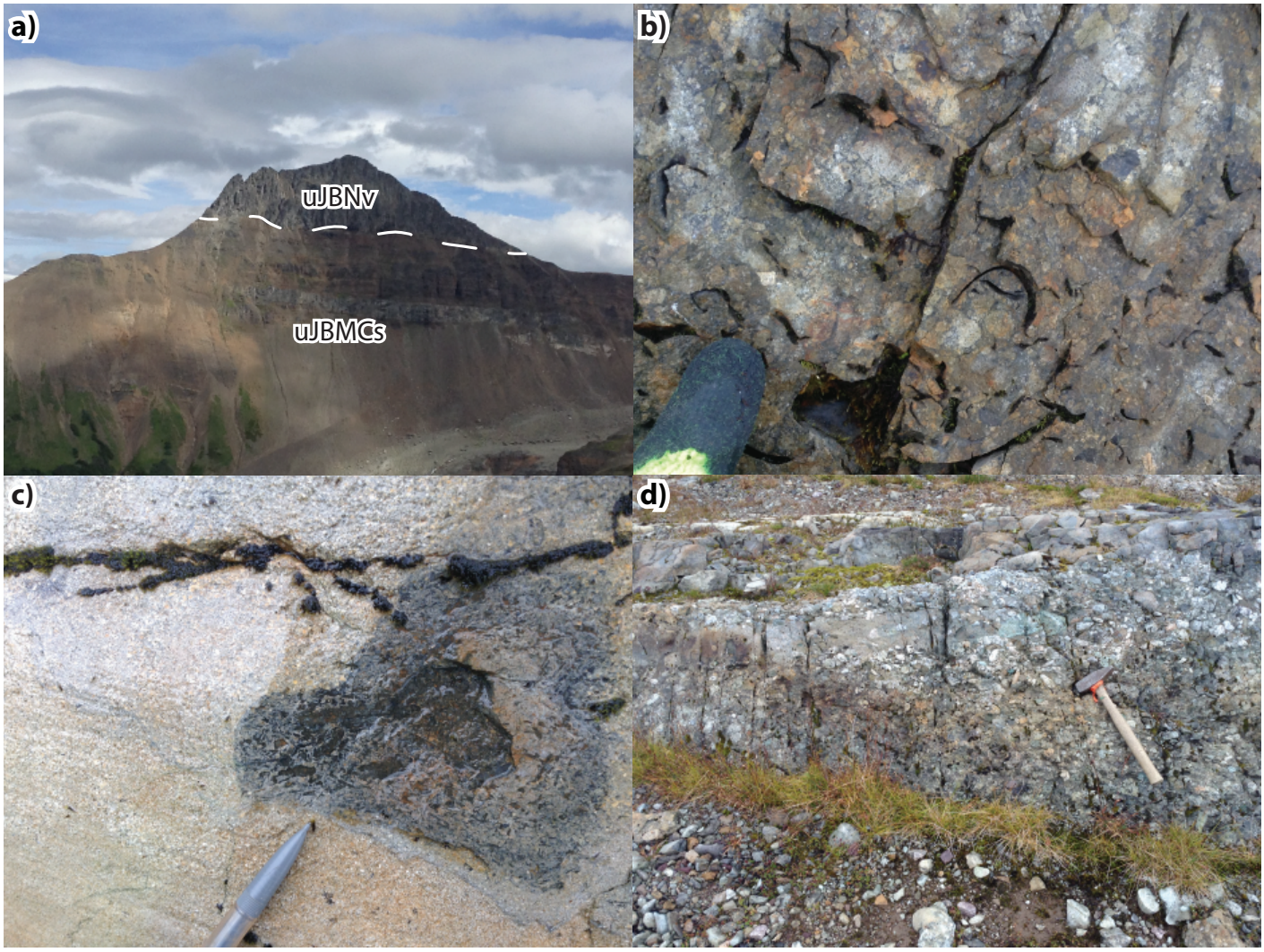

Figure 2.8: Photographs of the Bowser Lake Group: (a) Muskaboo Creek assemblage overlain by the Netalzul volcanics with an erosional boundary, western Paleo Peak. Photograph is looking to the north; (b) coquina in the Muskaboo Creek assemblage; (c) andesite lapilli breccia of the Netalzul volcanics with bivalve fragment; and (d) polymict conglomerate of the Trout Creek assemblage with notable sandstone lenses.

contains abundant bivalve fossil casts. Lapilli tuffs contain plagioclase-phyric andesite and lesser white, aphanitic rhyolite fragments. One lapilli breccia contains abundant bivalve and belemnite fossils; it is interpreted as a volcanic debris flow that incorporated an unconsolidated fossil bed (Figure 2.8b). Andesite flows have aphanitic chilled margins and peperitic textures along contacts with sandstone. Lenses of hyaloclastite occur within sandstone beds adjacent to andesite flows (Figure 2.8c).

An andesitic lapilli tuff on the north slope of Paleo Peak with trace quartz phenocrysts in fragments was evaluated for U-Pb zircon geochronology. This sample yielded texturally-variable zircons with some crystals with resorption pits. Twelve analyses were discarded as probable inherited grains based on their range of older ages similar to nearby volcanic units and the likelihood of lapilli tuff to incorporate foreign material. The four youngest concordant overlapping analyses returned a weighted mean $^{206}Pb/^{238}U$ age of 154.0 ± 4.6 Ma (Figure 2.6). This result supports the Oxfordian age for the Netalzul volcanics based on fossils collected from intercalated sedimentary strata outside of the Search area (Tipper and Richards, 1976).

Trout Creek Assemblage

The Trout Creek assemblage is an informal subdivision of the Bowser Lake Group identified by Tipper and Richards (1976). They defined it as polymict cobble conglomerate with volcanic, plutonic and sedimentary rock clasts interbedded with sandstone and siltstone that underlies, and in part interfingers with, the Netalzul volcanics. Regionally, the Trout Creek assemblage has been incorporated into the Muskaboo Creek shelf assemblage based on the presence of widespread marine sandstone and siltstone (Evenchick et al., 2008; Evenchick et al., 2010). We identify a conglomerate unit locally overlying the Netalzul volcanics that is sufficiently different

from the Muskaboo Creek assemblage to warrant distinction as a separate unit. We assign it to the Trout Creek assemblage because the nature and significance of this unit best corresponds to that originally described by Tipper and Richards (1976), with the exclusion of predominantly marine sandstone that is now assigned to the Muskaboo Creek assemblage. Trout Creek is an informal lithologic assemblage rather than a formation as mapped by Richards (1990) in the Hazelton area, because it apparently occurs under the Netalzul volcanics in that region whereas it overlies the same unit in the current study area. It represents uplift of the Skeena arch and exhumation of plutonic and volcanic rocks, with paleoflow indicators recording a source region to the south-southeast (Tipper and Richards, 1976).

Coarse conglomerate and sandstone occur in the saddle between Quinlan Mountain and Zymo Ridge and makes up most of Zymo Ridge (Figure 2.1 inset a). This conglomeratic unit was interpreted by Angen et al. (2017) to belong to the Bulkley Canyon Formation of the Skeena Group. New ages outlined below, and the acknowledgement that no earliest Cretaceous conglomerate is recognized in the Skeena Group by Bassett and Kleinspehn (1997), encourages a reinterpretation of this conglomerate-rich section as the Trout Creek assemblage of the Bowser Lake Group. This area was previously identified as Trout Creek assemblage by Woodsworth et al. (1985), who interpreted it to be a klippe separated from other Bowser Lake Group strata by a thrust fault. New observations suggest that it conformably overlies Netalzul volcanics and is conformably overlain by fine-grained sandstone to mudstone of either the Bowser Lake Group or Skeena Group (Figure 2.1 inset a).

The Trout Creek assemblage is ~200 m thick at this location and consists of approximately 60% cobble conglomerate interbedded with sandstone and siltstone. Beds of conglomerate, 5 to 30 m thick, contain subrounded to well-rounded clasts of volcanic, plutonic and sedimentary lithologies, including chert, in a coarse sand matrix. Cross-stratified arkosic beds occur throughout; brown-weathering recessive pods up to 2 m long in some sandstone beds reflect the presence of calcite cement. Plant debris is typical in finer-grained beds. Locally-imbricated clasts in conglomerate and cross-stratification in sandstone are consistent with paleoflow towards the northwest and northeast (Figure 2.8d). The lower contact is obscured but bedding is parallel to that in underlying Netalzul volcanics that interfinger with the Muskaboo Creek assemblage. A clastic dike that cuts the lowermost interbedded conglomerate and sandstone beds contains subangular to subrounded fragments of felsic volcanic rocks and chert, similar to the underlying Muskaboo Creek assemblage. The contact is therefore interpreted to be conformable.

Detrital zircons collected from a silty sandstone at the base of the Trout Creek assemblage returned a youngest (concordant) zircon age of 149.7 ± 4.1 Ma within a unimodal peak at ~155 Ma (Figure 2.9). The age of the Trout Creek assemblage at this locality is therefore as old as latest Late Jurassic. The unimodal peak corresponds to the age of the immediately underlying Netalzul volcanics, which must be the main source of detritus. The occurrence of plutonic and chert clasts within conglomerate suggests a much more heterogeneous source region for most of the Trout Creek assemblage and may record rapid uplift of the Skeena arch.

The Trout Creek assemblage is interpreted to be a delta facies, similar to the Eaglenest assemblage recognized in the northern Bowser basin by Evenchick and Thorkelson (2005). The predominance of cobble conglomerate, mixed marine and plant fossils, local clast imbrication and sand shadows are consistent with deltaic sedimentation, but could also represent a beach or shallow shelf. As noted by Tipper and Richards (1976), the presence of volcanic and plutonic clasts and paleocurrent indicators indicate flow to the northwest, and reflect uplift and erosion of the Hazelton Group and Triassic and Jurassic plutons in the Skeena arch.

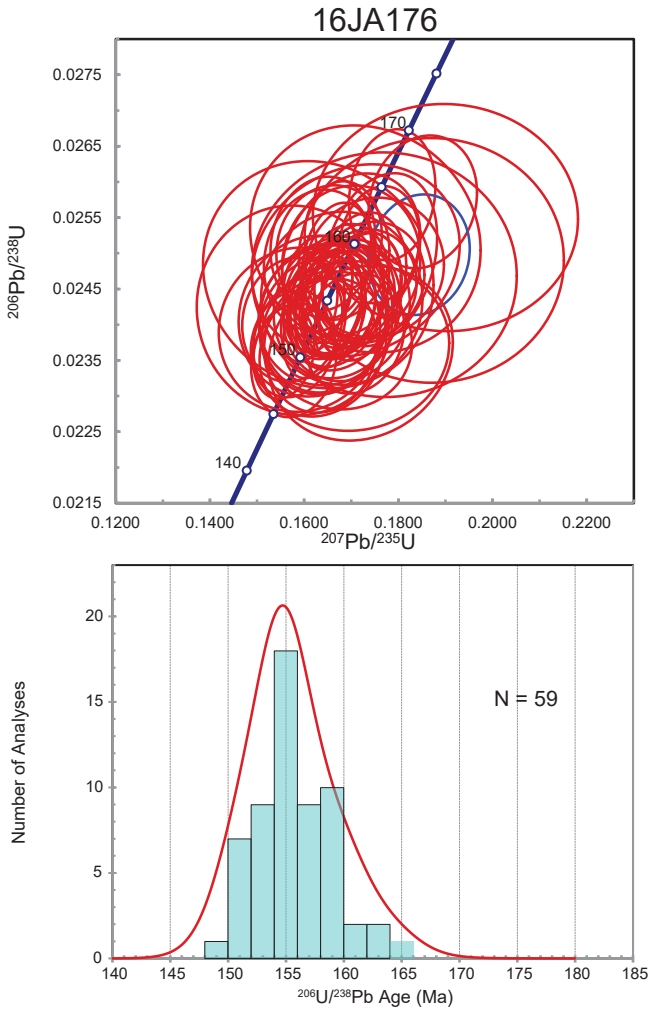

Figure 2.9: U-Pb plots for detrital zircon sample 16JA176: (a) standard Concordia, error ellipses are plotted at 2σ; (b) probability density plot of $^{206}Pb/^{238}U$ ages, red line reflects relative probability.

Skeena Group

The Skeena Group is a dominantly Lower, but locally Upper, Cretaceous sequence of marine to non-marine sedimentary rocks and locally significant accumulations of volcanic rocks (Bassett and Kleinspehn, 1997). It was first introduced by Duffell (1959) and was subsequently subdivided by Bassett and Kleinspehn (1997). The Skeena Group occurs in the Search study area in discontinuous exposures between Zymo Ridge in the northwest and Hudson Bay Mountain in the northeast, in the Telkwa Coalfields, and an isolated exposure east of the Clore River (Figure 2.1).

Bulkley Canyon Formation

Bassett and Kleinspehn (1997) introduced the Bulkley Canyon Formation to include marine to non-marine Lower Cretaceous clastic rocks of the Skeena Group. The Bulkley Canyon Formation is extensive in the Telkwa Coalfields and from Coal Creek north through Kitsuns Creek (Figure 2.1). In the Telkwa Coalfields area fine-grained sandstone, siltstone, coal, and minor conglomerate of Aptian to Albian age (Palsgrove and Bustin, 1991) rest unconformably on volcanic rocks of the Telkwa Formation. Similar coal-bearing strata occur in the vicinity of Coal Creek, southeast of Ashman Ridge (Figure 2.1). Bassett and Kleinspehn (1997) report palynological ages as old as Berriasian (ca. 144 Ma), which overlap in age with samples collected from the underlying Bowser Lake Group. A gradational lower contact has been identified within the Bowser basin, where Lower Cretaceous shallow marine strata of the Muskaboo Creek assemblage are overlain by fluvial strata of the Bulkley Canyon Formation (Smith and Mustard, 2005, 2006). The upper portion of the Bulkley Canyon Formation north of Coal Creek, referred to as the Kitsuns Creek Member (Bassett and Kleinspehn, 1997), contains more conglomerate, including detritus shed from the partly coeval Rocky Ridge Formation. Albian–early Cenomanian macrofaunal and pollen assemblages constrain the age of the Kitsuns Creek Member (Bassett and Kleinspehn, 1997).

The Bulkley Canyon Formation was only identified at one locality north of Paleo Peak (Figure 2.1 inset b). Here it occurs as granule to cobble conglomerate of the Kitsuns Creek Member. It contains subangular to subrounded fragments of plagioclase- and hornblende-phyric andesite, rhyolite, chert, sandstone, siltstone, feldspar, and quartz in a calcite-ankerite cement. Fresh surfaces are greenish-grey and weathered surfaces are red-orange. This exposure is at the base of a shallowly north-dipping package of Skeena Group. The contact between this north-dipping package and the east-dipping Muskaboo Creek assemblage farther south is not exposed; based on the contrasting bedding orientations it is either a major fault or an angular unconformity. The type section of the Kitsuns Creek Member is ~5 km ENE of this exposure, where it is also shallowly north-dipping but gradationally overlies finer-grained lower Bulkley Canyon Formation (Bassett and Kleinspehn, 1997). A conformable contact is reported farther north within the Bowser Basin (Smith and Mustard, 2005; Smith and Mustard 2006). Evidence for a conformable contact between the Bowser Lake and Skeena groups farther north and the lack of intervening finer-grained Bulkley Canyon Formation at this locality support a faulted contact.

Rocky Ridge Formation

The Rocky Ridge Formation is a Lower to Upper Cretaceous, subaerial to subaqueous, alkaline basalt to andesite within the Skeena Group (Richards, 1990). It is highly variable in thickness, ranging from <10 m to <1 km (Bassett and Kleinspehn, 1997). The Rocky Ridge Formation is made up of interbedded basalt flows and basaltic volcaniclastic rocks; flows contain ubiquitous 4–8 mm pyroxene phenocrysts, rare plagioclase and/or hornblende phenocrysts, and calcite and zeolite amygdules (Bassett and Kleinspehn, 1996). The Rocky Ridge Formation occurs at one locality southwest of Paleo Peak, where it is interpreted to overlie undifferentiated Skeena Group (Figure 2.1). It is separated from well-bedded Smithers Formation to the east by an inferred west-dipping normal fault. This locality was not revisited during the current study.

Plutonic Rocks

Mississippian to Permian(?) Delta Plutonic Suite

Mississippian plutonic rocks occur sporadically in the western Search area. They are exposed due east of Kitimat and along the Williams Creek valley (Figure 2.1) where they are typically strongly foliated diorite, granodiorite, tonalite, and gabbro (Nelson et al., 2008a). Two samples of foliated tonalite from the Williams Creek valley returned U-Pb zircon ages of 324.0 ± 0.8 Ma and 325 +9/-1 Ma (Nelson, 2017; Nelson and Friedman, 2017). The Delta River pluton east of Kitimat also returned a Mississippian U-Pb zircon age of ~331 Ma (van der Heyden, 1989) (Figure 2.1). These Mississippian intrusive rocks are herein referred to as the informal Delta plutonic suite. They are interpreted to be the plutonic equivalent of the coeval Mount Attree volcanics, which range in age from Mississippian to Early Permian.

Late Triassic Miligit Plutonic Suite

Late Triassic plutonic rocks are only recognized in the northern Howson Range, immediately north of Telkwa Pass (Figure 2.1). They are referred to herein as the Miligit plutonic suite. Two distinct phases are recognized: medium-grained, equigranular quartz diorite northeast of Limonite Creek, and porphyritic granodiorite southwest of Limonite Creek. The Late Triassic age of intrusions in this area was first identified by Deyell et al. (2000), who reported a U-Pb zircon ID-TIMS age of 212.0 ± 0.6 Ma. The location of this sample as plotted on Figure 2.1 (inset e), is based on a sketch map in Deyell et al. (2000).

Quartz Diorite Phase

Northeast of Limonite Creek, steep terrain is underlain by white, black and green quartz diorite to diorite of the Miligit plutonic suite (Figure 2.1 inset e). It is equigranular and mostly medium-grained, with subordinate coarse and fine-grained textures, consisting of 35–50% subhedral plagioclase, 2–20% quartz and 15–50% mafic minerals (hornblende >> pyroxene; Figure 2.10a). Fine-grained varieties occur as dikes that are equigranular or plagioclase- hornblende-phyric. Discontinuous ductile shear bands locally cut fine-grained Miligit suite dikes. Alteration within the pluton includes variable sericite alteration of plagioclase and replacement of mafic minerals by aggregates of epidote, magnetite and chlorite. The pluton is interpreted to intrude intensely altered mafic volcanic rocks tentatively assigned to the Mount Attree volcanics, which underlie the saddle at the headwaters of Limonite Creek. Red and dark green, well-bedded volcanic rocks assigned to the Telkwa Formation are exposed east of this quartz diorite pluton (Figure 2.1). The contact was not observed but is interpreted to be nonconformable.

A sample of quartz diorite was collected to confirm the age reported by Deyell et al. (2000). Sample 16JA076 yielded subhedral zircons that are all < 100 µm and exhibit sector zoning. Two analyses were rejected as discordant. The remaining 12 concordant analyses return a $^{206}Pb/^{238}U$ weighted mean age of 217.3 ± 1.4 Ma (Figure 2.6). This age confirms a Late Triassic age but is considerably older than the ID-TIMS age reported by Deyell et al. (2000), suggesting that there may be multiple phases of intrusions within the pluton. The occurrence of multiple cross-cutting textural phases supports such an interpretation.

Porphyritic Granodiorite Phase

Southwest of Limonite Creek, a more felsic, porphyritic granodiorite phase of the Miligit plutonic suite is exposed. It contains 15% plagioclase to 8 mm, 8% biotite to 3 mm, 2% hornblende to 4 mm, and trace magnetite to 2 mm in a light grey groundmass of quartz and K-feldspar (Figure 2.10b). It contains 3% microdiorite xenoliths. As with the more mafic phase, alteration includes sericitization of feldspars and chlorite and epidote alteration of mafic minerals.

A sample of this intrusion was collected for U-Pb zircon geochronology, to test if it is part of the texturally similar Eocene Nanika plutonic suite. Sample 16JA087 yielded prismatic zircons up to 150 µm long with well-developed oscillatory zoning. A single analysis was rejected for discordance; the remaining 19 analyses return a weighted mean $^{206}Pb/^{238}U$ age of 211.2 ± 1.7 Ma (Figure 2.6). The confirms that this felsic porphyritic intrusion is part of the Late Triassic Miligit plutonic suite. The contained mafic xenoliths could have been sourced from the somewhat older dioritic phase.

Early Jurassic Kleanza Plutonic Suite

The Kleanza plutonic suite refers to Early Jurassic heterogeneous plutonic rocks in the western Skeena arch. The Kleanza suite forms part of a northeast-trending batholith between Terrace and the Howson Range formerly called the Kleanza pluton (Figure 2.1). Gareau et al. (1997) reported an age of 200 +13/-3 Ma for coarse-grained biotite granite of the Kleanza suite ~2 km northeast of the mouth of the Zymoetz River (~2.5 km north of where the Zymoetz River intersect Search study area boundary). A 180.8 ± 2.6 Ma age was subsequently reported by Gehrels et al. (2009) in the headwaters of Kleanza Creek, indicating a protracted Early Jurassic magmatic history for the Kleanza pluton. An Early Jurassic intrusion near Hirsch Creek in the southern Search area is included with the Kleanza plutonic suite as well, based on a U-Pb zircon age of 198.9 ± 3.2 Ma (Gehrels et al., 2009).

Two plutons in the Howson Range south of Telkwa Pass are assigned to the Kleanza plutonic suite: a large (15 km wide) irregular pluton that underlies rugged topography in the Howson Range south of Telkwa Pass (Figure 2.1), and a small (~1 km wide), irregular stock of the Kleanza plutonic suite south of Outcast Peak (Figure 2.1 inset f). In this area, the Kleanza plutonic suite is equigranular, coarse-grained quartz monzodiorite to granodiorite with 35–50% euhedral plagioclase, 5–15% anhedral K-feldspar, 15–25% quartz, 10–15% hornblende, 3–5% biotite, and 1–3% magnetite; plagioclase crystals are euhedral and K-feldspar crystals are subhedral (Figure 2.10c). Two analyses of a sample of altered quartz diorite collected by H. Tipper approximately 1 km south of Top Lake returned K-Ar ages of 192.9 ± 8 Ma and 210.2 ± 9 Ma (Wanless et al., 1974; recalculated by Breitsprecher and Mortensen, 2004). The accuracy of these two ages are considered unreliable but they indicate a Late Triassic to Early Jurassic age for the Kleanza suite.

A sample of the Kleanza plutonic suite stock south of Outcast Peak was collected for U-Pb zircon geochronology based on the interpretation that it may belong to the Miligit suite and was responsible for the higher degree of alteration within the Mount Attree volcanics before deposition of the lower Telkwa Formation (Figure 2.1 inset f). Sample 16JA199 returned predominantly prismatic, slightly elongate zircons up to 15 µm that exhibit oscillatory and sector zoning. Seven older analyses were rejected as probable xenocrysts or antecrysts. The remaining 13 analyses yield a weighted mean $^{206}Pb/^{238}U$ age of 196.5 ± 1.2 Ma (Figure 2.6).

Late Cretaceous Bulkley Plutonic Suite

The Bulkley plutonic suite refers to widespread dikes, small stocks, and less common larger plutons in the Intermontane Belt (Woodsworth et al., 1991). The 'Bulkley intrusions' were originally identified by Carter (1982) to refer to calc-alkaline granite to diorite within the Skeena arch. Their range has

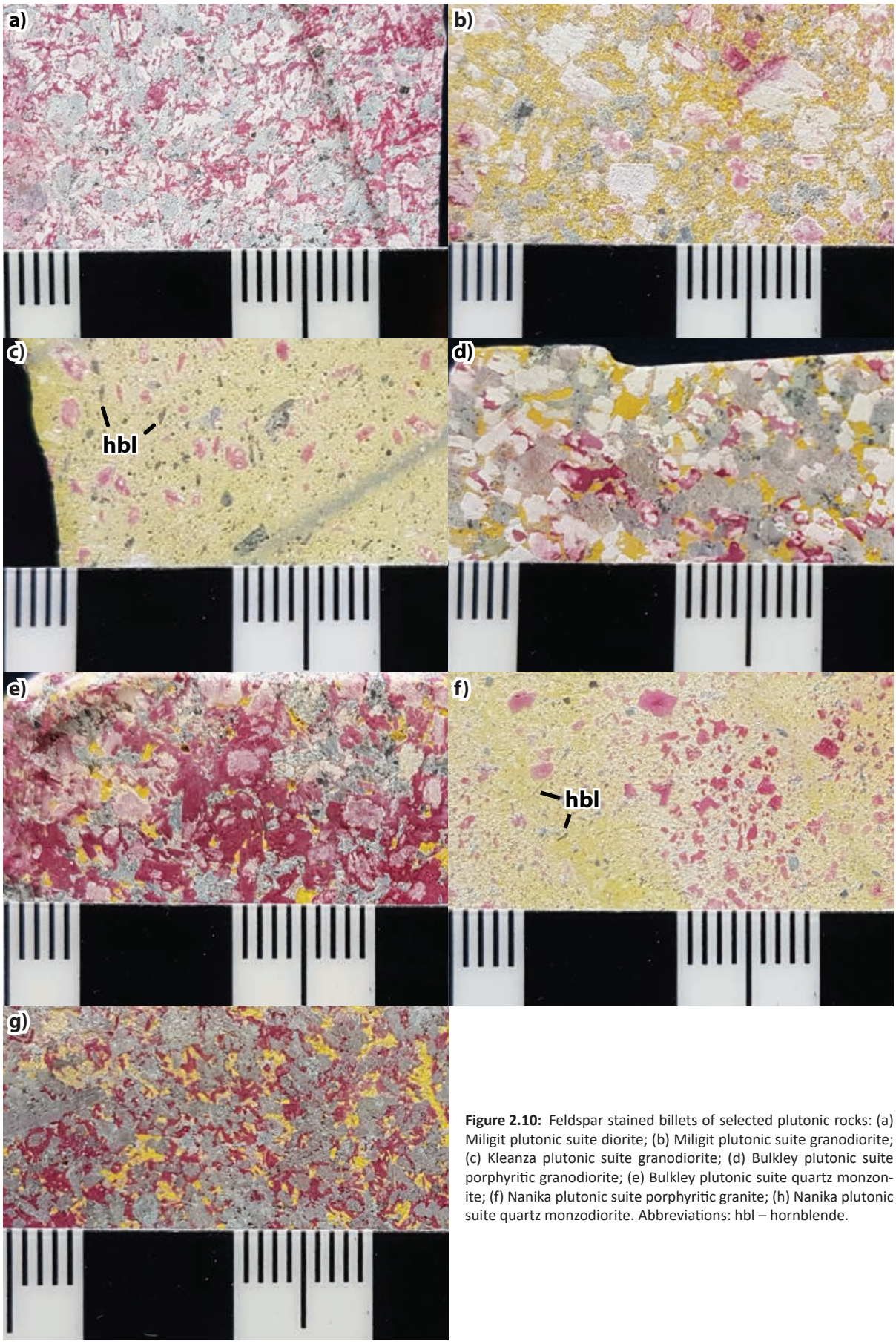

Figure 2.10: Feldspar stained billets of selected plutonic rocks: (a) Miligit plutonic suite diorite; (b) Miligit plutonic suite granodiorite; (c) Kleanza plutonic suite granodiorite; (d) Bulkley plutonic suite porphyritic granodiorite; (e) Bulkley plutonic suite quartz monzonite; (f) Nanika plutonic suite porphyritic granite; (h) Nanika plutonic suite quartz monzodiorite. Abbreviations: hbl – hornblende.

since been extended northwards into the Bowser Basin and southwards to Tahtsa Lake (MacIntyre, 1985). Small (100 m to 2 km diameter) stocks, dikes and sills of known or presumed Late Cretaceous age occur throughout the Search area east of the Coast Plutonic Complex. Three distinct phases of the Bulkley suite were recognized during the current study: a porphyritic granodiorite phase, a biotite diorite phase, and an equigranular quartz monzonite phase.

Porphyritic Granodiorite Phase

A typical phase of the Bulkley plutonic suite is plagioclase-hornblende-phyric granodiorite. Phenocrysts include 10– 45% plagioclase crystals up to 8 mm, 10–25% hornblende up to 4 mm, all in a light grey groundmass of aphanitic quartz and K-feldspar with 1–3% disseminated magnetite. It locally contains up to 5% quartz up to 2 mm and up to 3% biotite up to 2 mm. Hornblende occurs as equant to slightly elongate crystals with aspect ratios up to 3:1 (Figure 2.10d). This phase is well represented on Paleo Peak in the vicinity of the Hidden Valley prospect and near the Louise Lake prospect, where minimally altered plutonic rocks were identified. Friedman and Panteleyev (1997) established a Late Cretaceous age for Louise Lake porphyry with a U-Pb zircon age of 87.5 +4.9/-2.0 Ma from intensely clay- and sericite-altered feldspar porphyry. A sample of the characteristic plagioclase-hornblende-phyric granodiorite phase of the Bulkley plutonic suite was collected ~1 km west of the Louise Lake prospect (16JA202). It yielded prismatic, slightly elongate zircons up to 200 µm with well-developed oscillatory zoning. All 20 analyses are concordant and overlapping. They returned a weighted mean $^{206}Pb/^{238}U$ age of 85.8 ± 0.7 Ma (Figure 2.6). A previous 73.9 ± 3 Ma K-Ar hornblende age (Wanless et al., 1973 recalculated by Breitsprecher and Mortensen, 2004) has been reported for plagioclase-phyric diorite on Paleo Peak (Figure 2.1 inset b). A similar plagioclase-phyric diorite dike on Ashman Ridge (sample 16JA214) was also collected to test the hypothesis that a string of magnetic highs between Louise Lake and Hobbes FM zone correspond to Bulkley suite intrusions. This sample (16JA214) returned only three elongate zircon fragments with sector zoning. They yielded a weighted mean $^{206}Pb/^{238}U$ age of 92.1 ± 9.8 Ma (Figure 2.6). This result, while of low confidence, at least supports the interpretation that magnetic highs along this trend correspond to Bulkley plutonic suit intrusions.

Biotite Diorite Phase

A suite of diorite intrusions on Zymo Ridge are tentatively assigned to the Bulkley plutonic suite. These equigranular to plagioclase-phyric, fine- to medium-grained intrusions cut the upper Jurassic Trout Creek assemblage (Figure 2.1 inset a). They contain 40–55% plagioclase, 0–20% pyroxene, 5–20% hornblende, 0–25% biotite, and trace to 2% pyrite. Plagioclase exhibits minimal sericite alteration, and pyroxene and hornblende both exhibit weak chlorite alteration. Similar mafic dikes surrounding Ventura Peak and Cariboo Mountain are also included with the Bulkley plutonic suite. The dikes are fine grained, dark green-grey, and locally contain plagioclase, hornblende or pyroxene phenocrysts. One dike on the northwest ridge of Ventura Peak contains 15% plagioclase megacrysts up to 1 cm by 3 mm in a dark grey, fine-grained groundmass. Where observed on Ventura Peak, these dikes are moderately quartz-sericite-gypsum-altered and contain Cu sulfides (see Section 4).

A sample of biotite gabbro on Zymo Ridge was collected for U-Pb zircon geochronology. Sample 16JA154 yielded subhedral zircon crystals rarely greater than 50 µm. The zircons are round, consistent with abrasion or resorption into a magma that was undersaturated with respect to zircon, and many exhibit low luminescence rims surrounding high luminescence cores in cathodoluminescence imagery. Laser ablation analysis targeted cores only because the rims were too narrow to be analyzed. One analysis was discarded as it is ~20 m.y. older than all other analyses, and three were discarded due to discordance. The 15 remaining analyses return a weighted mean $^{206}Pb/^{238}U$ age of 167.4 ± 1.9 Ma (Figure 2.6). This is older than the Upper Jurassic Trout Creek assemblage that the sampled intrusion crosscuts, indicating that all the contained zircons must be inherited.

Equigranular Quartz Monzonite Phase

Equigranular, medium- to coarse-grained quartz monzonite to diorite forms a second phase of the Bulkley plutonic suite. It forms a 500 m long tadpole-shaped intrusion in the western cirque of Paleo Peak and as a 1.7 km long oval intrusion, as well as <5 m wide dikes in the Tatsi Creek area (Figure 2.1 insets b and g). In both localities this phase is white, pale pink, or white and black depending on K-feldspar content. It contains 30–55% plagioclase, 0–25% K-feldspar, 3–15% quartz, 5–10% hornblende, 0–15% biotite, 0–25% pyroxene, and 1–3% magnetite; plagioclase is euhedral to subhedral, whereas K-feldspar is anhedral (Figure 2.10e). Feldspars are weakly sericite-altered and mafic minerals are moderately altered to chlorite and epidote. Near the Tatsi prospect, this phase is cut by quartz veins and mineralization (Tennant and Tompson, 1995).

A dike of equigranular, medium-grained quartz monzodiorite cuts the foliation in the Telkwa Formation in the Tatsi Creek area. Sample 16JA117 from this dike yielded small (rarely greater than 40 µm) equant zircons with weak oscillatory zoning. One ca. 200 Ma zircon was rejected as inherited from the host Telkwa Formation and two analyses were rejected for discordance. Six concordant, overlapping analyses returned a weighted mean $^{206}Pb/^{238}U$ age of 79.3 ± 1.4 Ma (Figure 2.6). The equigranular quartz monzodiorite is therefore another textural variant of the Bulkley plutonic suite and is not Early Jurassic as previously interpreted (Angen et al., 2017).

Eocene Plutonic Suites

Eocene intrusive rocks in the Search area include the Nanika and the Carpenter plutonic suites. The Nanika suite refers to small (100 m to 2 km diameter) plutons, dikes, and sills of granite to granodiorite; they have been called the Kastberg intrusions, the Alice Arm intrusions and the Nanika intrusions east, west and south of the Bowser Basin, respectively (Woodsworth et al., 1991). They can be coarse-grained and equigranular, aphanitic, or porphyritic. Gabbro and monzodiorite intrusions south of Houston are referred to as the Goosly Lake intrusions (Church, 1971). The Carpenter plutonic suite forms a series of large (10-20 km diameter) equant bodies including the Carpenter Lake, Williams Creek and Kitimat River plutons and associated dikes in the Coast Plutonic Complex. They are typically coarse-grained, titanite-bearing, hornblende and biotite granodiorite to granite (Gareau et al., 1997; Nelson et al., 2008a; Nelson et al., 2008b). Available ages on the Carpenter suite include a mixed zircon and titanite U-Pb age of 52.6 +1.2/-1.8 Ma from the Carpenter Lake Pluton ~1 km outside of the Search area (Gareau et al., 1997). Only the Eocene granite and gabbro dikes of the Nanika suite, which were observed during the current investigation, are discussed in more detail.

Nanika Plutonic Suite

Beige porphyritic granite dikes (and sills) occur throughout the Howson Range. In the Limonite Creek and Tatsi Creek areas they strike N to NE and dip steeply or follow folded bedding planes (Figure 2.1 insets e and h). Individual dikes are <5 m wide and can be traced for up to 2.5 km along strike. A single Nanika plutonic suite dike was recognized on the north slope of Ventura Peak where it strikes NNW and dips steeply (Figure 2.1 inset c). It is 5–10 m wide and continues for at least 5 km along strike. These granite dikes contain 10–25% plagioclase, 0–15% K-feldspar, 5–15% quartz, 10–15% biotite, 5–10% hornblende and trace to 3% magnetite in a fine-grained grey to beige to pale pink groundmass of quartz and K-feldspar; hornblende forms very slender needles with aspect ratios of up to 10:1 (Figure 2.10f).

A porphyritic granite sill in the Tatsi Creek map area was collected for U-Pb zircon geochronology to establish the age of these characteristic intrusions. Sample 16JA123 yielded prismatic slightly elongate zircons up to 200 µm with well developed oscillatory zoning. A single analysis at ca. 200 Ma was rejected as a probable xenocryst incorporated from the Telkwa Formation into which the sill intrudes. The remaining nine concordant, overlapping analyses returned a weighted mean $^{206}Pb/^{238}U$ age of 52.7 ± 1.1 Ma (Figure 2.6). This is within error of a previous result from fine-grained, equigranular to biotite-feldspar porphyritic granite near Limonite Creek, which returned a U-Pb zircon age of 52.2 ± 0.1 Ma (Deyell et al., 2000).

A medium-grained equigranular quartz monzodiorite dike with locally pegmatitic margins crosscuts one of the porphyritic sills described above in the Tatsi Creek area. The interior of the dike contains 7% quartz, 30% hornblende, 8% pyroxene, and 55% plagioclase (Figure 2.10g). Along the pegmatitic margins are hornblende crystals, locally >5 cm long. Hornblende and pyroxene are euhedral to subhedral whereas quartz and feldspars are subhedral to anhedral. This dike is assigned to the Nanika plutonic suite but may better correlate with the Goosly Lake intrusions of Church (1971).

Others

In addition to the plutonic suites described above, there are abundant intrusions of uncertain affinity throughout the Search area. They were identified during regional mapping but have neither been dated nor confidently assigned to plutonic suites. In particular, a plethora of small (0.1–2 km wide) stocks and dikes without age control may belong to either the Bulkley or Nanika plutonic suite. These intrusions were mapped as a wide array of granite, granodiorite, quartz diorite, quartz monzonite, felsite, and quartz±feldspar±hornblende±biotite porphyry (Richards and Tipper, 1976; MacIntyre et al., 1989b; Desjardins et al., 1990a; Desjardins et al., 1990b).

Metamorphic Rocks

The area southeast of Pass Peak in the southeastern tip of the Search area is underlain by undifferentiated mylonite, schist and gneiss (Figure 2.1). This area was mapped as Permian metasedimentary rocks by Richards and Tipper (1976), as undifferentiated metamorphic rocks by Woodsworth et al. (1985) and has been assigned to the Central Gneiss Complex. It is tentatively interpreted to be part of the same intensely deformed, amphibolite facies, Permian to Jurassic metasedimentary and metavolcanic assemblage identified at Atna Peak to the south by Evenchick (1979). It may be a northern continuation of the Gamsby metamorphic complex, which outcrops extensively west of Whitesail Lake (van der Heyden, 1989).

3. STRUCTURAL GEOLOGY

Introduction

The northeastward orientation of the Skeena arch is interpreted to reflect the orientation of a long-lived zone of structural anisotropy. Four deformation events are recognized for this region; two have accommodated strain subparallel to the Skeena arch trend. Evidence of these deformations are apparent from aeromagnetic and orthophoto interpretation, historical data compilations, and from targeted regional and detailed mapping. A structural framework developed through aeromagnetic lineament analysis defines three main structural trends: east-northeast, north-northwest, and west-northwest. These main trends are also observed in structures observed

in outcrop, but some individual lineaments lack an obvious surface expression in the field.

The structural patterns of the Skeena arch have historically been ascribed mostly to Eocene 'block faulting' (MacIntyre et al., 1989a; Struik and MacIntyre, 2001; MacIntyre, 2007). This interpretation stems from the observation that most of the exposed rocks east of the Coast Belt, and particularly east of the Howson Range, are sub-greenschist facies volcanic rocks of the Hazelton Group that are preserved in well-bedded, typically homoclinal panels. These internally undeformed panels are bound by (mostly inferred) predominantly ENE- and NNW-trending faults that exhibit mutually cross-cutting relationships (Figure 2.1). Observations from the present project suggest that this block-faulting pattern likely reflects the reactivation of older structures during Eocene extension and transtension.

Evidence for older deformation events is locally preserved. Recognition of northeast-trending folds in the Zymoetz Group (Paleozoic) that are apparently cut off along the basal Hazelton unconformity prompted Nelson et al. (2006) to suggest that at least the westernmost portion of the Skeena arch underwent northwest-southeast shortening prior to the Jurassic. Subsequent recognition of similarly oriented folds affecting the Hazelton Group and Bowser Lake Group requires a generation of post-Jurassic folding, and suggests that the orientation of the Skeena arch reflects a long-lived structural anisotropy (Nelson et al., 2008a; Angen, 2009). The mid-crustal record of this structural anisotropy is preserved as northeast-trending ductile shear zones in the Coast Belt west-southwest of the Skeena arch (Evenchick, 1979; Heah, 1991). Preferential northeast elongation of Jurassic and Cretaceous intrusions indicate that this long-lived structural corridor periodically controlled magma emplacement.

Geophysical Interpretation

The structural interpretation was developed using a newly-constructed structural lineament map to identify the predominant trends in the western Skeena arch. A dataset stacking procedure similar to that developed by Sánchez et al. (2014) was modified to accommodate the datasets that were available. An initial lineament map was generated through manually digitizing linear trends in reduced-to-pole (RTP), first vertical derivative (1VD), and tilt-angle filters applied to data from the Search phase 1 aeromagnetic survey (Precision GeoSurveys Inc., 2016). Lineaments recorded include any curvilinear trends of continuous or discontinuous low magnetic response (magnetite destructive) or high magnetic response (magnetite additive), as well as curvilinear breaks that juxtaposed domains of differing magnetic response. The aeromagnetic lineament map was then assessed against upward continued aeromagnetic data (1500 m and 3000 m), isostatic residual gravity data, a digital elevation model (DEM), and existing geological mapping; each lineament was assigned a value of 1 if it was recognized in a given dataset and a value of 0 if it was not. The sum of all binary dataset values for a given lineament is referred to as its reliability index (Sánchez et al., 2014). In this study, the reliability index varies between 1 and 6. The resulting lineament map highlights two prominent trends that are nearly orthogonal to each another: NNW-trending and ENE-trending (Figure 3.1).

In many cases, well-constrained geological mapping and orthophoto interpretation preclude attributing a recognized lineament to the surface expression of a fault, therefore these lineaments were not transferred directly to the updated geological map (Figure 2.1). However, there is a correlation between the predominant lineament trends and the orientations of structural features that were recognized during mapping and the compilation of historical data. The identified lineaments may reflect deeper structural anisotropies that lack direct surface expressions. Overall, the combined geological and geophysical constraints contributed to establishing a new structural framework for the western Skeena arch.

The Search Phase 1 aeromagnetic data were collected by aircraft that flew flight lines along a prescribed draped surface with respect to topography. This resulted in highly variable ground clearances, particularly in the southwestern portion of the study area which has very steep topography (Precision GeoSurveys Inc., 2016) and the correlations of the magnetic signal with the topography are apparent. Topographic features and varying ground clearances may cause artifacts and false magnetic gradients (Grauch and Campbell, 1984; Luyendyk, 1997) which, in some cases, can be removed with mathematical transformation. However, because topographic features frequently reflect structural breaks, coincident topographic and magnetic lows cannot be ruled out as false lineaments. The possibility of false lineaments adds a degree of uncertainty to structural interpretations of the magnetic data for this region.

Structural Events and their Relative Timing

Pre-Jurassic NW-SE Contraction

Northeast-striking ductile foliations and folds occur in the Zymoetz Group and Delta plutonic suite between the Zymoetz River and Chist Creek and near the Limonite Creek prospect (Figure 2.1 and Figure 2.1 inset e). The age of deformation in both regions is constrained by cross-cutting Late Triassic to Early Jurassic nonfoliated intrusive rocks. Steeply southeast-dipping foliations occur in volcanic rocks assigned to the Mount Attree Formation of the Zymoetz Group at the Limonite Creek prospect (Figure 3.2). The fabric represents the alignment of muscovite and quartz ribbons. Shear sense indicators in this area are ambiguous and stretching lineations are not well developed. Deformation is tentatively constrained as pre-Late Triassic

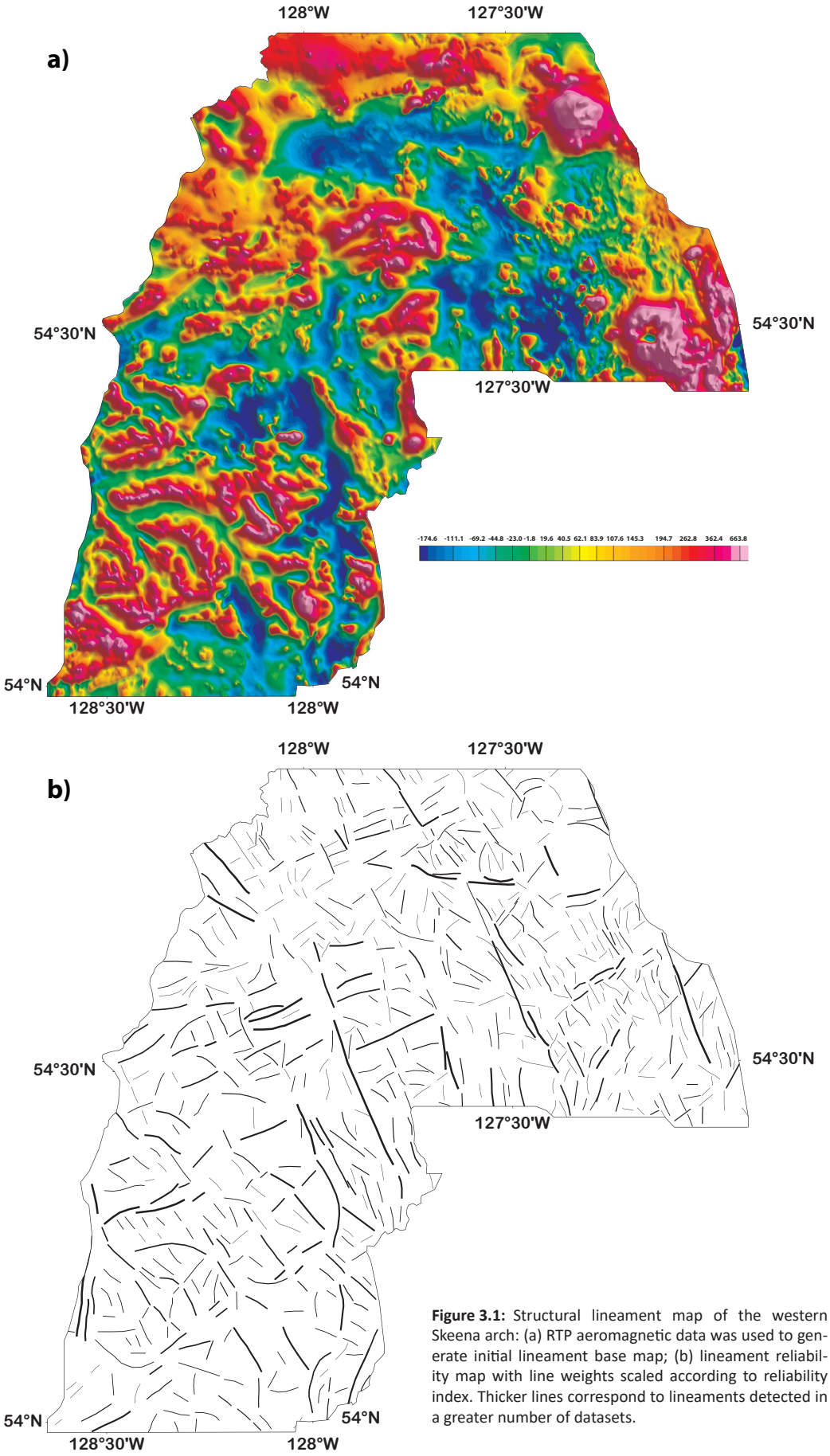

Figure 3.1: Structural lineament map of the western Skeena arch: (a) RTP aeromagnetic data was used to generate initial lineament base map; (b) lineament reliability map with line weights scaled according to reliability index. Thicker lines correspond to lineaments detected in a greater number of datasets.

Figure 3.2: Foliation in tuff at Limonite Creek.

because adjacent intrusions of the Miligit plutonic suite do not exhibit a ductile foliation. A similar relationship is observed near Chist Creek, where foliations in the Zymoetz Group are axial planar to northeast-trending folds. Steeply-southeast-dipping foliation in the Delta intrusive complex south of Chist Creek is truncated by a dioritic phase of the Kleanza pluton, indicating pre-Jurassic deformation (Nelson et al., 2008a).

Early Cretaceous NW-SE Contraction

Northeast-trending structures associated with NW-SE contraction are widely distributed throughout the western Skeena arch. Examples include northwest-vergent reverse and thrust faults and folds with locally-developed axial planar cleavage. Folds affect strata as young as Early Cretaceous. This deformation has contributed to the regional map pattern of the western Skeena arch (Figure 2.1). The oldest stratified rocks occur in the core of a regional anticline with younger strata dipping to the north and east away from the core (Nelson et al., 2008a; Angen, 2009). Open to tight folds are recognized in the Zymoetz Group within the core of the Skeena arch anticline between Williams Creek and Kleanza Creek (Nelson et al., 2008a). Folds within the Telkwa Formation are rare. Well-bedded tuffs of the upper Telkwa Formation in the southern Howson Range exhibit open folds (Figure 2.1). Northeast-trending folds are well developed in the Kitselas facies of the Telkwa Formation northwest of the Skeena River (Nelson et al., 2008a; Barresi et al., 2015b). The Bowser Lake Group is deformed into broad, open, northeast-trending folds in the Zymo Ridge and Paleo Peak map areas (Figure 2.1).

Zymo Ridge

Well-bedded conglomerate, sandstone and mudstone of the Bowser Lake and Skeena groups along Zymo Ridge are deformed into broad, open, shallowly to moderately NE-plunging folds with wavelengths of ~2 km (Figure 2.1 inset a). Similarly-oriented, outcrop-scale folds in the cores of larger folds have wavelengths of 10 to 20 m (Figure 3.3a).

Fine-grained rocks have a steeply NW- and less commonly SE-dipping spaced cleavage in which microlithons between cleavage foliae are spaced from 1 to 10 cm (figure 3.3b). This spaced cleavage is interpreted as axial planar to the NE-plunging folds as it is relatively consistent regardless of bedding orientation. The intersection of this cleavage, likely generated by pressure solution, with bedding-parallel partings, results in a pencil cleavage. Minor refraction of cleavage is present between sandstone and siltstone layers (Figure 3.3b). Pervasive southwest dipping joints are observed throughout the Zymo Ridge area (Figure 3.3c). These joints correspond to the AC (profile) plane of folds (Figure 3.3d).

Tatsi Creek

Well-bedded Telkwa Formation tuffs in the southern Howson Range are deformed into NE-trending folds and displaced across a NW-vergent thrust fault. A NW-vergent fold was observed in the cirque west of Mount Desdemona (Figure 3.4a). In the northern headwall, it is accentuated by a pale purple marker tuff that is offset ~50 m across the fault. Bedding varies between shallowly SE- and steeply NW-dipping (Figure 3.4b). Folds were also identified through air photo interpretation in areas where steep terrane restricted access. Shallowly S- to SE-dipping quartz veins at the Tatsi prospect host bornite, chalcopyrite, galena, sphalerite, electrum, and native silver (Figure 2.1 inset g)(Tennant and Tompson, 1995). Slickenlines along the margins of one such vein have an azimuth of 150° and a plunge of 19° (Figure 3.4b). En-echelon vein sets have enveloping surfaces parallel the SE-dipping veins. Individual veins within the sets dip variably to the northwest, consistent with top-to-the-northwest sense of shear (Figure 3.4c). Cleavage in one fine ash tuff is oblique to bedding, dipping shallowly to the southeast, consistent with northwest vergence (Figure 3.4d).

Upper Zymoetz River

Thrust faults were identified near the upper Zymoetz River, from the mouth of Coal Creek to Hudson Bay Mountain by Richards and Tipper (1976). These faults are well-represented by aeromagnetic data due to a greater magnetic response from the rocks in the hanging wall (Figure 2.2). South and east of McDonnell Lake, a thrust fault places undifferentiated Telkwa Formation volcanic rocks on top of undifferentiated Bowser Lake Group sedimentary rocks (Figure 2.1). At the latitude of Sandstone Lake another thrust places Middle Jurassic Smithers Formation and undifferentiated Bowser Lake Group sedimentary rocks on top of Upper Jurassic Bowser Lake Group volcanic rocks (Netalzul volcanics) to the north (Figure 2.1). A similar stacking order occurs north of Hudson Bay Mountain except that the footwall of the lower thrust includes the type exposure of the Trout Creek assemblage of the Bowser Lake

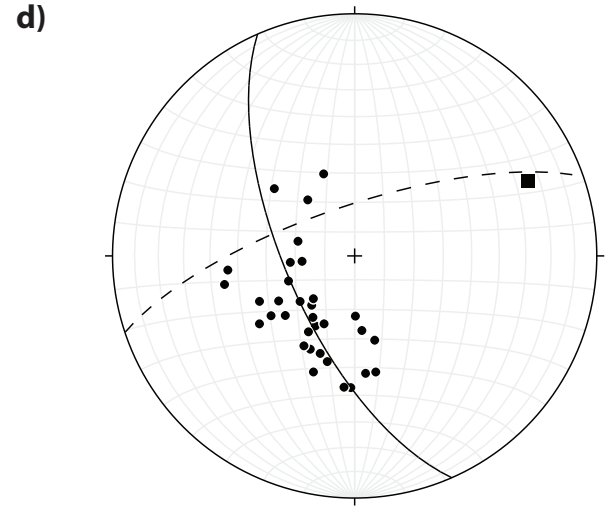

Figure 3.3: Structures in the Zymo Ridge area: a) panorama of parasitic northeast-plunging fold. Dashed white lines trace bedding in two adjacent outcrops that dip to the north and northeast. Photo looking oblique to the hinge line of the fold; b) refraction of foliation in siltstone and sandstone beds. Dashed white lines trace spaced cleavage and dashed black lines trace bedding; c) AC joints in Skeena Group sandstone. Dashed black line traces orientation of joints. White dashed lines trace bedding through hinge of a NE-plunging syncline in the distance; d) lower hemisphere, equal area stereonet plot showing the orientation of structures in the Zymo Ridge area excluding data from south of Red Canyon Creek. Black circles are poles to bedding. Black square corresponds to the fold axis calculated using eigenvalues of bedding measurements. Dashed line represents average orientation of cleavage. Solid line represents average orientation of AC joints.

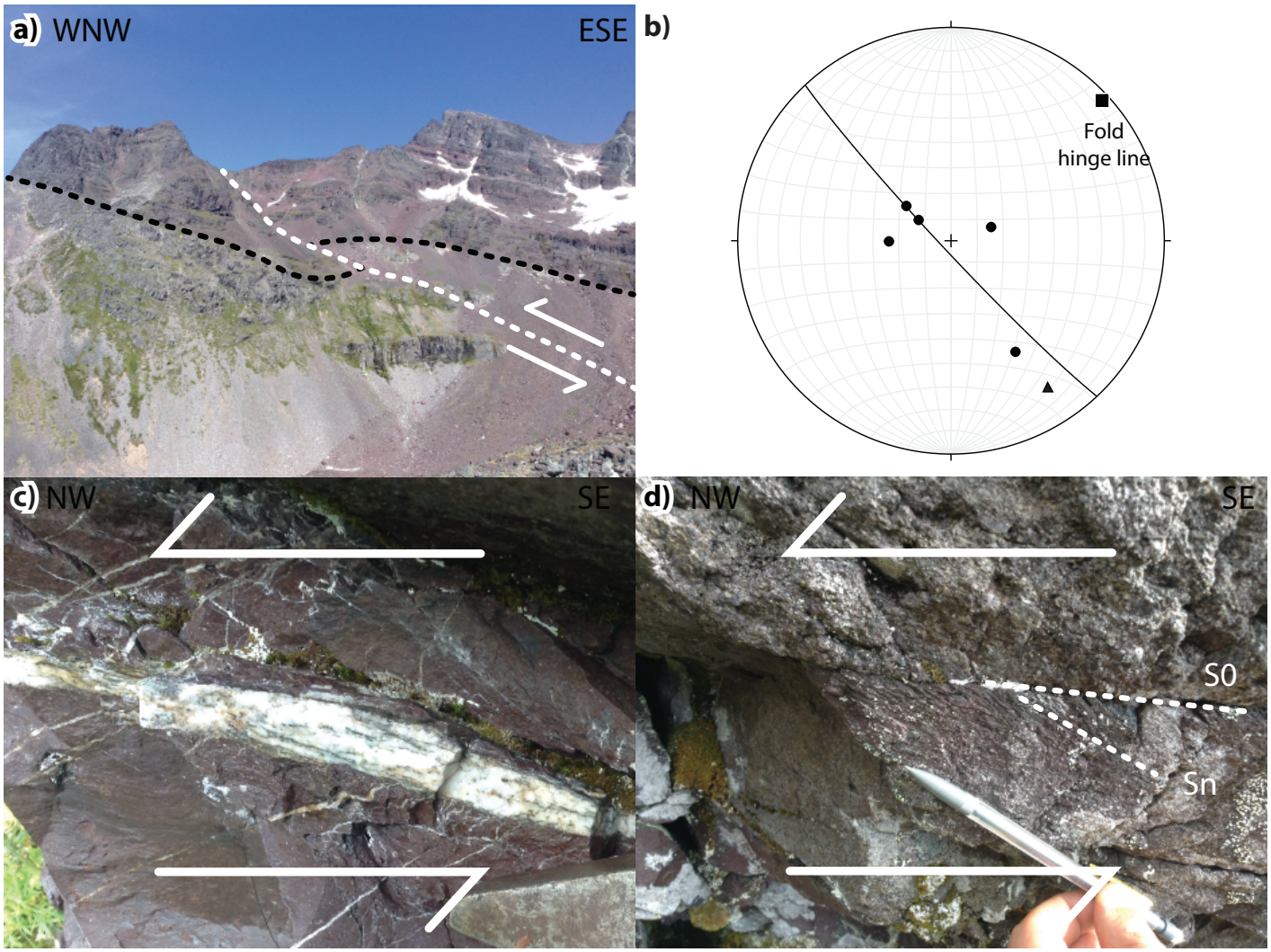

Figure 3.4: Structural features in the Tatsi map area: a) northwest-vergent thrust fault with minor fold. Dashed white line indicates trace of thrust. Black dashed lines indicate contact between pale purple marker crystal tuff and well bedded red tuffs; b) lower hemisphere, equal area stereonet projection of structural elements in the Tatsi map area. Black circles are poles to bedding. Black triangle is a slickenline on the surface of the mineralized vein in Figure 3.4c. Black square corresponds to the fold axis calculated using eigenvalues of bedding measurements. The solid black line represents best-fit great circle of bedding; c) a south-southeast dipping mineralized vein that crosscuts weakly folded northwest dipping veinlets. Interpreted sense of shear is top to the north-northwest; d) weak south-southeast dipping foliation developed in fine red tuff indicating north-northwest vergence.

Group (Tipper and Richards, 1976). The thrusts in this area are therefore Early Cretaceous or younger.

Kleanza Creek

The Kleanza suite intrusions are locally bound by NE-striking reverse faults (Figure 2.1; Woodsworth et al., 1985). The reverse faults along the Kleanza Creek corridor are interpreted to correlate with a similarly oriented top-to-the-northwest reverse fault mapped along the Skeena River southwest of Terrace (Heah, 1991). Heah (1991) reported penetrative steeply SE-dipping foliation along the Skeena River west of Terrace and East of Shames River; he interpreted it to be related to a reverse fault placing Permian rocks structurally above Early Jurassic rocks. Despite similarity in orientation and deformation style of these reverse faults to pre-Jurassic features described above, these reverse faults must be younger than Early Jurassic.

Pass Peak

A curvilinear N to NE-striking high strain zone occurs on the southeast slope of Pass Peak in the southern-southeastern corner of the Search area (Figure 2.1). It has been recognized through aeromagnetic and orthophoto interpretation combined with historic structural measurements. Steeply SE-dipping foliation was documented in the vicinity of Pass Peak by Woodsworth et al. (1985). This high strain zone is continuous with a NE-trending high-strain zone previously identified at Atna Peak approximately 10 km to the south-southwest where it forms an upright, isoclinal, northeast-trending fold (Evenchick, 1979). Evenchick (2001) assigned folding at Atna Peak to Early Cretaceous NW-SE shortening based on an unpublished age of a synkinematic intrusion. This high strain zone appears to be truncated to the northeast by an east-side-down normal fault along the Clore River (Figure 2.1).

Mid Cretaceous NE-SW Contraction

Northwesterly, orogen-parallel folds and faults that predominate the structural fabric of the Bowser Basin north of the Skeena arch are relatively sparse across the Skeena arch. A few SW-vergent thrusts are recognized in Skeena Group sedimentary rocks in the Telkwa Coalfields (Figure 2.1)(Ryan, 1993). Rare NW-trending folds are preserved in the Telkwa Formation; they are open folds with km-scale wavelengths. One example identified at the southeast end of Microwave ridge occurs in a series of fault bound blocks with internally homoclinal layering (Rahimi et al., 2018). Another example is on the west side of Hudson Bay Mountain where an east-dipping thrust plate of Telkwa formation is thrust westward over an overturned syncline of younger Saddle Hill (red tuff) and Smithers Formation marine sedimentary rocks. If pre-existing structural anisotropy contributed to generating Early Cretaceous NE-trending folds, that anisotropy could have also inhibited development of NW-trending folds.

Eocene Extension

Six NNW-trending structural corridors contribute to the present-day topography of the western Skeena arch. From west to east, they correspond to the Lakelse Lake to Kitsumkalum Lake valley (western limit of current map area), the Clore River valley, the Kitnayakwa and Zymoetz river valleys, the Burnie lakes valley to Mulwain Creek, the Sinclair to Kitsuns creek valleys, and the approximate location of Goathorn Creek along the eastern limit of the current map area (Figure 2.1). These are part of a system of faults that continues east to the Babine Lake area where they have accommodated normal sense of shear that affects Eocene intrusions (MacIntyre and Villeneuve, 2001).

The western limit of the Search map area corresponds to the eastern margin of the Kitsumkalum graben (Nelson and Kennedy, 2007). A west-side-down normal fault defines the eastern side of the graben on Fire Mountain (Figure 2.1). An Eocene pluton of the Carpenter intrusive suite is interpreted to be truncated by this west-side-down fault (Figure 2.1). The northern continuation of this fault (outside of the current study area) juxtaposes Cretaceous sedimentary rocks of the Skeena Group in its hanging wall to the west against amphibolite facies metamorphic rocks and a Paleocene pluton with ductile deformation in its footwall to the east (Nelson and Kennedy, 2007). The age of plutonic rocks truncated by this fault provide an older age constraint on graben formation in the western Skeena arch.

East of the Kitsumkalum graben is a horst that corresponds with rugged topography including the O.K. Range and continuing south to Pass Peak (Figure 2.1). This horst contains greenschist to amphibolite facies strata and intrusive rocks. Significant east-side-down normal shear along the upper Clore River is required to juxtapose amphibolite facies mylonitic gneiss of the Central Gneiss Complex near Pass Peak against lower greenschist facies Telkwa Formation volcanic rocks to the east (Figure 2.1). The apparent throw across this fault decreases to the north until it can no longer be recognized north of Kleanza Creek (Figure 2.1).

The Howson Range represents a second major horst bound by steep normal faults along the Kitnayakwa/Zymoetz river valleys to the west and the Burnie lakes valley to the east (Figure 2.1). The basal Hazelton Group is exposed in the horst, along with underlying Zymoetz Group and Miligit plutonic suite intrusions. Near the confluence of the Kitnayakwa and Zymoetz rivers, the Howson Range horst is flanked to the west by upper Hazelton Group volcanic rocks and minor Bowser Lake Group sedimentary rocks (Figure 2.1). Continuity of magnetic features related to the Kleanza pluton preclude significant offset across the Zymoetz River north of Telkwa Pass (Figure 2.2). The eastern bounding fault of the Howson Range horst is best represented near Serb Creek where it offsets a magnetic high corresponding to an Eocene Nanika suite pluton and has localized emplacement of subvertical sheeted dikes.

The large-scale extensional faults described above are reflected by minor faults throughout the western Skeena arch (Figure 2.1). Good examples were observed in the Zymo Ridge, Paleo Peak, Tatsi Creek and Outcast Peak areas. A set of south-striking faults separates sedimentary rocks at Zymo Ridge into three folded panels with apparent west-side-down sense of shear. A minor east-side-down normal fault occurs in the Tatsi Creek area (Figure 2.1 inset g). This same fault is interpreted to continue northwards to Outcast Peak where it offsets the base of the Hazelton Group (Figure 2.1 inset f). A similar NNW-striking, east-side-down normal fault transects the NE-trending fold at Paleo Peak (Figure 2.1 inset b).

Relatively minor faults associated with NW-SE extension are also recognized in this region. They include northwest-side-down normal faults in the Telkwa Coalfields area where they crosscut mid to Late Cretaceous northeast-vergent thrust faults (Figure 2.1)(Ryan, 1993). NW- and SE-side-down normal faults also crosscut NW-vergent thrusts in the vicinity of Coal Creek (Figure 2.1)(Richards and Tipper, 1976). The relative timing of E-W and NW-SE extensional deformation in the western Skeena arch is ambiguous, with apparent mutually cross-cutting relationships (Figure 2.1).

Discussion

The pre-Jurassic deformation identified in the western Skeena arch may correspond to the Late Permian to Early Triassic Tahltanian orogeny that is recognized in northern Stikine terrane (Souther, 1972; Read, 1983; Read, 1984). Subsequent deformation has modified fabrics formed during the Tahltanian orogeny throughout most of northern Stikine terrane. In the western Skeena arch, pre-Jurassic foliation and folds are

predominantly NE-trending. Nelson (2017) suggested that a fundamental pre-existing northeast-oriented structural anisotropy localized emplacement of the Jurassic Kleanza pluton and equivalents. These rare occurrences of ductile foliation truncated by Late Triassic to Early Jurassic intrusions are interpreted to record that early structural anisotropy.

The second generation of NW-SE contractional deformation in the western Skeena arch is interpreted to be an Early Cretaceous event. A maximum age of earliest Early Cretaceous is indicated by the occurrence of folds and cleavage within the Trout Creek assemblage at Zymo Ridge (Figure 2.1 inset a). This contractional deformation is correlated with similarly oriented structures documented through the western Skeena fold belt and locally within the Stikine arch to the north as well as minor zones within the Coast Belt (Evenchick, 2001). NE-trending folds and thrust faults in the Stikine arch affect Jurassic rocks and are overlapped by the Late Cretaceous Sustut Group, supporting an Early Cretaceous age for NW-SE contractional deformation in that region as well (Read, 1983; Read et al., 1989).

It has been suggested that the NE-trending folds within the Skeena fold belt may reflect the influence of basin geometry or basement structures on a predominantly northeast-trending deformation event (Sutherland Brown, 1960; McMechan, 2007). Although this interpretation may adequately explain some NE-trending structures within the belt, it would be difficult to achieve the fold interference patterns and the magnitude of estimated NW-SE shortening estimated in some portions of the Skeena Fold belt without convergence in that direction (Evenchick, 2001). The occurrence of NE-trending folds and related faults affecting Hazelton Group and older stratigraphy as well as Bowser Lake Group in the western Skeena arch indicates that NE-trending folds are not due to basin geometry but that they reflect NW-SE shortening. It may be that Early Cretaceous NW-SE shortening only developed where pre-existing structural anisotropies were present to accommodate it. The parallel orientation of pre- and post-Jurassic contraction-related features in the western Skeena arch suggests reactivation of a structural anisotropy.

Overall, the Skeena arch region is a large-scale zone of orogen-normal, E-NE-trending lineaments that were susceptible to reactivation as weak structural zones during both compressional and extensional events. Alignment of Early Jurassic plutons such as the Kleanza plutonic suite show that these weak structural zones functioned as magma pathways, presumably with mild NW-trending extension. Conversely, pre-Triassic and Early Cretaceous compressional events resulted in northeast-oriented fold and fault trends along the same structural corridor. A sinistral, orogen-parallel, compressional direction is documented elsewhere within the Cretaceous Skeena fold and thrust belt (Evenchick, 2001), but nowhere is it as well-expressed as within the Skeena arch region.

4. MINERAL OCCURRENCES

Introduction

Host to more than 220 mineral occurrences, the western Skeena arch is a highly prospective region for metallic mineral deposits. The mineral occurrences have been assigned to diverse deposit models including porphyry, epithermal, volcanogenic massive sulphide (VMS), and a variety of polymetallic Cu-(Ag-Au-Pb-Zn) veins. The latter are abundant, but typically small, and therefore most have received little modern exploration attention—with the exception of those that were historically mined (e.g., Copper Queen mine, refer to Stock MINFILE 093L 085; MINFILE, 2020). Among the vein-type occurrences, are numerous examples that are classified as conforming to the volcanic-hosted redbed-copper mineral-deposit model, and others that are assigned to a variety of intrusion-related and sub-volcanic mineral-deposit models. There are 54 mineral occurrences that are ambiguously classified as both, despite their apparent mutually exclusive genetic origins (MINFILE, 2020).

Most of the mineralization in the Skeena arch is interpreted to be genetically related to Late Cretaceous and Eocene magmatism (MacIntyre, 2006; MacIntyre, 2007). Significant exploration efforts in the western Skeena arch have focused primarily on porphyry copper systems that are associated with these two magmatic episodes. There are two NI-43-101-compliant resources in the western Skeena arch; both occur in and surrounding Late Cretaceous porphyry intrusions of the Bulkley plutonic suite west of Smithers: the Louise Lake Cu-Mo-Au-As porphyry deposit and the Davidson Cu-Mo porphyry deposit. The Sunsets, Hidden Valley and Hobbes/Zymo FM developed prospects are also interpreted to be genetically related to Bulkley plutonic suite, whereas the Serb Creek developed prospect is interpreted to be related to Eocene Nanika plutonic suite.

Exploration activity in the region has been limited in recent years and focused on high-grade vein-type occurrences including Empire (Kruse and Stuart, 2017), Midas (Goeppel and Turna, 2017a), Copperhead (Goeppel and Turna, 2017b), and locally on the Zymoetz claims (Wasteneys and Yang, 2013). Although these vein occurrences themselves are unlikely to represent economically viable orebodies, they may indicate proximity to larger zones of porphyry and epithermal mineralization. This relationship is apparent on Hudson Bay Mountain where the Davidson Cu-Mo deposit is surrounded by several polymetallic vein occurrences with fewer occurrences assigned to subvolcanic Cu-Au and intrusion-related Au-pyrrhotite vein deposit models (Figure 2.1). A similar relationship occurs around the Sunsets Creek porphyry prospect, but in this area the surrounding occurrences are mainly assigned to the subvolcanic Cu-Au deposit model with a few assigned to the volcanic redbed Cu deposit model (Figure 2.1). An improved understanding of these vein-type occurrences will lead to better exploration decision making in attempts to vector towards economic mineralization.

Four new mineral occurrences were identified during Search project mapping, and 21 mineralized and altered rock samples were collected. Two new occurrences are on the northwestern flank of Ventura Peak; these are examples of the vein-type mineralization described above and emphasize the mineral potential of the region. The other two new occurrences, located on the western flank of Paleo Peak, are interpreted to represent Middle Jurassic VMS targets, whose potential was not previously recognized in this region. The following section details these four new occurrences. Analytical techniques and assay results are provided in Appendix C.

Volcanogenic Massive Sulphide

Middle Jurassic marine sedimentary rocks of the Quock Formation are lateral equivalents of the Iskut River Formation that hosts the Eskay Creek deposit (Gagnon et al., 2012). Recognition of felsic volcanic rocks and sulphide-bearing fragments within dark grey mudstone of the Quock Formation at two new showings on the western flank of Paleo Peak indicates proximity to volcanic activity within the basin, and the potential for VMS-style mineralization.

Neocal

The Neocal mineral occurrence is in a cirque on the western slope of Paleo Peak (Figure 4.1a) where it is hosted by the Quock Formation. This is the same locality that contains *Neocalamites* fossils and has returned a zircon $^{206}Pb/^{238}U$ age of 159.0 ± 2.1 Ma (see Section 2). Feldspar-phyric rhyolite and semi-massive sulphide fragments occur within mudstone (Figure 4.1b). Pyrite is the most abundant sulphide mineral, with traces of chalcopyrite identified in thin section. Two samples that were analysed (16JA024 a and b) lacked anomalous geochemical results. A semi-massive sulphide layer occurs within sandstone to granule conglomerate of the Bowser Lake Group ~100 m stratigraphically above the Neocal occurrence. The layer is up to 50 cm thick and can be traced for 50 m along strike. An assay sample from this horizon (16JA005) also lacked anomalous geochemical results.

Neonorth

The Neonorth occurrence is on the northwestern ridge of Paleo Peak, ~1.5 km north of the Neocal occurrence at the same stratigraphic level (Figure 2.1 inset b). It is represented at the surface by a bright red gossan (Figure 4.1c). The gossan reflects weathering of disseminated pyrite and pyrrhotite within fragments and in the groundmass of phyllic-altered felsic lapilli tuff with rare plagioclase-phyric fragments (Figure 4.1d). The lapilli tuff is cut by series of 1–2 m wide basalt dikes that make up 10–20% of the exposure. An assay sample of pyritic lapilli tuff collected at the Neonorth occurrence (16JA011) lacked anomalous results.

Discussion

Although the few samples from these new sulphide mineral occurrences lacked anomalous geochemical assay results for base metals, they indicate that the Quock Formation in this region may have the potential to host VMS-style mineralization. Eskay Creek and related VMS prospects are limited, geologically, to a narrow rift or series of rifts which localized magma and hydrothermal activity (Alldrick et al., 2005). It is possible that similar rifts may occur elsewhere in the Stikine terrane, but have not yet been recognized due to younger overlying strata. Volcanic activity and coeval sulphide precipitation at Neocal and Neonorth may be distal expressions of hydrothermal activity along a structural corridor, potentially similar to the Eskay rift. Barresi et al. (2015a) identified a correlation between primitive E- to N-MORB basalt and Middle Jurassic VMS mineralization along the Eskay rift. Any primitive basalt flows recognized within the Quock Formation stratigraphy should be considered good indicators of prospectivity and proximity.

Polymetallic Vein and Volcanic Redbed Cu

Polymetallic vein and volcanic redbed Cu occurrences are ubiquitous in the western Skeena arch. Many occurrences described in BC MINFILE reports are ambiguously labelled as both. In reality, there is likely considerable overlap between these deposit styles and the presence of one does not preclude the presence of the other. The two types may be preferentially spatially associated, and potentially even genetically associated. Two new showings that have similarities with polymetallic and volcanic redbed Cu mineralization are located on the flanks of Ventura Peak (Figure 2.1).

CuLater

The CuLater occurrence is 7 km north-northwest of Ventura Peak (Figure 2.1) where there is evidence for at least two generations of potentially independent hydrothermal activity. A rhyolite dome and breccia of the Telkwa Formation contains variable intensities and distributions of quartz-sericite-pyrite (QSP) alteration at surface exposures across a north-trending, 300 x 200 m area (Figure 4.2a). Fuchsite-altered felsic (?) volcanic rocks and quartz veins occur as fragments within the overlying red tuff (Figure 2.7b). Alteration of the rhyolite therefore occurred before deposition of the red tuff. Given that the QSP alteration is spatially limited to the extent of the flow dome, it can be reasonably interpreted as syngenetic with respect to the Early Jurassic Telkwa Formation. Grab samples of altered and brecciated rhyolite (16JA032A, 16JA032C, 16JA033) did not yield anomalous geochemical results for metals.

Base and precious metal mineralization at the CuLater prospect overprints the earlier alteration. It occurs in quartz±carbonate±barite veins and as disseminated sulphides within a diorite dike. Veins contain chrysocolla, chalcopyrite and

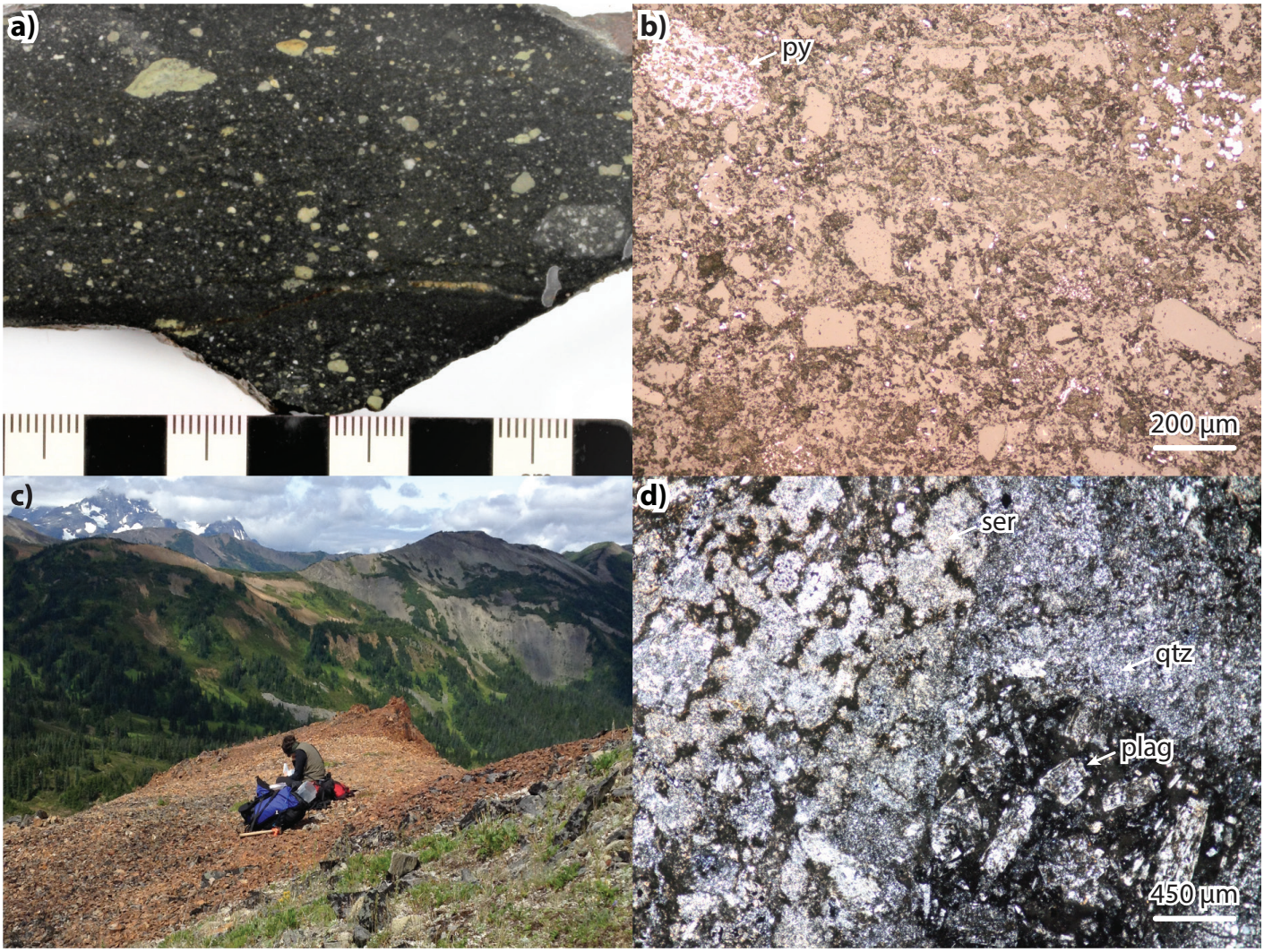

Figure 4.1: Characteristics of VMS-style mineral occurrences in the western Skeena arch: (a) photograph of cut slab of Quock Formation mudstone from the Neocal occurrence (16JA024a) exhibiting angular volcanic fragments, some of which contain disseminated pyrite; (b) reflected-light photomicrograph of 16JA024a; (c) photograph of gossan at Neonorth occurrence; (d) polarized-light photomicrograph of 16JA011 exhibiting plagioclase-phyric lapilli and strong quartz-sericite-pyrite alteration. Abbreviations: plag – plagioclase, py – pyrite, qtz – quartz, ser – sericite.

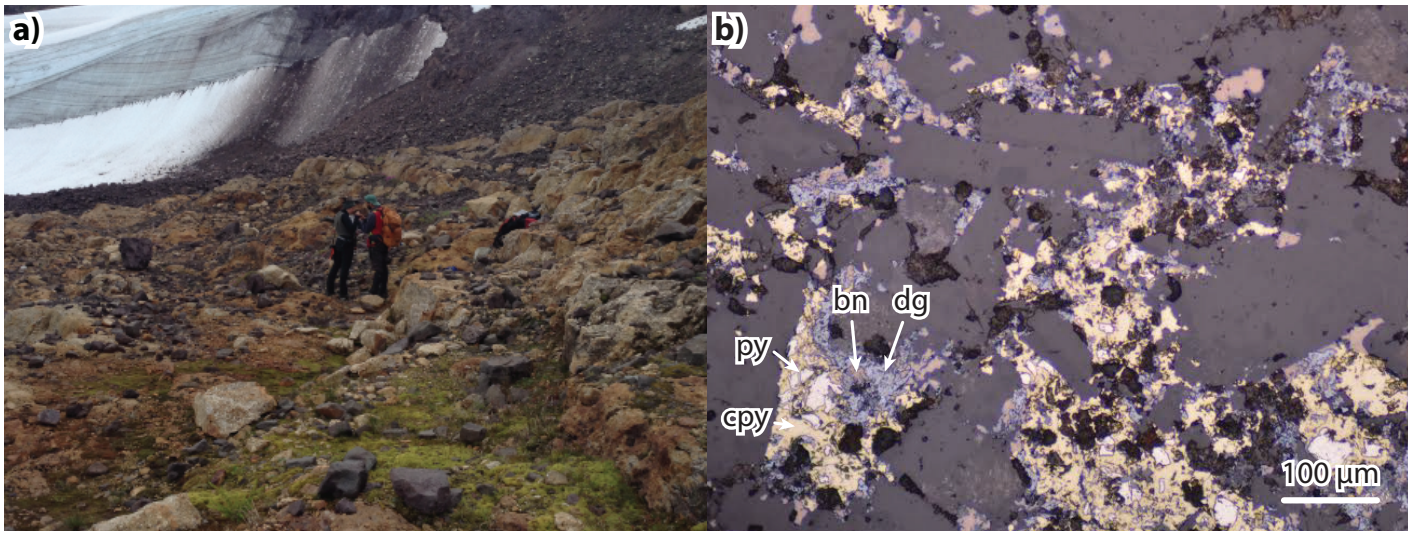

Figure 4.2: Characteristics of alteration and mineralization at the CuLater occurrence: (a) photograph of gossanous rhyolite of the Telkwa Formation; (b) thin section of sulphide zoning in diorite dike. Abbreviations: bn – bornite, cpy – chalcopyrite, dg – digenite, py – pyrite

sulfosalts. Three vein samples returned 0.08% Cu, 7.5 g/t Ag and 0.7 g/t Au (16JA035); 0.54% Cu, 12.5 g/t Ag (16JA038B); and 0.80% Cu, 0.12% Zn, 39.6 g/t Ag, and 0.25 g/t Au (15JA038C). The latter two have >0.2% Sb. The gangue mineralogy of the veins includes quartz, carbonate (including rhodochrosite) and barite. The metal tenor in the veins, consisting of generally low Cu and Au relative to other metals, and the limited alteration halos are consistent with polymetallic vein mineralization (Lefebure and Church, 1996). A sample collected from a fine-grained diorite dike at CuLater (16JA038A) returned values of 3.03% Cu and 25.5 g/t Ag.

Sulfide minerals in the dyke exhibit a distinctive zoned pattern from pyrite cores to chalcopyrite, bornite, and outermost digenite rims (Figure 4.2b). A similar zonation is reported for many of the sediment-hosted redbed Cu deposits at the deposit scale, with more reduced sulphide species present distally in the direction of fluid flow (Brown, 1992). The outwards Cu enrichment in Cu sulphide species at CuLater is interpreted to represent an initially pyrite-rich dike that acted as a reactive (reducing) host to oxidized copper-bearing fluids. This mineralization could be classified as volcanic-hosted redbed Cu mineralization, or it could be due to lower temperature hydrothermal activity related to the nearby polymetallic vein mineralization. The zoning pattern within the dike suggests that mineralization at CuLater is epigenetic—post-dating emplacement of the diorite dike that crosscuts the Telkwa Formation—and therefore younger than Early Jurassic. No younger age constraints on mineralization are available.

Blackberry

Approximately 4 km southwest of the CuLater occurrence, a plagioclase-megacrystic andesite dike contains coarse sulphides with the same zoning pattern as observed at CuLater. A sample of this dike has returned 0.38% Cu and 1.2 g/t Ag (Table C.1). Polymetallic quartz veins identified down-slope from the Blackberry showing have returned distinctly higher Au assay results: up to 0.58 g/t Au with 37 g/t Ag and 2.05 % Cu (Wasteneys and Yang, 2013).

Tourmaline Alteration

Widespread quartz+tourmaline±epidote alteration occurs in Telkwa Formation rhyolite along the northeastern ridge of Ventura Peak, approximately 1.5 km southeast of the CuLater occurrence and 3 km northeast of the Blackberry occurrence. Tourmaline-bearing alteration is interpreted to postdate devitrification of the rhyolite, as it occurs radially within spherulites (Figure 2.5c). The tourmaline in this area remains an unexplained anomaly. Tourmaline is a typical alteration mineral in a wide range of hydrothermal ore deposits (Slack, 1996). It is possible that it reflects alteration related to younger intrusion-related fluids in the northern Howson Range, such as the Eocene porphyry system at Serb Creek.

Discussion

The two new occurrences discovered on Ventura Peak could reasonably be assigned to volcanic redbed Cu, or to one of the intrusion-related vein-type deposit models. The dike-hosted, disseminated mineralization, in particular, has elevated Cu and Ag but low Zn and Au, typical of volcanic-hosted redbed Cu mineralization formed from low-temperature fluids which do not efficiently transport Au (Lefebure and Church, 1996). However, their concentration within dikes rather than within porous stratigraphic horizons is inconsistent with the volcanic-hosted redbed Cu deposit model. The geographic association of these occurrences with quartz veins with Au could be coincidental, or it could indicate that the dike-hosted mineralization reflects limited interaction of a higher temperature fluid, capable of transporting Au and Si in addition to Cu and Ag, with a reactive pyrite-bearing host. The presence of strong quartz+tourmaline±epidote alteration proximal to both occurrences indicates that a significant hydrothermal—potentially magmato-hydrothermal—system was active in this region.

The volcanic-hosted redbed Cu occurrences are interpreted to reflect distal, low temperature mineralization related to the hydrothermal systems that were driven by the same heat responsible for polymetallic vein, epithermal, and porphyry mineralization. The relative abundances of these mineral occurrences could potentially be used in conjunction with other exploration tools to vector towards the centre of porphyry systems.

5. CONCLUSION

The NE-trending Skeena arch was first characterized as a paleotopographic high that formed during the Middle Jurassic without apparent deformation or plutonism (Tipper and Richards, 1976). It is now interpreted to reflect a fundamental, long-lived structural anisotropy that transects Stikine terrane beyond much of its Mesozoic history. This anisotropy contributed to strain localizing and to focused episodic magmatic activity from the Triassic to the Eocene. Northeast-trending foliations and folds in the Zymoetz Group, which are crosscut by Late Triassic to Early Jurassic intrusions, preserve an early phase of deformation that is aligned with the orientation of the arch. The strong preferential alignment of Late Triassic to Early Jurassic intrusions suggests that they were localized by crustal-scale magma conduits that may have been under transient extension (Nelson, 2017). Subsequent folds of the same orientation affect uppermost Upper Jurassic to Lower Cretaceous rocks of the Trout Creek assemblage. This second phase of deformation is interpreted to reflect reactivation of the Skeena arch anisotropy during sinistral transpressional plate convergence (Evenchick,

2001). The same crustal-scale anisotropy is interpreted to have remained a magma conduit into the Late Cretaceous and Eocene, contributing to the widespread porphyry and related mineralization across the Skeena arch.

The stratigraphic descriptions outlined herein support previous interpretations that the Skeena arch became a northeast-trending topographic highland between the Middle Jurassic and Early Cretaceous. Before the Middle Jurassic, this part of Stikine terrane was characterized by NW-trending volcanic belts. Laterally continuous, uppermost Triassic, tuff beds in the lower Telkwa Formation in the Howson Range contrast with coeval high-standing volcanic edifices to the west (Barresi et al., 2015b). The Telkwa Formation in the Howson Range represents the fringes of these stratovolcanoes; transitional to submarine deposition represented by the Babine shelf and Kotsine marine facies are farther east (Tipper and Richards, 1976). Submarine conditions persisted in the Middle Jurassic across most of Stikine terrane, extending as far south as Telkwa Pass in the western Skeena arch (Figure 2.1). The uppermost Upper Jurassic to Lower Cretaceous cobble conglomerate of the Trout Creek assemblage records uplift and erosion of the central Skeena arch. We speculate that the uplift of the Skeena arch as a paleotopographic high capable of shedding detritus to form the Trout Creek assemblage during the Late Jurassic is an early manifestation of the same strain that generated folds within the Trout Creek assemblage. The Skeena arch developed into a northeast-trending paleotopographic high because deformation was localized along a fundamental structural anisotropy of that orientation.

The structural anisotropy was also responsible for the mineral prospectivity of this region. Both Late Cretaceous and Eocene porphyry and related mineral occurrences, as well as newly-identified Middle Jurassic VMS occurrences, are dependent on magma emplacement into the upper crust. Barresi et al. (2015a) hypothesized that established structures, present in the northern Eskay rift but not in the southern portion, acted as efficient magma pathways allowing for the emplacement of hot, primitive magma into the upper crust which was capable of generating large hydrothermal cells and, ultimately, larger deposits. Although our samples from newly-recognized VMS-type occurrences lacked significant geochemical results for metals, the long-lasting structural anisotropy beneath the Skeena arch suggests that this region may also be prospective for Middle Jurassic rift-related VMS mineralization similar to the Eskay Creek deposit. Localization of Late Cretaceous and Eocene magmas along this northeasterly trending structural corridor is a first order constraint on porphyry and related mineralization within the Skeena arch.

6. ACKNOWLEDGEMENTS

This project benefited from the technical input and support of numerous individuals. Jeff Kyba provided invaluable insight during field traverses and late night discussions on the geology of central British Columbia. Guillaume Lesage, Alexina Boileau, Stephanie Fogg, and Joel Knickle provided excellent assistance in the field. Ryan Hinds and SilverKing Helicopters provided outstanding helicopter service. The MDRU operations team provided invaluable support: Johanna McWhirter with project management, Tarn Khare with administration, and Sara Jenkins and Mana Rahimi with GIS solutions and map layout. Glen Garratt and the entire Eastfield Resources team are thanked for their support and for access to drill core and thin sections from the Hobbes property. Thoughtful reviews of the report were provided by Brady Clift and Lawrence Aspler. Finally, we thank Stephanie and Peter McGuiness for their efforts in expediting and their unending hospitality.

7. REFERENCES

Alldrick, D. J., Nelson, J. L. and Barresi, T. (2005): Geology and Mineral Occurrences of the Upper Iskut River Area: Tracking the Eskay Rift through Northern British Columbia (Telegraph Creek NTS 104G/1, 2; Iskut River NTS 104B/9, 10, 15, 16); *in* Geological Fieldwork 2004, British Columbia Ministry of Energy and Mines, British Columbia Geological Survey Paper 2005-1, p. 1–30.

AMEC (2009): Overall geotechnical evaluation of proposed Northern Gateway Pipeline Route; for Northern Gateway Pipelines Inc., available at https://www.acee-ceaa.gc.ca/050/documents_staticpost/cearref_21799/2213/Volume3/Vol_3_Appendix_E-1.pdf

Angen, J. J. (2009): Geospatial Structural Analysis of the Terrace Area, West-Central British Columbia (NTS 103I/08, 09, 10, 16); *in* Geological Fieldwork 2008, British Columbia Ministry of Energy and Mines, British Columbia Geological Survey Paper 2009-1, p. 21–34.

Angen, J. J., Nelson, J. L., Rahimi, M. and Hart, C. J. R. (2017): Mapping in the Tatsi and Zymo ridge areas of west-central British Columbia: Implications for the origin and history of the Skeena arch; *in* Geological Fieldwork 2016, British Columbia Ministry of Energy and Mines, British Columbia Geological Survey Paper 2017-1, p. 35–48.

Angen, J. J., Rahimi, M., Nelson, J. L. and Hart, C. J. R. (2019a): Bedrock geology, Search phase I project area, western Skeena arch, west-central British Columbia; Geoscience BC Map 2019-03-01, MDRU Map 17-2018 and BCGS Open File 2019-07, scale 1:150 000.

Angen, J. J., Rahimi, M., Nelson, J. L. and Hart, C. J. R. (2019b): Aeromagnetic correlation with bedrock geology, Search phase I project area, western Skeena arch, west-central British Columbia; Geoscience BC Map 2019-03-02, MDRU Map 18-2018 and BCGS Open File 2019-08, scale 1:150 000.

Barresi, T. (2015): Tectono-magmatic and metallogenic evolution of the late Triassic to middle Jurassic Hazelton Group in northwest British Columbia; unpublished MSc thesis, Dalhousie University.

Barresi, T., Nelson, J. L., Dostal, J. and Gibson, H. (2015a): Geochemical constraints on magmatic and metallogenic processes: Iskut River Formation, volcanogenic massive sulfide-hosting basalts, NW British Columbia, Canada; Canadian Journal of Earth Sciences, v. 52, p. 1–20.

Barresi, T., Nelson, J. L., Dostal, J., Friedman, R. and Gibson, H. (2015b): Evolution of the Hazelton arc near Terrace, British Columbia: stratigraphic, geochronological, and geochemical constraints on a Late Triassic – Early Jurassic arc and Cu–Au porphyry belt; Canadian Journal of Earth Sciences, v. 52, p. 466–494.

Bassett, K. N. (1995): A basin analysis of the Lower to mid-Cretaceous Skeena Group, west-central British Columbia: implications for regional tectonics and terrane accretion; unpublished MSc thesis, University of Minnesota.

Bassett, K. N. and Kleinspehn, K. L. (1996): Mid-Cretaceous transtension in the Canadian Cordillera: Evidence from the Rocky Ridge volcanics of the Skeena Group; Tectonics, v. 15, p. 727–746.

Bassett, K. N. and Kleinspehn, K. L. (1997): Early to middle Cretaceous paleogeography of north central British Columbia: stratigraphy and basin analysis of the Skeena Group; Canadian Journal of Earth Sciences, v. 34, p. 1644–1669.

Boghossian, N. D. and Gehrels, G. E. (2000): Nd isotopic signature of metasedimentary pendants in the Coast Mountains between Prince Rupert and Bella Coola, British Columbia; Geological Society of America Special Paper 343, p. 77–87.

Breitsprecher, K. and Mortensen, J. K. (2004): BC Age 2004A-1: A database of isotopic age determinations for rock units from British Columbia; BC Ministry of Energy and Mines, BC Geological Survey, Open File 2004-03 (Release 2.0), 7766 records.

Brown, A. C. (1992): Sediment-hosted Stratiform Copper Deposits; Geoscience Canada, v. 19, p. 125–141.

Brown, D. A., Logan, J. M., Gunning, M. H., Orchard, M. J. and Bamber, W. E. (1991): Stratigraphic evolution of the Paleozoic Stikine Assemblage in the Stikine and Iskut rivers area, northwestern British Columbia; Canadian Journal of Earth Sciences, v. 28, p. 958–972.

Carter, N. C. (1974): Geology and geochronology of porphyry copper and molybdenum deposits in west-central British Columbia; unpublished PhD thesis, The University of British Columbia.

Carter, N. C. (1981): Porphyry copper and molybdenum deposits, west-central British Columbia; BC Ministry of Energy and Mines, Bulletin 64, 150 p.

Carter, N. C. and Kirkham, R. V. (1969): Geological Compilation Map of the Smithers, Hazelton, and Terrace Areas, BC, (parts of NTS 93L, M and 103I); Dept. of Mines & Petroleum Resources, Map 69-1.

Church, B. N. (1971): Geology of the Owen Lake, Parrott Lakes, and Goosly Lake area; *in* Geology Exploration and Mining in British Columbia 1970, BC Ministry of Energy and Mines, BC Geological Survey, p. 119–125.

Colpron, M. C. and Nelson, J. L. (2011): A digital atlas of terranes for the northern Cordillera; accessed online from Yukon Geological Survey (www.geology.gov.yk.ca).

Cui, Y. and Russell, J. K. (1995): Magmatic origins of calc-alkaline intrusions from the Coast Plutonic Complex, southwestern British Columbia; Canadian Journal of Earth Sciences, v. 32, p. 1643–1667.

Cui, Y., Miller, D. M., Schiarizza, P. and Diakow, L. J. (2017): British Columbia digital geology; BC Ministry of Energy and Mines, BC Geological Survey, Open File 2017-8, 9 p.

Desjardins, P., Lyons, L., Pattenden, S., MacIntyre, D. G. and Hunt, J. A. (1990a): Geology of the Thautil River area; Ministry of Energy and Mines, Open File Map 1990-5, scale 1:50 000.

Desjardins, P., MacIntyre, D. G., Hunt, J. A., Lyons, L. and Pattenden, S. (1990b): Geology of the Thautil River map area (93L/6); *in* Geological Fieldwork 1989, British Columbia Ministry of Energy and Mines, British Columbia Geological Survey Paper 1990-1, p. 91–99.

Deyell, C. L., Thompson, J. F. H., Friedman, R. M. and Groat, L. A. (2000): Age and origin of advanced argillic alteration zones and related exotic limonite deposits in the Limonite Creek area, central British Columbia; Canadian Journal of Earth Sciences, v. 37, p. 1093–1107.

Diakow, L. J., Webster, I. C. L., Richards, T. A. and Tipper, H. W. (1997): Geology of the Fawnie and Nechako ranges,

southern Nechako Plateau, central British Columbia (93F/2,3,6,7); *in* Diakow, L. J., Metcalfe, P. and Newell, J. (eds.), Interior Plateau Geoscience Project: Summary of Geological, Geochemical and Geophysical Studies (NTS 092N; 092O; 093B; 093C; 093F; 093G; 093K), BC Ministry of Energy and Mines, Paper 1997-2, p. 7–30.

Duffell, S. (1959): Whitesail Lake Map-Area, British Columbia; Geological Survey of Canada, Memoir 299, 123 p.

Duffell, S. and Souther, J. G. (1964): Geology of Terrace Map-Area, British Columbia; Geological Survey of Canada, Memoir 329.

Evenchick, C. (1979): Stratigraphy, structure, and metamorphism of the Atna Peak area, British Columbia; unpublished BSc thesis, Carleton University.

Evenchick, C. A. (1991): Geometry, evolution, and tectonic framework of the Skeena fold belt, north central British Columbia; Tectonics, v. 10, p. 527–546.

Evenchick, C. A. (2001): Northeast-trending folds in the western Skeena Fold Belt, northern Canadian Cordillera: a record of Early Cretaceous sinistral plate convergence; Journal of Structural Geology, v. 23, p. 1123–1140.

Evenchick, C. A. and Thorkelson, D. (2005): Geology of the Spatsizi River map area, north-central British Columbia; Geological Survey of Canada, Bulletin 577, p. 276.

Evenchick, C. A., Poulton, T. P. and McNicoll, V. J. (2010): Nature and significance of the diachronous contact between the Hazelton and Bowser Lake groups (Jurassic), north-central British Columbia; Bulletin of Canadian Petroleum Geology, v. 58, p. 235–267.

Evenchick, C. A., Mustard, P. S., McMechan, M., Ritcey, D. H. and Smith, G. T. (2008): Geology, northeast Terrace and northwest Smithers, British Columbia; Geological Survey of Canada, Open File 2008-10, scale 1:125 000.

Ferri, F., Mustard, P. S., McMechan, M., Ritcey, D., Smith, G. T., Boddy, M. and Evenchick, C. (2005): Skeena and Bowser Lake groups, west half Hazelton map area (93M); in Summary of Activities 2005, BC Ministry of Energy and Mines, p. 113–131.

Friedman, R. and Panteleyev, A. (1997): U-Pb age of mineralized feldspar porphyry sills at the Louise Lake Cu-Mo-Au-As deposit, Smithers map area, west-central British Columbia (NTS 93L); *in* Geological Fieldwork 1996, British Columbia Ministry of Energy and Mines, British Columbia Geological Survey Paper 1997-1, p. 227–232.

Friedman, R. M. and Armstrong, R. L. (1995): Jurassic and Cretaceous Geochronology of the Southern Coast Belt, British Columbia, 49° to 51° N, *in* Miller, D.M. and Busby, C. (eds.), Jurassic Magmatism and Tectonics of the North American Cordillera; Geological Society of America Special Paper 299, p. 95–121.

Gabrielse, H. and Yorath, C. J. (1991): Tectonic Synthesis, in Geology of the Cordilleran Orogen in Canada (G2); DNAG, Geology of North America, Geological Society of America.

Gagnon, J. F. (2010): Stratigraphic and Tectonic Evolution of the Jurassic Hazelton Trough–Bowser Basin, Northwest British Columbia, Canada; unpublished PhD thesis, University of Alberta.

Gagnon, J. F., Barresi, T., Waldron, J. W. F., Nelson, J. L., Poulton, T. P. and Cordey, F. (2012): Stratigraphy of the upper Hazelton Group and the Jurassic evolution of the Stikine terrane, British Columbia; Canadian Journal of Earth Sciences, v. 49, p. 1027–1052.

Gareau, S. A., Friedman, R. M., Woodsworth, G. J. and Childe, F. (1997): U-Pb ages from the northeastern quadrant of Terrace map area, west-central British Columbia; Geological Survey of Canada; Geological Survey of Canada, Current Research no. 1997-A/B, 1997 p. 31–40. doi: 10.4095/208598

Garwin, S., Hall, R. and Watanabe, Y. (2005): Tectonic setting, geology, and gold and copper mineralization in Cenozoic magmatic arcs of Southeast Asia and the West Pacific; *in* Hedenquist, J.W., Thompson, J.F.H., Goldfarb, R.J. and Richards, J.R. (eds.), Economic Geology One Hundredth Anniversary Volume, Society of Economic Geologists.

Gehrels, G.E. (2001): Geology of the Chatham Sound region, southeast Alaska and coastal British Columbia; Canadian Journal of Earth Sciences, v. 38, p. 1579–1599.

Gehrels, G., Rusmore, M., Woodsworth, G., Crawford, M., Andronicos, C., Hollister, L., Patchett, J., Ducea, M., Butler, R., Klepeis, K., Davidson, C., Friedman, R., Haggart, J., Mahoney, B., Crawford, W., Pearson, D. and Girardi, J. (2009): U-Th-Pb geochronology of the Coast Mountains batholith in north-coastal British Columbia: constraints on age and tectonic evolution; Geological Society of America Bulletin, v. 121, p. 1341–1361.

Glen, R. A. and Walshe, J. L. (1999): Cross-structures in the Lachlan orogen: The Lachlan transverse zone example; Australian Journal of Earth Sciences, v. 46, p. 641–658.

Goeppel, N. and Turna, R. (2017a): Geological and geochemical assessment report on the Midas property, Skeena Mining

Division, British Columbia; Ministry of Energy and Mines, Assessment Report 36876, 434 p.

Goeppel, N. and Turna, R. (2017b): Geological, geochemical and geophysical assessment report on the Copperhead property, Omineca Mining Division, British Columbia; BC Ministry of Energy and Mines, Assessment Report 36901, 195 p.

Gow, P. A. and Walshe, J. L. (2005): The role of preexisting geologic architecture in the formation of giant porphyry-related Cu±Au deposits: Examples from New Guinea and Chile; Economic Geology, v. 100, p. 819–833.

Grauch, V. J. S. and Campbell, D. L. (1984): Does draping aeromagnetic data reduce terrain-induced effects?; Geophysics, v. 49, p. 75–80.

Gunning, M. H., Bamber, E. W., Brown, D. A., Rui, L., Mamet, B. L., and Orchard, M. J. (1994): The Permian Ambition Formation of northwestern Stikinia, British Columbia; *in* Embry, A. F., Beauchamp, B. and Glass, D. J. (eds.), Pangea: Global Environments and Resources; Canadian Society of Petroleum Geologists, Memoir 17, p. 589–619.

Hanson, D. J. and Klassen, R. W. (1995): The Louise Lake copper-molybdenum-gold-arsenic high-level porphyry system, west-central British Columbia. *in*: Schroeder, T. G. (ed.), Porphyry Deposits of the Northwestern Cordillera of North America, Special Volume 46, Canadian Institute of Mining, Metallurgy and Petroleum, p. 416–421.

Heah, T. S. T. (1991): Mesozoic ductile shear and Paleogene extension along the eastern margin of the Central Gneiss Complex, Coast Belt, Shames River area, near Terrace, British Columbia; unpublished M.Sc. thesis, The University of British Columbia, 155 p.

Heidrick, T. L. and Titley, S. R. (1982): Fracture and dike patterns in Laramide plutons and their structure and tectonic implications, American Southwest; *in* Advances in Geology of the porphyry copper deposits, University of Arizona Press.

Israel, S., Schiarizza, P., Kennedy, L. A., Friedman, R. M. and Villeneuve, M. (2006): Evidence for Early to Late Cretaceous sinistral deformation in the Tchaikazan River area, southwestern British Columbia: Implications for the tectonic evolution of the southern Coast belt; *in* Haggart, J. W., Enkin, R. J. and Monger, J. W. H. (eds.), Paleogeography of the North American Cordillera: Evidence For and Against Large-Scale Displacements; Geological Association of Canada, Special Paper 46, p. 331–350.

Israel, S., Beranek, L., Friedman, R. M. and Crowley, J. L. (2014): New ties between the Alexander terrane and Wrangellia and implications for North America Cordilleran evolution; Lithosphere, v. 6, p. 270–276. doi: 10.1130/L364.1

Kapp, P. A. and Gehrels, G. R. (1998): Detrital zircon geochronology and regional correlation of metasedimentary rocks in the Coast Mountains, southeastern Alaska; Canadian Journal of Earth Sciences, v. 5, p. 269–279.

Kruse, S. and Stuart, D. (2017): Juggernaut discovers new zones with channel samples grading 11.2 grams per tonne gold equivalent over 4.6 metres, 16.8 grams per tonne gold equivalent over 5 metres, and 59 grams per tonne gold equivalent over 2 metres, in outcrop on empire, Juggernaut Exploration Limited, Press Release, November 29, 2017.

Lefebure, D. and Church, B. N. (1996): Polymetallic Veins Ag-Pb-Zn+/-Au; *in* Lefebure, D. and Höy, T. (eds.), Selected British Columbia Mineral Deposit Profiles, Volume 2 - Metallic Deposits, BC Ministry of Energy and Mines, Open File 1996-13, p. 67–70.

Luyendyk, A. P. (1997): Processing of airborne magnetic data; AGSO Journal of Australian Geology and Geophysics, v. 17, p. 31–38.

Mahoney J. B., Gordee, S. M., Haggart, J. W., Friedman, R. M., Diakow, L. J. and Woodsworth, G. J. (2009): Magmatic evolution of the eastern Coast plutonic complex, Bella Coola region, west-central British Columbia, Geological Society of America, Bulletin, v. 121, p. 1362–1380.

MacIntyre, D. G. (1985): Geology and mineral deposits of the Tahtsa Lake district west central British Columbia; BC Ministry of Energy and Mines, BC Geological Survey, Bulletin 75, 79 p.

MacIntyre, D. G. (2006): Geology and Mineral Deposits of the Skeena Arch, West-Central British Columbia: A Geoscience BC Digital Data Compilation Project; *in* Geological Fieldwork 2005, British Columbia Ministry of Energy and Mines, British Columbia Geological Survey Paper 2006-1, p. 303–312.

MacIntyre, D. G. (2007): Geology and Mineral Deposits of the Skeena Arch, West-Central British Columbia (Parts of NTS 093E, L, M; 094D; 103I, P) Update on a Geoscience BC Digital Data Compilation Project; *in* Geological Fieldwork 2006, British Columbia Ministry of Energy and Mines, British Columbia Geological Survey Paper 2007-1, p. 333–340.

MacIntyre, D. G. and Villeneuve, M. E. (2001): Geochronology of mid-Cretaceous to Eocene magmatism, Babine porphyry copper district, central British Columbia; Canadian Journal of Earth Sciences, v. 38, p. 639–655.

MacIntyre, D. G., Ash, C. and Britton, J. (1994): Skeena Arcview Data (NTS 93E,L,M; 94D, 104A,B, 103G,H,I,J,P); BC Ministry of Energy and Mines, Open File 1994-14.

MacIntyre, D. G., Desjardins, P. and Tercier, P. (1989a): Jurassic stratigraphic relationships in the Babine and Telkwa ranges (93W10, 11; 14, 15); *in* Geological Fieldwork 1988, British Columbia Ministry of Energy and Mines, British Columbia Geological Survey Paper 1989-1, p. 195–208.

MacIntyre, D. G., Desjardins, P., Tercier, P. and Koo, J. (1989b): Geology of the Telkwa River area, NTS 93L/11; BC Ministry of Energy and Mines, Open File Map 1989-16, scale 1:50 000.

MacIntyre, D. G., Villeneuve, M. E. and Schiarizza, P. (2001): Timing and tectonic setting of Stikine Terrane magmatism, Babine–Takla lakes area, central British Columbia; Canadian Journal of Earth Sciences, v. 38, p. 579–601.

McClelland, W. C. and Gehrels, G. E. (1990): Geology of the Duncan Canal shear zone: Evidence for Early to Middle Jurassic deformation of the Alexander terrane, southeastern Alaska; Geological Society of America Bulletin, v. 102, p. 1378–1392.

McKeown, M., Nelson, J. and Friedman, R. (2008): Newly Discovered Volcanic-Hosted Massive Sulphide Potential within Paleozoic Volcanic Rocks of the Stikine Assemblage, Terrace Area, Northwestern British Columbia (NTS 103I/08); *in* Geological Fieldwork 2007, British Columbia Ministry of Energy and Mines, British Columbia Geological Survey Paper 2008-1, p. 102–116.

McMechan, M. (2007): Nature, origin and tectonic significance of anomalous transverse structures, southeastern Skeena Fold Belt, British Columbia; Bulletin of Canadian Petroleum Geology, v. 55, p. 262–274.

Mihalynuk, M. G. (1987): Metamorphic, structural and stratigraphic evolution of the Telkwa Formation: Zymoetz River area (NTS 103 I/8 and 93L/5), near Terrace, British Columbia. MSc thesis, University of Calgary. doi:10.11575/PRISM/11828.

MINFILE (2020): MINFILE digital data; British Columbia Ministry of Energy and Mines, British Columbia Geological Survey, https://www.minfile.ca

Monger, J. W. H. (1977): Upper Paleozoic rocks of the western Canadian Cordillera and their bearing on Cordilleran evolution; Canadian Journal of Earth Sciences, v. 14, p. 1831–1858. doi: 10.1139/e77-156

Monger, J. W. H., Price, R. A. and Tempelman-Kluit, D. J. (1982): Tectonic accretion and the origin of the two major metamorphic and plutonic welts in the Canadian Cordillera; Geology, v. 10, p. 70–75.

Monger, J. W. H., Wheeler, J. O., Tipper, H. W., Gabrielse, H., Harms, T., Struik, L. C., Campbell, R. B., Dodds, C. J., Gehrels, G. and O'Brien, J. (1991): Upper Devonian to Middle Jurassic assemblages, Part B: Cordilleran terranes; *in* Gabrielse, H. and Yorath, C. J. (eds.), Geology of the Cordilleran Orogen in Canada, Geological Survey of Canada, p. 281–327.

Nelson, J. L. (2017): Composite pericratonic basement of west-central Stikinia and its influence on Jurassic magma conduits: examples from the Terrace-Ecstall and Anyox areas; *in* Geological Fieldwork 2016, British Columbia Ministry of Energy and Mines, British Columbia Geological Survey Paper 2017-1, p. 61–82.

Nelson, J. L. (2009): Terrace project year 4: Extension of Paleozoic volcanic belt and indicators of VMS-style mineralization near Kitimat, NTS 103I/02, 07; *in* Geological Fieldwork 2008, British Columbia Ministry of Energy and Mines, British Columbia Geological Survey Paper 2009-1, p. 7–20.

Nelson, J. L. and Friedman, R. (2017): U-Pb and geochemical data from late Paleozoic and Jurassic rocks of western Stikinia and the Coast Mountains; British Columbia Ministry of Energy and Mines, British Columbia Geological Survey GeoFile 2017-1.

Nelson, J. L. and Kennedy, R. (2007): Terrace regional mapping project year 2: new geological insights and exploration targets (NTS 103I/16S, 10W), west-central British Columbia; *in* Geological Fieldwork 2006, British Columbia Ministry of Energy and Mines, British Columbia Geological Survey Paper 2007-1, p. 149–162.

Nelson, J. L., Barresi, T., Knight, E., and Boudreau, N. (2006): Geology and mineral potential of the Usk Map area (NTS 103I/09), Terrace, British Columbia; *in* Geological Fieldwork 2005, British Columbia Ministry of Energy and Mines, British Columbia Geological Survey Paper 2006-1, p. 117–134.

Nelson, J. L., Colpron, M. and Murphy, D. C. (2007): Northern Cordilleran terranes and their interactions through time; GSA Today: v. 17, no. 4/5, p. 4–10. doi: 10.1130/GSAT01704-5A.1.

Nelson, J. L., Kyba, J., McKeown, M. A. and Angen, J. J. (2008a): Terrace regional mapping project, year 3: contributions to stratigraphic, structural and exploration concepts, Zymoetz River to Kitimat River, east-central British Columbia (NTS

103I/08); *in* Geological Fieldwork 2007, British Columbia Ministry of Energy and Mines, British Columbia Geological Survey Paper 2008-1, p. 159–174.

Nelson, J. L., Kyba, J., McKeown, M. A. and Angen, J. J. (2008b): Geology of the Chist Creek map area (NTS 103I/08); BC Ministry of Energy and Mines, BC Geological Survey, Open File 2008-3, scale 1:50 000.

Nelson, J. L., Colpron, M. and Israel, S. (2013): The Cordillera of British Columbia, Yukon and Alaska: Tectonics and metallogeny, *in* Colpron, M., Bissig, T., Rusk, B.G. and Thompson, J. F., (eds.), Tectonics, Metallogeny and Discovery: The North American Cordillera and Similar Accretionary Settings. Society of Economic Geologists Special Publication, 17, Chapter 3, p. 53–103.

Pálfy, J., Mortensen, J. K., Smith, P. L., Friedman, R. M., McNicoll, V. and Villeneuve, M. (2000): New U-Pb zircon ages integrated with ammonite biochronology from the Jurassic of the Canadian Cordillera; Canadian Journal of Earth Sciences, v. 37, p. 549–567.

Palsgrove, R. J. and Bustin, R. M. (1991): Stratigraphy, sedimentology and coal quality of the lower Skeena Group, Telkwa coalfield, central British Columbia (NTS 093L/11); BC Ministry of Energy and Mines, BC Geological Survey, Paper 1991-2, 59 p.

Patchett, P. J. and Gehrels, G. E. (1998) Continental Influence on Canadian Cordilleran Terranes from Nd Isotopic Study, and Significance for Crustal Growth Processes; The Journal of Geology, v. 106, p. 269–280. doi: 10.1086/516021.

Precision Geosurveys Inc. (2016): Search Project 2015 Airborne Magnetic Survey; Geoscience BC, Report 2016-02, 29 p.

Rahimi, M., Angen, J. J. and Hart, C. J. R. (2018): Application of ASTER Data to Identify Potential Alteration Zones on Microwave Ridge, Northeastern Search Project Area, West-Central British Columbia (part of NTS 093L); *in* Geoscience BC Summary of Activities 2017: Minerals and Mining, Geoscience BC, BC Geological Survey, Paper 2018-1, p. 7–22.

Read, P. B. (1983): Geology, Classy Creek (10J/2E) and Stikine Canyon (104J/1W), British Columbia; BC Ministry of Energy and Mines, BC Geological Survey, Open File 940.

Read, P. B. (1984): Geology Clastline River (I04G/lCE), Blue Lake, 104W/3W), Cake Hill, 104V/4W), and Stikine Canyon(104J/lE), British Columbia; Geological Survey of Canada, Open File 1080.

Read, P. B., Brown, R. L., Psutka, J. F., Moore, J. M., Journeay, J. M., Lane, R. A. and Orchard, M. J. (1989): Geology, More and Forrest Kerr creeks [parts of 104B/10, 15, 16 and 104G/1, 2]; Geological Survey of Canada, Open File 2094.

Richards, J. P. (2000): Lineaments revisited, Society of Economic Geologists Newsletter, v. 42, no. 1, p. 14–20.

Richards, J. P., Boyce, A. and Pringle, M. (2001): Geologic Evolution of the Escondida Area, Northern Chile: A Model for Spatial and Temporal Localization of Porphyry Cu Mineralization; Economic Geology, v. 96. doi: 10.2113/96.2.271.

Richards, T. A. (1990): Geology and mineral deposits of Hazelton [93M] map area, British Columbia; Geological Survey of Canada, Open File 2322. doi: 10.4095/131315.

Richards, T. A. and Tipper, H. W. (1976): Geology of Smithers Map-Area, British Columbia; Geological Survey of Canada, Open File 351, scale 1:250 000.

Roddick, J. A. (1983): Geophysical review and composition of the Coast Plutonic Complex, south of latitude 55°N, *in* Circum-Pacific Plutonic Terranes, Roddick, J. A. (ed.), Geological Society of America Memoir 159, p. 192–211.

Ryan, B. D. (1993): Geology of the Telkwa Coalfield, British Columbia; BC Ministry of Energy and Mines, BC Geological Survey, Open File 1993-21, scale 1:20 000.

Samson, S. D., Patchett, P. J., McClelland, W. C., Gehrels, G. E. (1991): Nd and Sr isotopic constraints on the petrogenesis of the west side of the northern Coast Mountains batholith, Alaskan and Canadian Cordillera; Canadian Journal of Earth Sciences, v. 28, p. 939–946.

Sánchez, M. G., Allan, M. M., Hart, C. J. R. and Mortensen, J. K. (2014): Extracting ore-deposit-controlling structures from aeromagnetic, gravimetric, topographic, and regional geologic data in western Yukon and eastern Alaska; Interpretation, v. 2, p. SJ75–SJ102.

Schmitt, H. A. (1966): The porphyry copper deposits in their regional setting. Geology of the Porphyry Copper Deposits-Southwestern North America; University of Arizona Press, v. 17, 34 p.

Slack, J. F. (1996): Tourmaline associations with hydrothermal ore deposits; Reviews in Mineralogy and Geochemistry, v. 33, p. 559–643.

Smith, G. T. and Mustard, P. S. (2005): The southern contact of the Bowser Lake and Skeena groups: unconformity or transition?; *in* Summary of Activities 2005, BC Ministry of Energy and Mines, BC Geological Survey, p. 152–156.

Smith, G. T. and Mustard, P. S. (2006): Supporting evidence for a conformable southern contact of the Bowser Lake and Skeena groups; *in* Summary of Activities 2006, BC Ministry of Energy and Mines, BC Geological Survey, p. 125–134.

Souther, J. G. (1972): Telegraph Creek Map Area, British Columbia; Geological Survey of Canada, Paper 71-44, 38 p.

Struik, L. C. and MacIntyre, D. G. (2001): Introduction to the special issue of Canadian Journal of Earth Sciences: The Nechako NATMAP Project of the central Canadian Cordillera; Canadian Journal of Earth Sciences, v. 38, p. 485–494.

Sutherland Brown, A. (1960): Geology of the Rocher Deboule Range; BC Ministry of Energy and Mines, BC Geological Survey, Bulletin 43, 78 p.

Tennant, S. J. and Tompson, W. D. (1995): Geological, geophysical and diamond drilling assessment report on the Tatsi gold-silver-copper prospect, Kitnayakwa River area, Omineca Mining Division, British Columbia; BC Ministry of Energy and Mines, Assessment Report 24175, 186 p.

Thomson, R. C., Smith, P. L. and Tipper, H. W. (1986): Lower to Middle Jurassic (Pliensbachian to Bajocian) stratigraphy of the northern Spatsizi area, north-central British Columbia; Canadian Journal of Earth Sciences, v. 23, p. 1943–1973.

Tipper, H. W. and Richards, T. A. (1976): Jurassic stratigraphy and history of north-central British Columbia; Geological Survey of Canada, Bulletin 270, 73 p.

Tosdal, R. M. and Richards, J. P. (2001): Magmatic and structural controls on the development of porphyry Cu±Mo±Au deposits; in Structural Controls on Ore Genesis; Reviews in Economic Geology, v. 14, p. 157–181. doi: 10.5382/Rev.14.06

van der Heyden, P. (1989): U-Pb and K-Ar geochronometry of the Coast Plutonic Complex, 53°N to 54°N, British Columbia, and implications for the Insular-Intermontane superterrane boundary; unpublished PhD thesis, The University of British Columbia, 526 p.

van der Heyden, P. (1992): A Middle Jurassic to early Tertiary Andean-Sierran arc model for the Coast Belt of British Columbia; Tectonics, v. 11, p. 82–97. doi: 10.1029/91TC02183.

van Straaten, B. I. and Nelson, J. L. (2016): Syncollisional late Early to early Late Jurassic volcanism, plutonism, and porphyry-style alteration on the northeastern margin of Stikinia; *in* Geological Fieldwork 2015, British Columbia Ministry of Energy and Mines, British Columbia Geological Survey Paper 2016-1, p. 113–143.

van Straaten, B. I. and Gibson, R. (2017): Late Early to Middle Jurassic Hazelton Group volcanism and mineral occurrences in the McBride-Tanzilla area, northwest British Columbia; *in* Geological Fieldwork 2016, British Columbia Ministry of Energy and Mines, British Columbia Geological Survey Paper 2017-1, p. 83–115.

Wanless, R. K., Stevens, R. D., Lachance, G. R. and Delabio, R. N. (1973): Age determinations and geological studies K-Ar isotopic ages, Report 11; Geological Survey of Canada, 139 p.

Wanless, R. K., Stevens, R. D., Lachance, G. R. and Delabio, R. N. (1974): Age determinations and geological studies K-Ar Isotopic ages, Report 12; Geological Survey of Canada, 78 p.

Wasteneys, H. and Yang, W. (2013): Technical report on stream sediment geochemistry for the Blackberry Creek Property; British Columbia Ministry of Energy and Mines, Assessment Report 33734, 199 p.

Woodsworth, G. J., Anderson, R. G. and Armstrong, R. L. (1991): Plutonic Regimes; *in* Gabrielse, H., and Yorath, C. J. (eds.), Geology of the Cordilleran Orogen in Canada, Geological Survey of Canada, p. 491–531.

Woodsworth, G. J., Hill, M. L. and van der Heyden, P. (1985): Preliminary geologic map of Terrace (NTS 103I East Half) map area, British Columbia; Geological Survey of Canada, Open File 1136, scale 1:125 000.

8. APPENDICES

Report accompanied by digital appendices (in boxes).

Appendix A. U-Pb Geochronology

A total of 14 samples were collected for U-Pb zircon geochronology. One is a detrital zircon sample and the remaining 13 are igneous samples. They were analyzed via Laser Ablation Inductively Coupled Plasma Mass Spectrometry (LA-ICP-MS) at the Pacific Centre for Isotopic and Geochemical Research (PCIGR) at The University of British Columbia.

Analytical Techniques

Zircon was separated from up to 20 kg samples according to standard methods including jaw crushing, disc milling, Wilfley™ table concentration, heavy liquids, and Frantz™ Isodynamic Magnetic separator. For igneous samples, approximately 30 zircons per sample (or as many as could be recovered if less than 30) were hand-picked under ethanol, mounted in 2.54 cm epoxy resin rounds, and polished to expose cross-sections. For the detrital zircon sample, all of the grains that could be recovered were mounted and polished. Zircons were imaged using a scanning electron microscope in cathodoluminescence (CL) mode to identify potential core and rim features as well as metamict zones and inclusions. Twenty zircons were analyzed per igneous sample with grains and ablation tracks selected to avoid the aforementioned features. All of the detrital grains were analysed. Prior to analyses, pucks were washed with dilute nitric acid and rinsed with de-ionized water. Analyses were carried out using a New Wave 213nm Nd-YAG laser in a New Wave 'Supercell' ablation chamber with data collection on a Thermo Finnigan Element2 ICP-MS. U-Pb isotopic concentrations and compositions were calibrated to zircon standard Plešovice [337.13 ± 0.37 Ma; (Sláma et al., 2008)] with analysis of Temora 2 [416.8 ± 1 Ma; (Black et al., 2004)] to assess quality control. Data reduction was carried out in Iolite 3.1 (Paton et al., 2011) using the VizualAge data reduction scheme (Petrus and Kamber, 2012). Time-resolved data were examined alongside CL images with ablation tracks plotted to identify and avoid portions of the signal that reflected potential Pb loss and/or the presence of older inherited cores or inclusions.

Results

Results of individual zircon analyses for igneous samples are presented in Table A.1. Results for individual detrital zircon grains are presented in Table A.2. Graphical plots, which are presented in the main text and final age calculations, which are summarized in Table 2.1, were produced using Isoplot 3.75 (Ludwig, 2012). In all graphical results, blue analyses were excluded from final age interpretations due to large errors, discordance, or interpretation as an inherited grain. Discordance was assessed in conjunction with analytical uncertainty following the procedure of Spencer et al. (2016); data that do not overlap Concordia at 2σ are considered discordant and are rejected from final age calculations. While the discordant data reflect some form of isotopic disturbance, the disturbance has a much greater influence on the $^{207}Pb/^{235}U$ ratio due to the low initial concentration of ^{235}U. Final ages reported in the text are weighted mean $^{206}Pb/^{238}U$ ages because all of the analyzed samples are much younger than 1.2 Ga (Gehrels et al., 2008). There does not appear to be a significant effect in the $^{206}Pb/^{238}U$ ratio of any of the discordant analyses so they could reasonably be included in the final age calculations; however, the influence of doing so would be negligible on the resulting age interpretations. If greater precision is desired, reanalysis via thermal ionization mass spectrometry is recommended.

Table A.1: U-Pb isotopic data from LA-ICP-MS analyses on zircon. Rho is error correlation coefficient. Decay constants are from Jaffey et al. (1971). Data are not corrected for common Pb.

Table A.2: U-Pb isotopic data from LA-ICP-MS analyses on detrital zircon grains. Rho is error correlation coefficient. Decay constants are from Jaffey et al. (1971). Data are not corrected for common Pb.

Appendix B. Magnetic Susceptibility

Magnetic susceptibility measurements were collected on outcrop exposures using a KT-9 (Exploranium Radiation Detection Systems, 1997) Kappameter. The KE-9 has an inductive coil diameter of 65 mm and utilizes an operating frequency of 10 kHz. It has a reported sensitivity of 1 x 10^{-5} SI units when used in standard mode on a flat surface (Exploranium Radiation Detection Systems, 1997). All measurements were collected in pin mode, where a pin holds the measuring coil a fixed distance above the surface of the rock, and a correction factor is applied to account for the separation. This is deemed to provide the most accurate value for rough surfaces if a minimum of five measurements are averaged (Exploranium Radiation Detection Systems, 1997). When operating in pin mode, a typical accuracy of ± 10% compared to laboratory measured values is estimated for the KT-9 Kappameter (Exploranium Radiation Detection Systems, 1997).

A total of ten measurements were collected within a single rock type at each station. If two major lithologies were present at an outcrop, they were treated separately. Care was taken to measure only reasonably flat, fresh surfaces. Measurements were randomly distributed across an approximately 25 m^2 area where possible. Limited outcrop exposure restricted the measurement area at some stations. All measurements as well as mininum, maxinum, and median values for each outcrop are compiled in Table B.1. The median value for each station is interpreted as the most likely value to correlate with readings obtained from airborne data.

Table B.1: Magnetic susceptibility data collected in the field.

Appendix C. Geochemistry

Exploration geochemistry

A total of 21 samples were collected for base and precious metal assays. Rock samples were sent to Bureau Veritas Ltd in Vancouver in two batches, one in 2014 and one in 2015, for processing and analysis.

Analytical Techniques

One kg of each sample was first crushed to 70% passing a 2 mm screen and then a 250g split was pulverized to 85% passing a 75 µm screen. A 0.5g split was digested in modified aqua regia (1:1:1 HNO_3:HCl:H_2O) and analyzed via ICP-MS for a suite of 37 elements. One sample was over limit for Cu. A 1 g split of this sample was digested in aqua regia and analysed via atomic absorption spectroscopy (AAS). The Bureau Veritas Ltd internal QAQC procedure was considered sufficient for these samples as they were collected to provide an initial indication of prospectivity only.

Results

The combined results of ICP-MS and AAS analyses are presented in Table C.1

Table C.1: Complete exploration geochemistry assay results for the Search project. Method codes correspond to Bureau Veritas analytical codes.

References

Black, L. P., Kamo, S. L., Allen, C. M., Davis, D. W., Aleinikoff, J. N., Valley, J. W., Mundil, R., Campbell, I. H., Korsch, R. J., Williams, I. S., and Foudoulis, C. (2004): Improved Pb-206/U-218 microprobe geochronology by the monitoring of a trace-element-related matrix effect; SHRIMP, ID-TIMS, ELA-ICP-MS and oxygen isotope documentation for a series of zircon standards; Chemical Geology, v. 205, p. 115–140.

Exploranium Radiation Detection Systems (1997): User's Guide KT-9 Kappameter, Rev. 1; Exploranium G.S. Limited, p. 1–80.

Gehrels, G. E., Valencia, V. A., and Ruiz, J. (2008): Enhanced precision, accuracy, efficiency, and spatial resolution of U-Pb ages by laser ablation-multicollector-inductively coupled plasma-mass spectrometry; Geochemistry, Geophysics, Geosystems, v. 9, p. 1–13.

Jaffey, A. H., Flynn, K. F., Glendenin, L. E., Bentley, W. C., and Essling, A. M. (1971): Precision Measurement of Half-Lives and Specific Activities of U-235 and U-238; Physical Review C, v. 4, p. 1889–1906.

Ludwig, K. R. (2012): Isoplot 3.75. A geochronological toolkit for Microsoft Excel; Berkeley Geochronology Center, Special Publication No. 5, 75 p.

Paton, C., Hellstrom, J., Paul, B., Woodhead, J., and Hergt, J. (2011): Iolite: Freeware for the visualisation and processing of mass spectrometric data; Journal of Analytical Atomic Spectrometry, v. 26, p. 2508–2518.

Petrus, J. A., and Kamber, B. S. (2012): VizualAge: A Novel Approach to Laser Ablation ICP-MS U-Pb Geochronology Data Reduction; Geostandards and Geoanalytical Research, v. 36, p. 247–270.

Sláma, J., Košler, J., Condon, D. J., Crowley, J. L., Gerdes, A., Hanchar, J. M., Horstwood, M. S. A., Morris, G. A., Nasdala, L., Norberg, N., Schaltegger, U., Schoene, B., Tubrett, M. N., and Whitehouse, M. J. (2008): Plešovice zircon — A new natural reference material for U–Pb and Hf isotopic microanalysis; Chemical Geology, v. 249, p. 1–35.

Spencer, C. J., Kirkland, C. L., and Taylor, R. J. M. (2016): Strategies towards statistically robust interpretations of in situ U–Pb zircon geochronology; Geoscience Frontiers, v. 7, p. 581–589.